PERFORMANCE OF HYPERBOLIC POSITION LOCATION TECHNIQUES FOR CODE DIVISION MULTIPLE ACCESS

by
George A. Mizusawa

Thesis submitted to the Faculty of the
Virginia Polytechnic Institute and State University
in partial fulfillment of the requirements for the degree of

MASTER OF SCIENCE
in
Electrical Engineering

Approved:

Dr. Brian D. Woerner
(Chairman)

Dr. Theodore S. Rappaport

Dr. Jeffery H. Reed

August 1996
Blacksburg, Virginia

Performance of Hyperbolic Position Location Techniques for Code Division Multiple Access

by

George A. Mizusawa

Committee Chairman: Dr. Brian D. Woerner

Electrical Engineering

Abstract

The Federal Communications Commission (FCC) recently adopted rules requiring cellular telephone, Personal Communication System (PCS) and Specialized Mobile Radio (SMR) licensees to provide two dimensional automatic location information (ALI) for a user requesting E-911 service. These wireless service providers will need to utilize effective position location (PL) technology in order to meet FCC rules. Hyperbolic PL systems are one such technology that can provide accurate PL information using the existing cellular/PCS infrastructure and without requiring additional hardware/software implementation within the mobile unit. In recent years, the IS-95 Code Division Multiple Access (CDMA) system has gained increasing popularity in North America because of the many advantages it offers over existing air interfaces. However, CDMA systems present some unique challenges to the effectiveness of hyperbolic position location systems.

This thesis investigates the performance of the hyperbolic PL technique in CDMA systems. The effect of multipath and shadowed mobile radio environments, the location of the user within the cell, and configuration and number of base stations on the accuracy of the hyperbolic PL technique is investigated. The effect of the power control scheme required in CDMA system operation on the performance of the hyperbolic system is also demonstrated. The simulation results provide insight to the limitations and effectiveness of hyperbolic position location systems within CDMA systems.

Acknowledgements

I would like to thank all my committee members. I owe a great debt of gratitude to Dr. Brian Woerner. His support, suggestions and advice provided me the guidance needed to complete this research work. I would also like to thank Dr. Jeffery Reed and Dr. Theodore Rappaport for their suggestions, corrections and advice on this work.

I would like to thank the Bradley Department of Electrical Engineering, General Motors and the I-95 Corridor Coalition for their generous financial assistance of this research effort.

I am grateful to all the members of the Mobile and Portable Radio Research Group (MPRG) who assisted me with this research effort. A special thanks to George Aliftiras, Don Breslin, Nitin Mangalvedhe and Mike Buehrer for their help with my thesis. The educational conversations and assistance they have provide me during my work is very much appreciated. I would also like to thank all MPRG staff members who have assisted me throughout my thesis work.

Lastly, and most of all, I would like to thank my wife, Penny, and daughter, Amber, for their support during my years at Virginia Tech. If it were not for their understanding and sacrifice, I would not have been able to complete this work for which I so much desired.

Contents

List of Tables

List of Figures

Chapter 1

Introduction

Wireless mobile radio systems have generated many new services in recent years. Cellular communication systems provide data and voice communication services with the convenience of mobility to their users. Paging systems provide paging services, brief messages in numeric, alphanumeric and voice formats, allowing their subscribers to receive messages virtually anywhere. With the development of new Personal Communications Systems (PCS), one can only expect an increase in the availability and types of service. However, one service that current wireless radio systems are unable to offer is effective and efficient emergency 9-1-1 service. This is primarily due to the inability of wireless mobile radio systems to provide accurate user position location (PL) information to the public safety answering points (PSAP). This problem has become evident to those who use and those who govern wireless services.

In 1994, the Federal Communications Commission (FCC) addressed this problem and proposed regulations that will require wireless service providers to provide Enhanced 9-1-1 (E-911) service in the near future [FCC94]. The National Association of State Nine-One-One Administrators (NASNA), the National Emergency Number Association (NENA), the Public-Safety Communications Officials (APCO) and the Cellular Telecommunications Industry Association (CTIA) have encouraged the FCC to adopt such regulations. The primary concern of the commission and these organizations is the inability of wireless service providers to provide automatic location information (ALI) to emergency service providers. This ALI information allows the emergency service agencies to provide fast and efficient emergency service to those in need of

assistance. While almost all wireline telephone service providers are capable of providing ALI information to the PSAP's, wireless service providers currently are not. In June 1996, the FCC adopted regulations requiring wireless service providers to implement E-911 [FCC96]. These regulations will affect all existing and future cellular and PCS service providers. To meet FCC regulations, wireless service providers will have to incorporate PL technology that will locate a user within an accuracy of 125 meters 67% of the time. In order for effective wireless E-911 to become a reality, these PL systems will have to provide accurate PL information of the user within the harshest environments, such as dense urban environments in which multipath and shadowing effects can greatly effect the accuracy of such systems.

1.1 Mobile Radio Position Location

Several different position location (PL) technologies present themselves as candidates for a mobile radio PL system. However, radio frequency (RF) PL systems have dominated the field because they offer the advantages of relatively low cost, ease of integration and potentially high accuracy. Radio frequency PL techniques also work with the existing cellular/PCS infrastructure, eliminating the need for external network implementations. Furthermore, radio frequency systems may operate, to a limited extent, in cases where other PL methods completely fail, such as when the line-of-sight (LOS) to the source is not available.

Radio frequency PL systems attempt to locate a source by direct measurements on radio signals traveling between the transmitter and receiver. These RF PL systems use time, phase or frequency measurements to first estimate the direction or range information of the signal propagation path, then utilize estimators that provide PL solutions from the measured data. The most widely used RF PL technique for geolocation of mobile users is the hyperbolic position location technique. The hyperbolic PL technique, also known as the time difference of arrival (TDOA) PL technique, utilizes cross-correlation techniques to estimate the TDOA of a propagating signal received at two receivers. This delay measurement defines a hyperbola of constant range difference from the receivers which are located at the foci. When multiple receiving stations are used, multiple hyperbolas are formed, and the intersection of the

set of hyperbolas provides the PL estimate of the source. The hyperbolic position location technique offers the advantages of not requiring additional hardware or software within the mobile unit, ability to resolve ambiguities in the PL estimate and minimizing the effect of noise within the mobile radio channel.

While hyperbolic PL systems can provide accurate PL estimation of a source given the appropriate conditions, geolocation of a mobile unit can be severely hindered by elements associated with the mobile radio channel. Multipath propagation can severely degrade the accuracy of PL techniques. This is a disadvantage common to all radio frequency PL systems. Proper base station positioning can be used to mitigate multipath effects. However, because cell coverage is a primary concern of wireless service providers, this may not be feasible alternative. When the mobile operates in shadowed environments, in which the line-of-sight (LOS) propagation path is obstructed by either man-made or natural structures, the signal propagation delays and attenuation experienced can also effect the accuracy of position location estimates. Furthermore, because the hyperbolic PL technique requires reception of a mobile's transmitted signal at multiple platforms, usually three or more base stations (BS), another problem lies with signal power levels at each receiving station. Because base stations in cellular/PCS systems are located to optimize cell coverage, the number of base stations receiving the signal with adequate power level may be limited. These mobile radio channel conditions present some unique challenges to the geolocation of a user within a cellular/PCS system.

1.2 Position Location in CDMA Systems

Development of CDMA systems within the U.S. is currently underway and it is expected to grow. To meet FCC wireless E-911 regulations, these systems must incorporate position location techniques that will acquire and provide accurate location information for a user requesting E-911 service to the PSAP's. However, position location systems within CDMA systems face some unique challenges.

First, if geolocation is implemented in the forward channel, the mobile unit would be required to make signal measurements and either relay the information to a Master

Switching Center (MSC), which would then perform the PL calculations based on the measurements, or perform the PL calculations and relay the PL estimate to the MSC. Accurate clock synchronization between the base stations and mobile unit would be required in order to achieve accurate PL estimation. This implementation would require additional hardware and/or software in the mobile unit, possibly increasing the power requirements, size and cost of the unit. Furthermore, to allow E-911 access for all users within a CDMA system, retrofitting of existing CDMA or dual mode AMPS/CDMA phones may be required.

The reverse link of a CDMA system also presents unique challenges. Since reverse channel transmissions originate from users dispersed within a cell, the reverse link is subject to the near-far problem. The near-far problem occurs when a mobile units power level at the base station is much higher than the power level of all other mobile users. This introduces interference in the signals of all other mobile users, degrades signal quality and system capacity. Consequently, a strict power control scheme is required which adjusts the transmitting power of all users accordingly to limit the amount of interference. Under this power control scheme, when a mobile unit's received power level increases as it moves in closer proximity to the base station, the mobile unit is directed to reduce its transmitting power. In this situation, the signal power levels at neighboring base stations will be lower because of the reduced transmitting power and increased transmitter-receiver distance. This results in low signal-to-noise ratio (SNR) at the neighboring BS's and leads to inaccuracies in PL estimation. This presents a major problem to reliable and accurate geolocation of mobile users [Gil96].

Although CDMA offers multipath interference rejection, multipath interference is only rejected if the multipath arrives with a delay of at least one chip interval of the CDMA code. Multipath arriving within the chip interval can introduce errors in the TDOA estimates, resulting in inaccurate PL estimation. This presents another limitation to the capabilities of hyperbolic position location systems. The extent to which these mobile radio channel elements effect the accuracy of the hyperbolic position location technique must be known if these detrimental effects are to be mitigated to provide improved PL performance.

Although CDMA system operation and the mobile radio channel introduce limitations to the PL estimation accuracy, CDMA systems are well suited for position location from a technical standpoint. Similar to the well-known Global Positioning System (GPS) [Par96], CDMA systems use high rate pseudo-noise (PN) sequences. The short duration of the PN "chip" allows for a high resolution TDOA estimation, resulting in accurate position location estimation of a mobile unit. To illustrate the improved TDOA resolution capabilities of high rate PN sequences, consider a single 16μs pulse from a BPSK signal, as seen in Figure 1.1. The normalized cross-correlation of the pulse, assuming a noise-free environment, results in a correlation peak that is rather broad. However, when the same pulse is spread using a high chip rate PN spreading sequence, as seen in Figure 1.2, the normalized cross-correlation results in a much narrower peak, which can be detected with a much greater resolution than the conventional pulse. This higher temporal resolution effectively reduces the uncertainty in the TDOA estimation and improves the accuracy of the position location estimate.

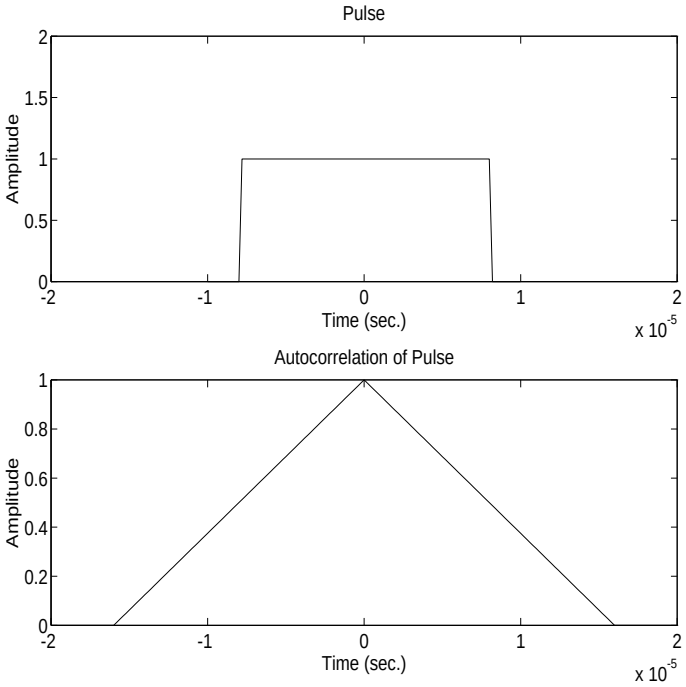

Figure 1.1: Single Pulse and Autocorrelation

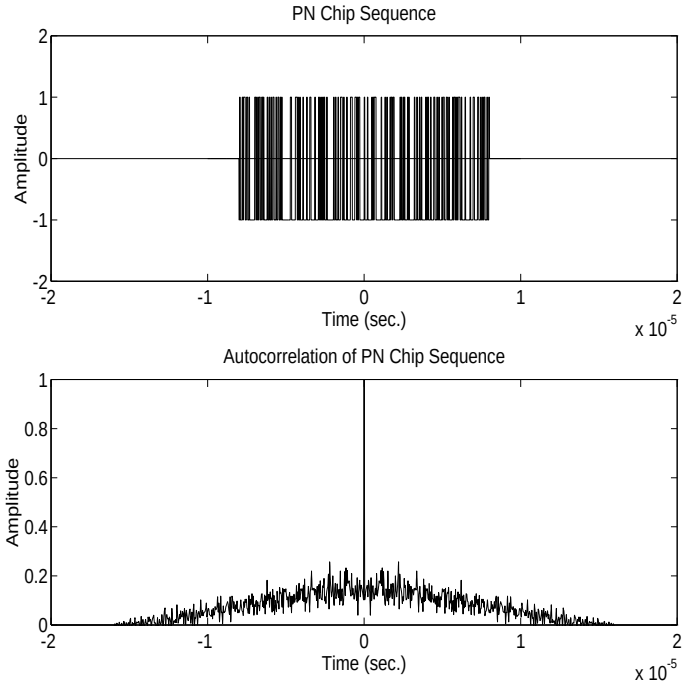

Figure 1.2: PN Spreading Sequence and Autocorrelation

1.3 E-911 and FCC Regulations

1.3.1 Enhanced 911

In 1965, American Telephone and Telegraph (AT&T) introduced the use of the phone number 911 for emergency purposes. Since its inception, this 911 emergency number has seen widespread use. A study by the FCC's Network Reliability Council indicates that 89 percent of the wireline access lines in the United Sates are served by some form of 911 service [Nat93]. Currently, about 260,000 calls nationwide are placed to 911 every day [FCC94]. The 911 telephone emergency number provides users with an easily memorized number for accessing emergency services within their area and allowing them to receive, and state and local governments to provide, fast response to emergency situations.

The initial implementation of 911 emergency service was developed to provide a forwarding arrangement with public safety agency's. The 911 call is received and translated by a telephone switch and directed to the appropriate public safety answering point (PSAP) over dedicated emergency telephone lines for response. However, this did not provide for the most efficient response time because the PSAP handling the call may not be the PSAP nearest to the caller and vital information, such as the caller's location or phone number, was not always available. Thus the need for a more efficient 911 service was conceived, which consequently lead to the development of the Enhanced 911 (E-911) service.

Enhanced 911 service, which is provided by approximately 85 percent of emergency 911 systems, aid emergency services personnel in achieving the shortest possible response time to emergency requests [FCC94]. The minimum E-911 service provides the PSAP with Automatic Number Identification (ANI) information of the calling party. The ANI, which indicates the calling party's phone number, permits call-back capability in the event the call is disconnected. A fully enhanced 911 service not only displays the ANI, but also permits the PSAPs to identify the calling party's address through use of an Automatic Location Identification (ALI) database. This ALI information also permits selective routing (SR) of the call to the appropriate PSAP for the identified location [FCC94].

However, while some wireless systems are capable of providing basic 911 service, few provide E-911 service. The ability of the public safety agencies to respond is severely hindered by the inability of wireless systems to provide the ALI information of the caller requesting assistance. This information is not accessible in the ALI database associated with wireline telephone users. Furthermore, wireless service providers are unable to provide call-back capability, the number of the caller, or indicate the type of service required. The inability of wireless service providers to offer comparable E-911 service to its customers has become a major safety issue that concerns the FCC, public safety organizations and the wireless industry.

1.3.2 FCC Regulations for Wireless E-911

In 1994, the Federal Communications Commission (FCC) proposed to amend its regulations to address issues raised by the provision of 911 and enhanced 911 (E-911) service through wireless communications systems [FCC94]. The FCC proposed to adopt rules that would require wireless services, in particular commercial mobile radio services (CMRS) that provide real time voice services, to include features that will make enhanced 911 services available to mobile radio callers. These features include Station Number Identification (SNI), Automatic Location Information (ALI), Selective Routing (SR), and other features for 911 calls provided over wireless systems.

The FCC recognized that in order to provide a functionally equivalent E-911 service to wireless customers, the mobile unit must be able to communicate to the base station (BS) the information required by E-911 service (ANI and ALI). The base station must be able to interpret this information, provide proper handling of 911 calls, and forward sufficient information to the PSAP to provide call-back capability, location information enabling selective routing, and the determination of the type of service to be provided. Proper handling of 911 calls includes giving 911 call priority over non-emergency calls and without required validation. However, because the nature of calls in progress is unknown, priority of 911 calls will not require the interruption of calls in progress.

In June 1996, the FCC adopted rules that require wireless service providers to implement E-911 and that compliance should be implemented in three steps [FCC96]. The

first step requires, within twelve months after the effective date of the rules, cellular telephone, Personal Communications Systems (PCS) and Specialized Mobile Radio (SMR) licensees to transmit to the PSAP's any 911 emergency calls from a handset that transmits a Mobile Identification Number (MIN), or its functional equivalent, without any interception by the carrier for credit checks or other validation procedures. The commission also allows the PSAPS the discretion to require cellular, PCS and SMR's licensees to transmit 911 calls that originate from phones that do not transmit the MIN, without any credit checks or validation. The second step, beginning twelve months after the effective date of the rules and to be completed by eighteen months, requires these same licensees to provide the PSAP with the callers phone number, and at a minimum, the location of the base station (BS) or cell site handling the 911 call. Furthermore, if the BS or cell site employs a sectored antenna, the information relayed to the PSAP would have to indicate the sector in which the 911 call is received. The third step allows PSAPs to require within five years after the effective date of rules, cellular, PCS and SMR licensees to obtain and relay two dimensional (2-D) position location of the mobile station within an accuracy of 125 meters ($\approx$ 400 feet) in 67 percent of all cases to the PSAP. This information would provide the PSAP with a relative precise location of the 911 caller requesting assistance. The first two goals are primarily networking and protocol design problems, and while they provide significant challenges, they are not the focus of this thesis. The third goal of 2-D PL is the primary topic studied in this thesis.

1.4 The Importance of Accurate PL Techniques

Emergency E-911 service has proven effective in aiding those in need of assistance. However, this is only true for wireline telephone customers. While some wireless systems are capable of providing basic 911 service, few, if any, are currently capable of providing enhanced 911 service. This raises public policy concerns because as the number of calls from wireless service users continues to rapidly increase, so do the number of emergency 911 calls originating from them. For example, the number of cellular calls in Massachusetts increased from 300 per month in 1987 to more than 15,700 per month in 1992 [FCC94].

In order for emergency services to provide comparable E-911 service to wireless service users, the location of the individual will have to be accurately known. This location information should not rely upon the caller's verbal instructions. For example, in Los Angeles County, more than 25% of the callers out of 600,000 cellular/mobile 911 calls made in 1992 could not identify their location [FCC94]. Consequently, the location of a user should be determined through passive position location techniques without requiring user intervention. These position location techniques will need to achieve high reliability and accuracy, especially in densely populated urban environments, to be effective. It is estimated that as many as 10% of all 911 calls originate from mobile radio service subscribers within major metropolitan areas [FCC94].

With the extreme growth of existing wireless communications systems, billions of dollars have been invested in the deployment of PCS. As the competition for consumers is expected to increase with this new system, a wireless service provider that provides effective E-911 service becomes more marketable and attractive to consumers, consequently gaining an advantage over the competition. As a result, the added cost of implementing a position location service can be offset by spreading the cost over more users.

1.5 Purpose of Research

The objective of this research is to simulate and evaluate the performance of the hyperbolic position location technique within CDMA systems in urban cellular environments. The pseudo-noise codes used in CDMA systems facilitate high resolution TDOA estimation which leads to accurate PL estimation. However, the mobile radio channel, base station configuration and CDMA operation present limitations to the accuracy of the hyperbolic PL systems. Multipath signal propagation corrupts time difference of arrival estimation, and shadowing due to made-made or natural structures degrade signal quality and introduce delays in the signal propagation time. The configuration of the base stations can also hamper position location accuracy, as indicated by the geometric dilution of precision (GDOP) factor. The power control scheme required of CDMA systems presents one of the most serious limitations to position location accuracy. Because of power control operation in CDMA systems,

signal power levels at neighboring base stations can be very low, resulting in inaccurate TDOA and PL estimation. The simulation software developed for this research investigates the effect of these channel and system parameters. The limitations due to these parameters must be overcome if accurate position location within CDMA is to become a reality.

1.5.1 Outline of Thesis

The remainder of this thesis is organized as follows. Chapter 2 provides an overview of code division multiple access and radio frequency position location techniques. The advantages of a wideband CDMA system over narrowband FDMA or TDMA and the power control scheme required of CDMA systems are discussed. The Direct Sequence Spread Spectrum (DS/SS) technique used in CDMA systems is presented. Classifications of radio frequency position location systems and a brief overview of direction finding and ranged-based position locations techniques is provided. A comparison of direction finding and hyperbolic position location systems, and factors limiting the use of the Global Positioning System (GPS) within cellular environments is provided.

Chapter 3 provides a detailed discussion of the time difference of arrival (TDOA) estimation techniques and algorithms used in hyperbolic position location systems. General models for time delay estimation and hyperbolic position location estimation are developed. The generalized cross-correlation (GCC) technique and frequency filters used in GCC TDOA estimation are reviewed. The hyperbolic position location algorithms commonly used to provide solutions to the position location problem are described. The advantages and disadvantages of each algorithm are discussed.

Chapter 4 discusses the simulation method used in this thesis. The general position location procedure within a CDMA system, as well as CDMA system parameters and operation, is discussed. The transmitter, receiver and the mobile radio channel models used are described. The path loss, multipath and shadowing models used in the simulation are developed, and the issue of AWGN noise power scaling is covered.

Chapter 5 presents the experimental results of the simulations. Performance measures include the root-mean square (RMS) PL error, geometric dilution of precision (GDOP) and circle of error probability (CEP) of the PL estimate. The performance

of the hyperbolic position location technique within a microcellular and macrocellular CDMA environment is presented. The performance of the hyperbolic position location system as a function of the location of a user within the cellular environment and signal-to-noise ratio (SNR) at the base stations is examined. Simulation results for hyperbolic position location system operation under a CDMA closed-loop power control scheme indicate how available power levels effect PL accuracy. The effect of path loss and observation window on performance is also investigated. The degradation in position location accuracy due to multipath and shadowed mobile radio channels is demonstrated.

Chapter 6 concludes this thesis by summarizing the results of the work and discussing future work.

Chapter 2

CDMA and Position Location Techniques

2.1 Code Division Multiple Access

In 1993, a U. S. digital cellular system based on code division multiple access (CDMA) was standardized as Interim Standard 95 (IS-95) by the Telecommunication Industry Association (TIA) [TIA93]. During the same year, the FCC allocated spectrum for Personal Communication Systems (PCS) operation in the United States. Blocks of spectrum within this band, as indicated by Figure 2.1, were licensed for PCS systems in 1994 and 1995. Those who licensed the blocks of spectrum are allowed to use any desired air interface provided that it complies with FCC rules. The CDMA IS-95 cellular standard, which is based on direct sequence spread spectrum (DS/SS) technology, offers several advantages over TDMA or FDMA based systems. Consequently, the CDMA has also been selected as one of the air interfaces for new PCS systems.

2.1.1 Advantages of CDMA Systems

In a CDMA system, each user's narrowband message is multiplied by a long pseudo-noise (PN) sequence, called the *spreading signal*. The PN sequence is comprised of random symbols called *chips* and has a chip rate which is in orders of magnitude

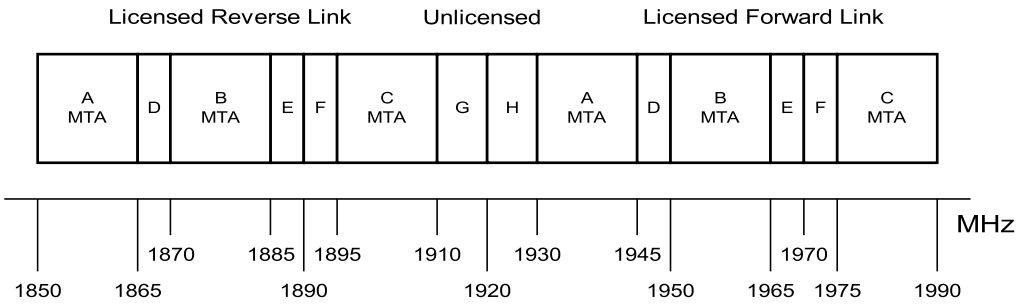

Figure 2.1: PCS Spectrum Licensing

greater than the data rate of the message. This effectively spreads the narrowband signal energy over a much larger bandwidth. Figure 2.2 illustrates the spreading effect of the PN sequence. In the figure, $b(t)$ is the baseband message signal with bit duration T, $a(t)$ is the spreading sequence with chip duration T_c, and $B(f)$ and $C(f)$ are the spectrum of the message before and after spreading respectively.

This spreading of the user's signal serves two purposes. First, it provides a simple form of security because it hides the user's signal within the noise floor. In order to receive the signal, a receiver must correlate the received signal with a locally generated replica of the PN carrier. As a result, only those receivers who have knowledge of the user's PN sequence can acquire the user's message. Second, it provides resistance to narrowband interference within the bandwidth of the signal. The decorrelation process used to despread the user's signal at the receiver spreads the energy of the narrowband interference over a much larger bandwidth causing it to be seen as noise.

In an ideal CDMA system, each user's signal would be spread by a unique PN code which is mutually orthogonal to the PN code of all other user's. The orthogonality of the PN sequences provides code diversity between each user's signal, allowing all user's to share the same spectrum, and thus explaining the name *code division multiple access*. When a particular user's signal is despread at the receiver through correlation with an identical PN sequence, all other user's PN sequences are highly uncorrelated and seen as noise. Thus CDMA offers resistance to multiple access interference. In practice, the base station in the forward channel of a CDMA system is able to simultaneously transmit user signals spread by orthogonal PN sequences. However, user signals in the reverse channel are asynchronous and non-orthogonal. A

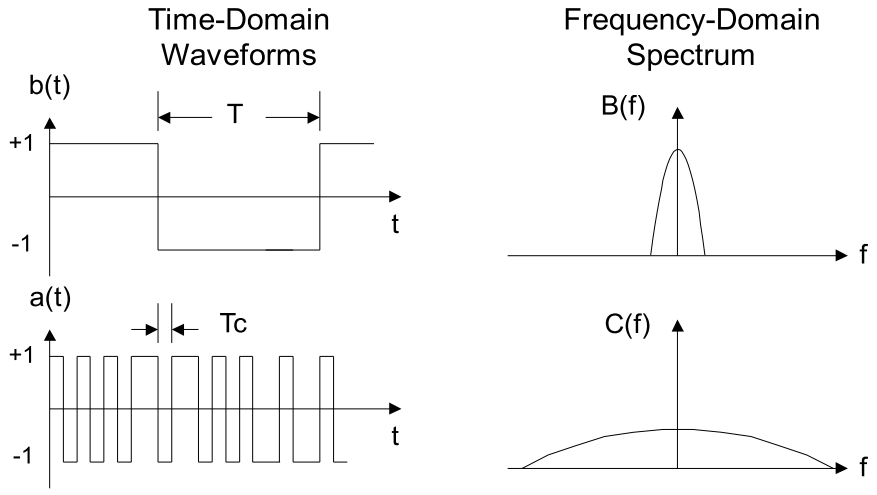

Figure 2.2: Spread Spectrum Encoding

CDMA system is considered asynchronous if the PN sequences from different user's are not chip and bit aligned [Lib95]. In the reverse channel, each user's PN sequence is generated based on the mobile unit's Electronic Serial Number (ESN). While each ESN is unique, they generally do not produce a PN sequence that is orthogonal to all other PN sequences. Consequently, the reverse channel is susceptible to multiple access interference.

Since each user is allowed to occupy the same duplex channel, CDMA systems do not require frequency reuse or channel allocation throughout the system, unlike TDMA and FDMA systems. Sharing of spectrum by all user's allows for *soft handoff* between cells, which is performed by the Master Switching Center (MSC). When a user approaches the cell boundary, the MSC can simultaneously monitor the unit from two or more base stations. The MSC is able to switch control of the user's call to the base station receiving the best version of the user's signal without changing frequencies. This greatly simplifies handoff strategies within a cellular/PCS environment.

Code division multiple access systems also offer resistance to multipath interference. When a user's signal is despread during the correlation process at the receiver, the locally generated replica of the user's PN code is aligned with the line-of-sight (LOS) signal, assuming that the LOS signal has the greatest signal power. When the LOS

and multipath components signal are separated by more than one chip, the multipath signal is highly uncorrelated and seen as noise. As a result, the interference due to multipath lying outside of one chip is minimized. However, useful signal energy within the multipath is lost. To make use of the signal energy within the multipath, multi-finger Rake receivers are commonly used at the base station and mobile unit. A general implementation of a Rake receiver is illustrated in Figure 2.3. Rake receivers are able to maximize the signal-to-noise ratio (SNR) of the signal by coherently combining signal energies from the LOS and multipath components.

Another advantage that CDMA systems offer is capacity improvement. The IS-54 and AMPS cellular standards have a hard limit on the number of user's that it can support because of the limited number of available channels. Since all user's within a CDMA system occupy the same channel, there is not a limited number of user channels that can be occupied. However, because the interference levels increase as the number of user's increase, there is a "soft" capacity limit in which CDMA systems can maintain acceptable signal quality. Capacity improvements are also realized by the systems ability to exploit the voice activity of a call. Typical voice activity during a normal conversation is approximately 40% or less. During the silent periods, in which there is no voice activity, the data rate of the variable rate speech encoder in the mobile unit is reduced, code symbols are repeated to maintain a constant code rate and the unit is instructed to reduce its transmit duty cycle. This reduces the interference contributed by the mobile unit. As a result, more user's can be accommodated within the same spectrum.

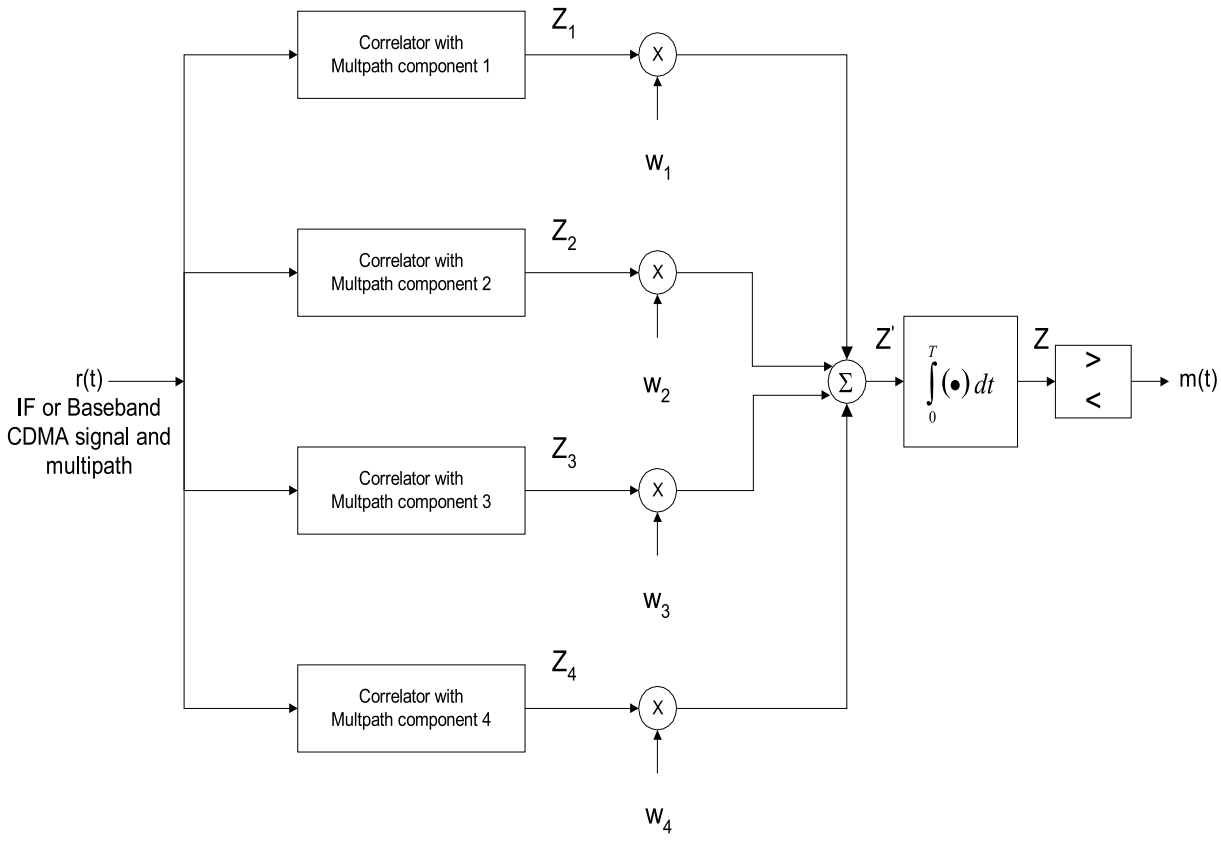

Figure 2.3: General Implementation of a Rake receiver

2.1.2 Power Control and the Near-Far Problem

Transmissions in the reverse link of a CDMA system originate from user's dispersed throughout the cell. As a result, received signal powers at the base station can vary widely. Stronger received signal levels raise the noise floor at the base station demodulators. Weaker signals are thereby received with power much lower than the noise floor and the probability that a weaker signal will be received is decreased. This creates a problem termed the *near-far problem*. In order to combat this problem, power control must be implemented. This power control assures that all transmissions from the mobile units within the cell are received with the same signal power at the base station.

Code division multiple access systems can use two types of power control: closed-loop power control at the base station or open-loop power control at the mobile unit. Closed-loop power control is implemented at the base station by rapidly sampling the radio signal strength indicator (RSSI) levels of each mobile and then sending a power change command over the forward link [Rap96]. Under open-loop power control, a mobile adjusts its power based on the strength of the signal it receives from the base station.

The power control required of CDMA systems presents a major problem for PL systems. In general, as the mobile moves closer to the base station handling the call, and consequently farther away from neighboring base stations, the received signal power from the mobile unit increases at the base station. Under a closed-loop power control scheme, the base station instructs the unit to reduce power to limit the amount of interference. However, this effectively reduces the signal power at the neighboring base stations. This can severely degrade the accuracy of the position location estimate and possibly eliminate the ability to geolocate the mobile unit. This problem is just one of many issues to be resolved if position location in CDMA systems is to become a reality.

2.1.3 Direct Sequence Spread Spectrum

Direct sequence spread spectrum (DS/SS) technology provides CDMA systems robustness against multipath and multiple access interference and improvements in capacity. To illustrate the operation of a DS/SS system, consider the conceptual representation of a DS/SS transmitter shown in Figure 2.4. It is assumed that the an information bearing signal $b(t)$ is BPSK modulated data. The ith bit of the information bearing signal is assumed to be an equiprobable independent random variable that takes on values of $b_i \in \{+1, -1\}$. The data signal $b(t)$ is described as

$$b(t) = \sum_{i=-\infty}^{\infty} b_i \Pi_T(t - iT), \tag{2.1}$$

where $\Pi_T(t)$ is a unit rectangular pulse of duration T and is described as

$$\Pi_T(t) = \begin{cases} 1, & 0 \leq t < T \\ 0, & t < 0, t \geq T. \end{cases} \tag{2.2}$$

The BPSK data is then spread by the PN sequence $a(t)$ given by

$$a(t) = \sum_{j=-\infty}^{\infty} a_j \Pi_{T_c}(t - jT_c), \tag{2.3}$$

where a_j is the jth chip of a discrete periodic PN sequence assigned to the user and assumed to be an equiprobable independent random variable that can take on values of $a_j \in \{+1, -1\}$. The PN chip has pulse shape $\Pi_{T_c}(t)$ which is limited in time to $[0, T_c)$ where $T_c \ll T$. The processing gain of a DS/SS system, N, is defined as the ratio T/T_c. Although not included in the conceptual DS/SS transmitter representation, pulse-shaping is normally performed to bandlimit the signal so as to meet FCC regulations. The PN spread signal is then RF modulated and amplified, resulting in a transmitted signal $s(t)$ described as

$$s(t) = \sqrt{2P} b(t) a(t) cos(\omega t), \tag{2.4}$$

where P is the power of the user's signal.

While there are many receiver structures for the reception of DS/SS signals, consider the conceptual representation of a correlation DS/SS receiver in Figure 2.5. This receiver performs the complementary operations of the DS/SS transmitter in Figure

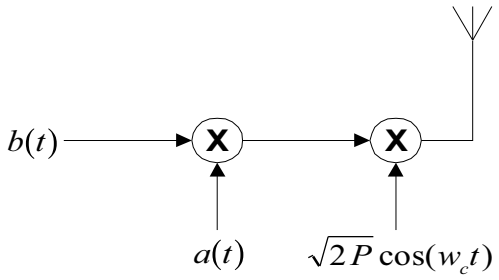

Figure 2.4: Direct Sequence Spread Spectrum Transmitter

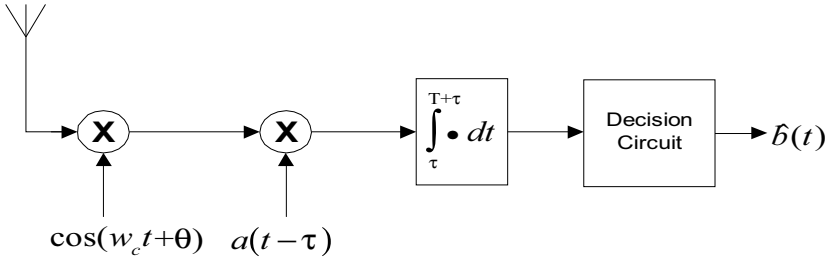

Figure 2.5: Direct Sequence Spread Spectrum Receiver

2.4. Assuming an additive white Gaussian noise channel and a finite propagation delay τ, the received signal is described as

$$r(t) = s(t-\tau) + n(t). \tag{2.5}$$

The received signal is demodulated to baseband where it is multiplied by a replica of the user's PN sequence. The multiplication by the identical PN sequence despreads the user's signal to its original narrowband form. The despread signal is then passed through a matched filter which forms a decision statistic, Z_i, for each received bit. The decision statistic is described by

$$Z = \int_{\tau}^{T+\tau} r(t)a(t-\tau)cos(\omega t + \theta)dt \tag{2.6}$$

or

$$Z_i = \int_{\tau}^{T+\tau} \sqrt{2P}b_i(t-\tau)a(t-\tau)cos(\omega t + \theta)a(t-\tau)cos(\omega t + \theta)dt, \tag{2.7}$$

where the effect of noise is assumed to be negligible and therefore is not included. The multiplication of the two PN sequences $a(t) \cdot a(t) = 1$ and the integration over one bit results in an estimate $\hat{b}_i$. Therefore, the statistic can be written as

$$Z_i = \sqrt{2P}\hat{b}_i(t) \int_0^T cos^2(\omega t)dt, \tag{2.8}$$

where

$$cos^2(\omega t) = \frac{1}{2}(1 - cos(2\omega t)). \tag{2.9}$$

The $\frac{1}{2}cos(2\omega t)$ term is filtered out, resulting in a decision of the ith bit

$$Z_i = \sqrt{\frac{P}{2}}\hat{b}_i(t). \tag{2.10}$$

A comparator then estimates the transmitted bit based on this decision statistic. In an noise-free channel, the resulting received message will be identical to the transmitted message.

To illustrate the multiple access interference resistance of DS/SS system, consider a multiuser CDMA system with two user's. The received signal can be described as

$$r(t) = s_1(t) + s_2(t), \tag{2.11}$$

where it is assumed that $s_1(t)$ is the signal of interest and $s_2(t)$ is the interference. The decision statistic for $s_1(t)$ will then be based on the decorrelation of both signals by the PN sequence used to generate $s_1(t)$ and is described in a simplified form as

$$Z_i = \int_0^T b_1(t)a_1(t)a_1(t)dt + \int_0^T b_1(t)a_1(t)a_2(t)dt. \tag{2.12}$$

If the PN sequences of both user's are truly orthogonal, the multiplication of both result in $a_1(t) \cdot a_2(t) = 0$, and the multiple access interference is eliminated.

To illustrate the multipath interference resistance of DS/SS systems, consider a mobile radio channel which produces a single multipath component. The received signal can be described as

$$r(t) = s_1(t) + \alpha s_1(t - T), \tag{2.13}$$

where α and T are the relative power and delay of the multipath. The decision statistic can be described in a simplified form as

$$Z_i = \int_0^T b_1(t)a_1(t)a_1(t)dt + \int_0^T \alpha b_1(t - T)a_1(t)a_1(t - T)dt. \tag{2.14}$$

If the PN sequence of the user is truly random and the multipath delay $T > T_c$, the two sequences, $a(t)$ and $a(t-T)$, will be uncorrelated and result in $a(t) \cdot a(t-T) = 0$. As a result, the interference of the multipath is eliminated. However, if the multipath lies within the chip interval, $T < T_c$, the decision statistic will be effected.

2.2 RF Position Location Systems

2.2.1 Classification of PL Systems

Radio frequency position location systems be can classified into two broad categories: direction finding (DF) and range-based PL systems. Each of these systems can be classified as a satellite or terrestrial based system, indicating whether the base station is located on the surface of the earth or in orbit around the earth. They can also be classified by their coverage area: world-wide coverage or local area coverage; by the number of measurements used: multilateration or trilateration; and by the type of measurement used: phase, time or frequency. An extensive list of PL system classifications is provided in [Law76]. These DF and range-based PL systems and techniques can be used individually or in a number of different configurations to produce a PL solution.

Direction finding systems estimate the position location of a source by measuring the direction of arrival (DOA), or angle of arrival (AOA), of the source's signal. The DOA measurement restricts the location of the source along a line in the estimated DOA. When multiple DOA measurements from multiple base stations are used in a triangulation configuration, the location estimate of the source is obtained at the intersection of these lines. Consequently, direction finding PL systems are also known as *direction of arrival* or *angle of arrival* PL systems.

Range-based PL systems can be categorized as either a ranging, range sum, or range difference PL system. The type of measurement used in each of these systems defines a unique geometry, or configuration, of the position location solution. Ranging PL systems locate the source by measuring the absolute distance between a source and the receiver. Range measurements are determined by estimating the time-of-arrival (TOA) of the signal propagating between the source and receiver. The TOA estimate defines a sphere of constant range around the receiver. The intersection of multiple spheres produced by multiple range measurements from multiple base stations provides the position location estimate of the user. Consequently, ranging systems are also known as *TOA* or *spherical* PL systems. Most practical ranging systems are unable to measure the range between the user and a base station directly, and as a

result, measurement of the range and a bias term is commonly performed. This bias term can be calculated using a additional range measurement by an additional base station. Ranging systems of this type are often called *pseudo-range* systems [Par96].

Range sum PL systems measure the relative sum of ranges between the source and receiver respectively. These systems measure the time sum of arrival (TSOA) of the propagating signal between two base stations to produce a range sum measurement. The range sum estimate defines a ellipsoid around the receiver, and when multiple range sum measurements are obtained, the position location estimate of the user is at the intersection of the ellipsoids. Consequently, range sum PL systems are also known as *TSOA* or *elliptical* PL systems.

Range difference PL systems measure the relative difference in ranges between the source and receiver respectively. These systems measure the time difference of arrival (TDOA) of the propagating signal between two base stations to produce a range difference measurement. The range difference measurement defines a hyperboloid of constant range difference with the base stations at the foci. When multiple range difference measurements are obtained, producing multiple hyperboloids, the position location estimate of the user is at the intersection of the hyperboloids. Consequently, range difference PL systems are also known as *TDOA* or *hyperbolic* PL systems. Throughout this thesis, systems of this class will be referred to as hyperbolic PL systems.

Range-based systems can also be classified as either *multilateration* or *trilateration* systems. Multilateration PL systems are those systems which utilize measurements from four or more base stations to estimate the three dimensional (3-D) location of the user. In a multilateration ranging PL system, four or more base stations produce four or more range measurements, and in a multilateration hyperbolic PL system, four or more base stations produce three or more range difference measurements. Trilateration PL systems are those which utilize measurements from three base stations to estimate the two dimensional (2-D) location of the user. In a trilateration ranging PL system, three range measurements are produced from the three base stations, while in a trilateration hyperbolic PL system, two range difference measurements are produced from three base stations. The additional measurement by ranging systems is required to reduce the ambiguities.

Radio frequency position location systems can be classified according to the type of measurement the estimate is based on: time, phase or frequency. Obviously, systems that utilize time or phase information to determine PL are considered time and phase systems respectively. Position location systems which measure the change in frequency of a signal transmitted signal are considered *Doppler systems*. When either the source or receiver is moving, the transmitted signal is subjected to a shift in frequency due to the Doppler effect. This change in frequency is proportional to the relative direction of movement and velocity of movement. By measuring the change in frequency, the rate of change between the user and base station can be determined. If the trajectory of the base station is known then the user's location can be uniquely determined from the Doppler frequency changes. Doppler systems generally require the velocity of either the receiver station or user to be high enough to generate an easily resolvable Doppler shift. Consequently, systems of this type are generally applicable to non-geosynchronous satellite based PL systems or PL estimation of high velocity vehicles.

2.2.2 Direction Finding PL Systems

Direction finding (DF) systems utilize multi-array antenna and direction of arrival (DOA) techniques to estimate the direction of the signal of interest. The DOA measurement restricts the source location along a line in the estimated DOA. When multiple DOA measurements from multiple base stations are used in a triangulation configuration, the location estimate of the source is obtained at the intersection of these lines. Figure 2.6 illustrates the two dimensional (2-D) PL solution of DF systems. While only two DOA estimates are required to estimate the PL of a source, multiple DOA estimates are commonly used to improve the estimation accuracy.

Direction of arrival estimation is performed by signal parameter estimation algorithms which exploit the phase differences, or other signal characteristics, between closely spaced antenna elements of an antenna array and employ phase-alignment methods for beam/null steering. The spacing of antenna elements within the antenna array is typically less than 1/2 wavelength of all received signals. This alignment is required to produce phase differences on the order of π radians or less to avoid ambiguities

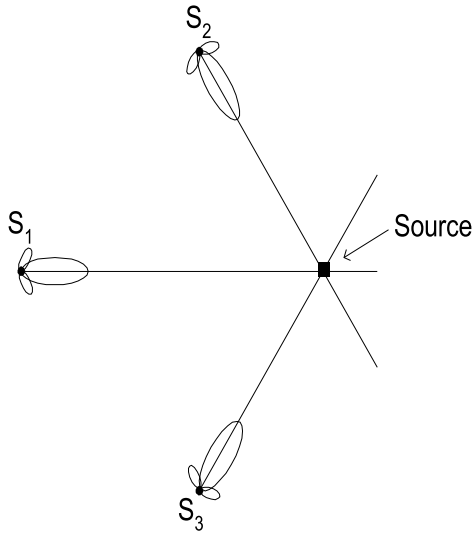

Figure 2.6: 2-D Direction Finding Position Location Solution

in the DOA estimate. The resolution of DOA estimators improves as the baseline distances between antenna elements increases. However, this improvement is at the expense of ambiguities. As a result, DOA estimation methods are often used with short baselines to reduce or eliminate the ambiguities and long baselines to improve resolution.

Although, direction finding methods can provide accurate DOA estimation given the appropriate conditions, they do suffer from elements encountered within the mobile radio channel. First, DOA estimation techniques estimate the direction of a source based on the strongest received signal, which is assumed to be the line-of-sight (LOS) signal. However, in shadowed environments such as encountered in urban areas, the true LOS signal path may be obstructed by the surrounding environment and only multipath components of the signal may exist. In this case, the DOA estimate will be the direction of the strongest multipath component, which leads to errors in the DOA estimate. Depending on the transmitter-receiver distance, these errors in the DOA estimate can lead to dramatic errors in the PL estimate. Even if the LOS signal is available, multipath has been shown to severely degrade the accuracy of DF methods. While angular accuracy's of several degrees are possible with these techniques, this generally does not provide an acceptable position location accuracy when using the triangulation configuration solution.

2.2.3 Ranging PL Systems

Ranging PL systems measure the absolute distance between a source and a set of base stations through the use of time-of-arrival (TOA) measurements. The TOA measurements are related to range estimates that define a sphere around the receiver. When measurements are made from receivers with known locations, the spheres described by the range measurements intersect at a unique point indicating the position location estimate of the source. Figure 2.7 illustrates the three dimensional (3-D) solution of the ranging PL system. If the spheres described by the range measurements intersect at more than one point, an ambiguous solution to the position location estimate results. Redundant range measurements, resulting in a multilateration ranging PL estimation, are commonly made to reduce or eliminate PL ambiguities.

To illustrate the ranging PL concept, consider a 3-D ranging PL system using N base stations. The time of arrival of a signal at each receiver is estimated and related to the range measurement by the relationship

$$R_i = c\, d_i, \tag{2.15}$$

where is the range measurement, c is the signal propagation speed and d_i is the TOA estimate at the ith receiver. The mathematical relationships between range measurements at N base stations, the coordinates of the known base station locations, and the coordinates of the source are

$$R_i = \sqrt{(X_i - x)^2 + (Y_i - y)^2 + (Z_i - z)^2} \quad for\ i = 1, 2, 3, ...N, \tag{2.16}$$

where (X_i, Y_i, Z_i) are the coordinates of the ith base station, R_i is the ith range estimate to the source and (x, y, z) is the location of the user. Equation 2.16 defines a N x 3 set of nonlinear equations whose solution is the location coordinates of the source. If the number of unknowns, or coordinates of the source to be solved, is equal the number of range measurements, the set of equations are consistent and a unique solution exists. However, if redundant measurements produce more range measurements than the number of unknowns, then the system is inconsistent and a unique solution may or may not exist. This generally requires an error criterion to be selected and iterative techniques to be employed to produce a solution. A least squares (LS) fit is commonly used to simultaneously solve these equations for both the position location and error coefficients.

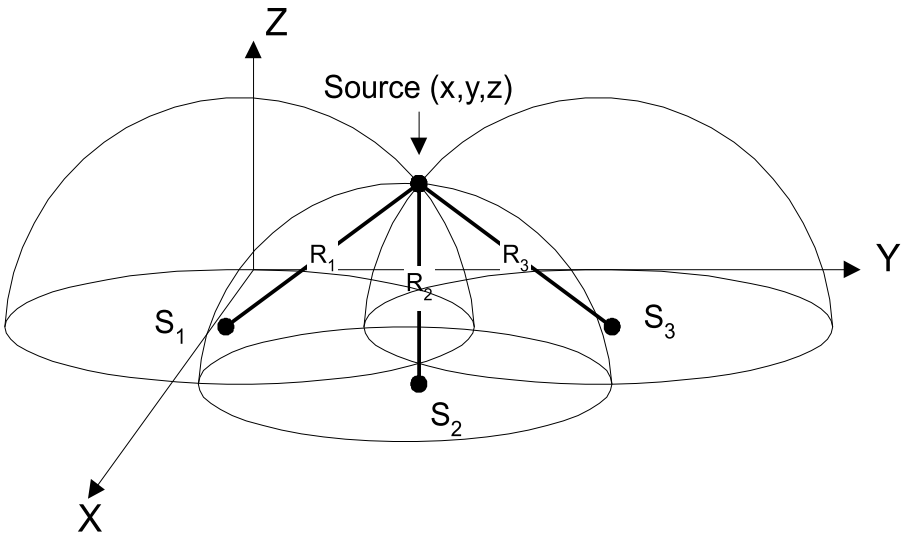

Figure 2.7: 3-D Ranging Position Location Solution

Accurate time or phase measurements in ranging PL systems requires strict clock synchronization between the source and base stations. This is accomplished through the use of stable clocks, such as the rubidium or cesium standard clocks used in GPS satellites, at both the source and base station. As such, ranging PL system may require additonal hardware implmentation in a mobile unit, resulting in additional power, size and weight requirements.

A disadvantage of the ranging PL technique is that accuracy is very dependent on system geometry. Highest accuracies are attained when all ranging spheres intersect at 90 degrees. Degradation in performance is experienced as the intersections deviate from this angle. For systems with fixed receivers and moving sources, such as cellular and PCS systems, the optimum situation will rarely be attained. Another disadvantage of this PL technique is that the errors in the TOA estimate common to all receivers are not treated before the position location estimate.

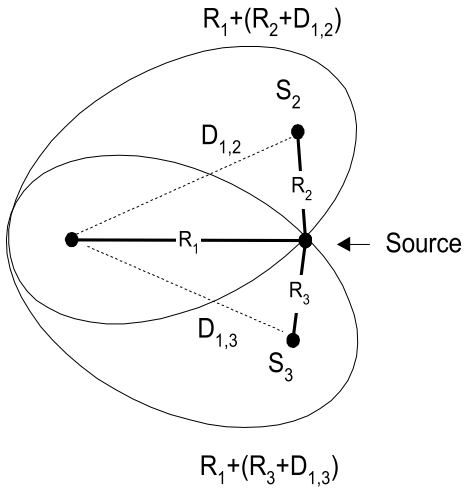

Figure 2.8: 2-D Elliptical Position Location Solution

2.2.4 Elliptical PL Systems

Elliptical PL systems locate a source by the intersection of ellipsoids describing the range sum measurements between multiple receivers. Figure 2.8 illustrates the 2-D solution of an elliptical location system. The range sum is determined from the sum of signal TOA's at multiple receivers. The relationship between range sum, $R_{i,j}$, and the TOA between receivers is given by

$$R_{i,j} = c\, d_{i,j} = R_i + R_j, \tag{2.17}$$

where c is the signal propagation speed and $d_{i,j}$ is the sum of TOA at receiver i and j. The range sum measurement restricts the possible source locations to a ellipsoid. The ellipsoids that describe the range sum between receivers is given by

$$R_{i,j} = \sqrt{(X_i - x)^2 + (Y_i - y)^2} + \sqrt{(X_j - x)^2 + (Y_j - y)^2}, \tag{2.18}$$

where (X_i, Y_i, Z_i) and (X_j, Y_j, Z_j) define the location of receiver i and j, and (x, y, z) is the position location estimate of the source. A source location can be uniquely determined by the intersection of three or more ellipsoids. Redundant range sum measurements can be made to improve the accuracy and resolve location solution ambiguities. This method offers the advantage of not requiring high precision clocks at the mobile. While there exist some systems that use this method, it appears that it offers no performance advantage over the spherical or hyperbolic configurations.

2.2.5 Hyperbolic PL Systems

Hyperbolic position location systems estimate the location of a source by the intersection of hyperboloids describing range difference measurements between three or more base stations. The range difference between two receivers is determined by measuring the difference in time of arrival of a signal between them. The relationship between range difference and the TDOA between receivers is given by

$$R_{i,j} = c\, d_{i,j} = R_i - R_j, \tag{2.19}$$

where c is the signal propagation speed and $d_{i,j}$ is the TDOA between receiver i and j. The TDOA estimate, in the absence of noise and interference, restricts the possible source locations to a hyperboloid of revolution with the receiver as the foci. Figure 2.9 illustrates a 2-D hyperbolic position location solution. In a 3-D system, the hyperboloids that describe the range difference, $R_{i,j}$, between receivers are given by

$$\begin{aligned} R_{i,j} &= \sqrt{(X_i - x)^2 + (Y_i - y)^2 + (Z_i - z)^2} \\ &\quad -\sqrt{(X_j - x)^2 + (Y_j - y)^2 + (Z_j - z)^2}, \end{aligned} \tag{2.20}$$

where (X_i, Y_i, Z_i) and (X_j, Y_j, Z_j) define the location of receiver i and j respectively, $R_{i,j}$ is the range difference measurement between base station i and j, and (x, y, z) are the unknown coordinates of the source. If the number of unknowns, or coordinates of the source to be determined, is equal to the number of equations, or range difference measurements, then the system is consistent and a unique solution exist. However, if redundant range difference measurements are made, then the system may be inconsistent and a unique solution may or may not exist. In this situation, some error criteria must be selected for determining the optimum solution to the system of equations.

If the source and receivers are coplanar, two dimensional (2-D) source location can be estimated from the intersection of two or more hyperboloids produced from three or more TDOA measurements, resulting in a hyperbolic trilateration solution. Three dimensional (3-D) source location estimation is produced by the intersection of three or more independently generated hyperboloids generated from four or more TDOA measurements, resulting in a hyperbolic multilateration solution.

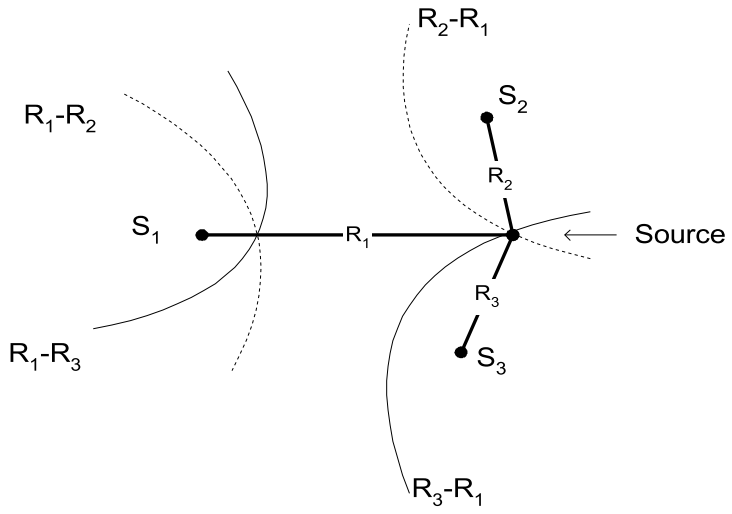

Figure 2.9: 2-D Hyperbolic Position Location Solution

If the hyperbola determined from multiple receivers intersects at more than one point, then ambiguity in the estimated position exists. This location ambiguity may be resolved by using a priori information about the source location, bearing measurements at one or more of the stations, or redundant range difference measurements at additional base station to generate additional hyperbolas.

A major advantage of this TDOA method is that it does not require knowledge of the transmit time from the source, as do TOA methods. Consequently, strict clock synchronization between the source and receiver is not required. As a result, hyperbolic position location techniques do not require additional hardware or software implementation within the mobile unit. However, clock synchronization is required of all receivers used for the PL estimate. Furthermore, unlike TOA methods, the hyperbolic position location method is able to reduce or eliminate common errors experienced at all receivers due to the channel.

2.3 Hyperbolic versus DF PL Systems

The two most commonly used PL techniques are direction finding (DF) and hyperbolic methods. While DF systems exploit the relative phase differences between closely spaced antenna elements and employ phase-alignment methods for beam/null steering to estimate the direction of arrival (DOA) of the signal of interest, hyperbolic methods exploit the relative time differences of a signal arriving at different receivers.

The requirements on accuracy and spatial resolution capabilities of array-based DF methods become more stringent as the distance between the sources and the receiving platform increases, since this decreases the differences between DOA's of the sources at the platform. In contrast, the requirements for accuracy and temporal resolution capabilities of time difference of arrival (TDOA) based methods become less stringent as the relative distance between base stations and the source increases, since this increases the TDOA between them.

The need for high resolution arises primarily when closely spaced sources give rise to multiple received signals that cannot be separated by preprocessing methods before the PL estimate is made. For instance, when cross correlating TDOA's of multiple signals that are not separated by more than the widths of their cross-correlation peaks, the peak cross correlation of the signal of interest usually cannot be resolved with conventional TDOA-based methods. To minimize this problem, the distance between platforms is typically made as large as possible to minimize overlap of adjacent peaks. This presents a fundamental resolution-limit problem for TDOA estimation of two closely spaced sources. The best performing array-based DF methods attempt to resolve the resolution problem in locating multiple signal sources by simultaneously estimating multiple DOA's rather than estimating the DOA of each signal as is commonly done by conventional beamformers and TDOA-based techniques.

Although DF techniques offer greater spatial resolution and the ability to simultaneously locate a number of signals, their complexity is typically much higher than that of TDOA techniques. They tend to be more complex because of the need for measurement, storage and usage of large amounts of array calibration data, with some exceptions such as the ESPRIT algorithm [Roy89], and because of the computationally intensive algorithms [Zis88]. The tradeoff between these systems is the highly

complexity high-resolution array-based DF methods and the simplicity of TDOA-based methods that require widely separated base stations.

2.4 GPS versus Terrestrial Position Location

The most widely known position location system is the Global Positioning System (GPS). The GPS is a satellite-based psuedo-ranging position location system that provides geolocation of user's with GPS receivers. The GPS is a proven technology that has found widespread use in military and navigation applications. It can reportedly provide position location accuracy's of less than 10 meters to military user's and 100 meters to commercial user's. A differential GPS (DGPS) has been developed that can improve the PL accuracy of the commercial operation. Although GPS has found wide acceptance in these application, the use of GPS for the geolocation of mobile user's within cellular and PCS system is limited.

First, while GPS provides accurate PL information for users within open and unobstructed areas, it has limited operation within urban and shadowed environments. The GPS requires at least three satellites to be in communication with the GPS receiver to provide 2-D position location for the user. Satellite blockage due to man-made or natural structures within urban and shadowed environments can render GPS inoperable. If universal position location coverage is to be provided, a position location system will have to be able to geolocate user's within these areas. Consequently, the existing terrestrial cellular infrastructure, which was designed to provide coverage of these regions, is ideal for the geolocation for mobile user.

Most importantly, use of GPS for the geolocation of mobile user's would require a mobile user to have a GPS receiver. At the present time, GPS receivers are not cheap enough or small enough to be incorporated into a mobile phone. Even if they were, mobile phone manufacturers may hesitate to include GPS receivers because of the added weight, size, power consumption and cost. Furthermore, use of GPS would require the retrofitting of the millions of existing cellular/PCS mobile phones. This is not a feasible alternative. A GPS receiver can be bought as a separate unit and interfaced with a mobile phone, however, this would add additional cost to the user.

2.5 Chapter Summary

Code division multiple access systems offer many advantages over existing cellular/PCS air interfaces. Multipath and multiple access interference rejection, narrowband interference suppression and capacity improvements offered by the CDMA air interface make it a favorable choice for cellular and PCS systems. However, position location of a mobile user within a CDMA system poses some unique challenges. Although the PN sequence used in CDMA systems, similar to that used in GPS, does offer the ability to provide high resolution position location estimation, multipath and shadowing experienced in mobile radio environments, the power control operation required of CDMA systems and the base station configuration present limitations to the effectiveness of position location systems.

Direction finding and range-based RF PL systems have been the most widely used position location techniques. Each method offers unique advantages and disadvantages to the geolocation of mobile user's. Direction finding systems can provide accurate PL estimation, however, they are usually very complex and are susceptible to multipath environments. Ranging PL systems require additional hardware or software within the mobile phone, and encounter ambiguity problems. Elliptical PL systems do not offer any advantage over ranging or hyperbolic PL systems. The hyperbolic PL technique has been the most widely used method for the geolocation of mobile user's. Hyperbolic PL systems do not require implementation within the mobile phone, are able to provide unambiguous PL solutions and can reduce the effect of errors introduced by noise that is common to all receivers. While each systems offers advantages and disadvantages, hyperbolic position location systems are more effective in combating the elements associated with mobile radio channels.

The Global Positioning System is an effective position location system. However, because GPS receivers are required in order to make use of GPS services, its use for the PL of mobile user's does not appear to be a feasible alternative at this time. Furthermore, coverage within urban and shadowed is limited because of satellite blockage. Consequently, a terrestrial PL system which utilizes the existing cellular/PCS infrastructure offers the advantages or not requiring a GPS receiver within the mobile unit and providing coverage where the satellite-based GPS system cannot.

Chapter 3

Hyperbolic Position Location Systems

3.1 Introduction

This chapter introduces the general models for the position location problem and the techniques involved in the hyperbolic position location method. Hyperbolic position location (PL) estimation is accomplished in two stages. The first stage involves estimation of the time difference of arrival (TDOA) between receivers through the use of time delay estimation techniques. The estimated TDOA's are then transformed into range difference measurements between base stations, resulting in a set of nonlinear hyperbolic range difference equations. The second stage utilizes efficient algorithms to produce an unambiguous solution to these nonlinear hyperbolic equations. The solution produced by these algorithms result in the estimated position location of the source. The following sections introduce the techniques and algorithms used to perform hyperbolic position location of a mobile user.

3.2 TDOA Estimation Techniques

The time difference of arrival (TDOA) of a signal can be estimated by two general methods: subtracting TOA measurements from two base stations to produce a relative TDOA, or through the use of cross-correlation techniques, in which the received signal at one base station is correlated with the received signal at another base station. The former method requires knowledge of the transmit timing, and thus, strict clock synchronization between the base stations and source. To eliminate the need for knowledge of the source transmit timing, differencing of arrival times at the receivers is commonly employed. Differencing the observed time of arrival eliminates some of the errors in TOA estimates common to all receivers and reduces other errors because of spatial and temporal coherence. While determining the TDOA from TOA estimates is a feasible method, cross-correlation techniques dominate the field of TDOA estimation techniques. As such, the discussion of TDOA estimation is limited to cross-correlation estimation techniques. In the following section, a general model for TDOA estimation is developed and the techniques for TDOA estimation are presented.

3.2.1 General Model for TDOA Estimation

For a signal, $s(t)$, radiating from a remote source through a channel with interference and noise, the general model for the time-delay estimation between received signals at two base stations, $x_1(t)$ and $x_2(t)$, is given by

$$\begin{aligned} x_1(t) &= A_1 s(t - d_1) + n_1(t) \\ x_2(t) &= A_2 s(t - d_2) + n_2(t), \end{aligned} \tag{3.1}$$

where A_1 and A_2 are the amplitude scaling of the signal, $n_1(t)$ and $n_2(t)$ consist of noise and interfering signals and d_1 and d_2 are the signal delay times, or arrival times. This model assumes that $s(t)$, $n_1(t)$ and $n_2(t)$ are real and jointly stationary, zero-mean (time average) random processes and that $s(t)$ is uncorrelated with noise $n_1(t)$ and $n_2(t)$. Referring the delay time and scaling amplitudes to the receiver with the shortest time of arrival, assuming $d_1 < d_2$, the model of (3.1) can be rewritten as

$$\begin{aligned} x_1(t) &= s(t) + n_1(t) \\ x_2(t) &= As(t - D) + n_2(t), \end{aligned} \tag{3.2}$$

where A is the amplitude ratio and $D = d_2 - d_1$. It is desired to estimate D, the time difference of arrival (TDOA) of $s(t)$ between the two receivers. It may also be desirable to estimate the scaling amplitude A. By estimating the amplitude scaling, selection of the appropriate receivers can be made. It follows that the limit cyclic cross-correlation and autocorrelations are given by

$$\begin{aligned} R^{\alpha}_{x_2x_1}(\tau) &= AR^{\alpha}_s(\tau - D)e^{-j\pi\alpha D} + R^{\alpha}_{n_2n_1}(\tau) && (3.3)\\ R^{\alpha}_{x_1}(\tau) &= R^{\alpha}_s(\tau) + R^{\alpha}_{n_1}(\tau) && (3.4)\\ R^{\alpha}_{x_2}(\tau) &= |A|^2R^{\alpha}_s(\tau)e^{-j\pi\alpha D} + R^{\alpha}_{n_2}(\tau), && (3.5) \end{aligned}$$

where the parameter α is called the cycle frequency [Gar92a]. If $\alpha = 0$, the above equations are the conventional limit cross-correlation and autocorrelations.

If $s(t)$ exhibits a cycle frequency α not shared by $n_1(t)$ and $n_2(t)$, then by using this values of α in the measurements in (3.3)-(3.5), we obtain through infinite time averaging

$$R^{\alpha}_{n_1}(\tau) = R^{\alpha}_{n_2}(\tau) = R^{\alpha}_{n_2n_1}(\tau) = 0 \quad (3.6)$$

and the general model for time delay estimation between base stations is

$$\begin{aligned} R^{\alpha}_{x_2x_1}(\tau) &= AR^{\alpha}_s(\tau - D)e^{-j\pi\alpha D} && (3.7)\\ R^{\alpha}_{x_1}(\tau) &= R^{\alpha}_s(\tau) && (3.8)\\ R^{\alpha}_{x_2}(\tau) &= |A|^2R^{\alpha}_s(\tau)e^{-j\pi\alpha D}. && (3.9) \end{aligned}$$

Accurate TDOA estimation requires the use of time delay estimation techniques that provide resistance to noise and interference and the ability to resolve multipath signal components. Many techniques have been developed that estimate TDOA D with varying degrees of accuracy and robustness. These include the generalized cross-correlation (GCC) and cyclostationarity-exploiting cross-correlation methods. Cyclostationarity-exploiting methods include the Cyclic Cross-Correlation (CYCCOR), the Spectral-Coherence Alignment (SPECCOA) method, the Band-Limited Spectral Correlation Ratio (BL-SPECCORR) method and the Cyclic Prony method [Gar94]. While signal selective cyclostationarity-exploiting methods have been shown in [Gar94] and [Gar92b] to outperform GCC methods in the presence of noise and interference, they do so only when spectrally overlapping noise and interference exhibit a cycle frequency different than the signal of interest. When spectrally overlapping

signals exhibit the same cycle frequency, as is encountered in multiuser CDMA systems, these methods do not offer an advantage over GCC methods. As such, only generalized cross-correlation methods for TDOA estimation are presented.

3.2.2 Generalized Cross-Correlation Methods

Conventional correlation techniques that have been used to solve the problem of TDOA estimation are referred to as generalized cross-correlation (GCC) methods. These methods have been explored in [Gar92a], [Gar92b], [Kna76], [Car87], [Rot71], [Hah73] and [Hah75]. These GCC methods cross-correlate prefiltered versions of the received signals at two receiving stations, then estimate the TDOA D between the two stations as the location of the peak of the cross-correlation estimate. Prefiltering is intended to accentuate frequencies for which high signal-to-noise (SNR) is highest and attenuate the noise power before the signal is passed to the correlator.

Generalized cross-correlation methods for TDOA estimation are based on (3.7) with $\alpha = 0$ [Gar92a]. Thus (3.7) is rewritten as

$$R^0_{x_2x_1}(\tau) = AR^0_s(\tau - D). \tag{3.10}$$

The argument τ that maximizes (3.10) provides an estimate of the TDOA D. Equivalently, (3.10) can be written as

$$R_{x_2x_1}(\tau) = R^0_{x_2x_1}(\tau) = \int_{-\infty}^{\infty} x_1(t)x_2(t-\tau)dt. \tag{3.11}$$

However, $R_{x_2x_1}(\tau)$ can only be estimated from a finite observation time. Thus, an estimate of the cross-correlation is given by

$$\hat{R}_{x_2x_1}(\tau) = \frac{1}{T}\int_0^T x_1(t)x_2(t-\tau)dt, \tag{3.12}$$

where T represents the observation interval. Equation (3.12) is based on the use of an analog correlator. An integrate and dump correlation receiver of this form is one realization of a matched filter receiver [Zie85]. The correlation process can also be implemented digitally if sufficient sampling of the waveform is used. The output of a discrete correlation process using digital samples of the signal is given by

$$\hat{R}_{x_2x_1}(m) = \frac{1}{N}\sum_{n=0}^{N-|m|-1} x_1(n)x_2(n+m)dt. \tag{3.13}$$

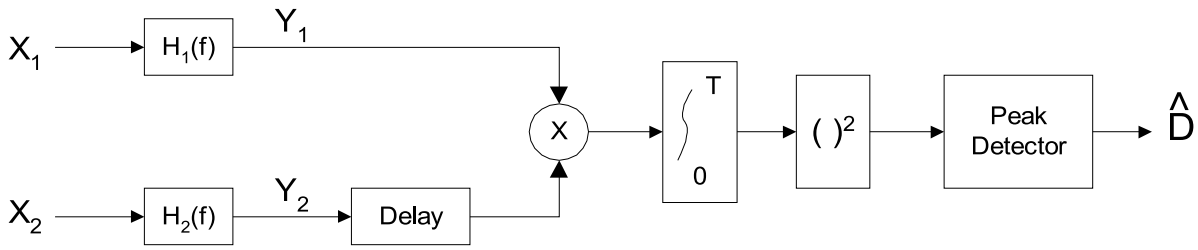

Figure 3.1: Generalized Cross-Correlation Method for TDOA Estimation

The cross-power spectral density function, $G_{x_2x_1}(f)$, related to the cross-correlation of $x_1(t)$ and $x_2(t)$ in (3.12) is given by

$$R_{x_2x_1}(\tau) = \int_{-\infty}^{\infty} G_{x_2x_1}(f)e^{j\pi f\tau}df \tag{3.14}$$

or

$$G_{x_2x_1}(f) = \int_{-\infty}^{\infty} R_{x_2x_1}(\tau)e^{-j\pi f\tau}dt. \tag{3.15}$$

As before, because only a finite observation time of $x_1(t)$ and $x_2(t)$ is possible, only an estimate $\hat{G}_{x_2x_1}(f)$ of $G_{x_2x_1}(f)$ can be obtained.

In order to improve the accuracy of the delay estimate, filtering of the two signals is performed before integrating in (3.12). As shown in Figure 3.1, each signal $x_1(t)$ and $x_2(t)$ is filtered through $H_1(f)$ and $H_2(f)$, then correlated, integrated and squared. This is performed for a range of time shifts, τ, until a peak correlation is obtained. The time delay causing the cross-correlation peak is an estimate of the TDOA $\hat{D}$. If the correlator is to provide an unbiased estimate of TDOA D, the filters must exhibit the same phase characteristics and hence are usually taken to be identical filters [Hah73].

When $x_1(t)$ and $x_2(t)$ are filtered, the cross-power spectrum between the filtered outputs is given by

$$G_{y_2y_1}(f) = H_1(f)H_2^*(f)G_{x_2x_1}(f), \tag{3.16}$$

where $*$ denotes the complex conjugate. Therefore, the generalized cross-correlation, specified by superscript G, between $x_1(t)$ and $x_2(t)$ is

$$R_{y_2y_1}^G(\tau) = \int_{-\infty}^{\infty} \Psi_G(f)G_{x_2x_1}(f)e^{j\pi f\tau}df, \tag{3.17}$$

where

$$\Psi_G(f) = H_1(f)H_2^*(f) \tag{3.18}$$

and denotes the general frequency weighting, or filter function. Because only an estimate of $R^G_{y_2y_1}(\tau)$ can be obtained, (3.17) is rewritten as

$$\hat{R}^G_{y_2y_1}(\tau) = \int_{-\infty}^{\infty} \Psi_G(f)\hat{G}_{x_2x_1}(f)e^{j\pi f\tau}df, \tag{3.19}$$

which is used to estimate the TDOA D. The GCC methods use filter functions $\Psi_G(f)$ to minimize the effect of noise and interference.

The choice of the frequency function, $\Psi_G(f)$, is very important, especially when the signal has multiple delays resulting from a multipath environment. Consider the optimal case in which $n_1(t)$ and $n_2(t)$ are uncorrelated and only one signal delay is present. The cross-correlation of $x_1(t)$ and $x_2(t)$ in (3.10) can be rewritten as

$$R^0_{x_2x_1}(\tau) = AR^0_s(\tau) \otimes \delta(t - D), \tag{3.20}$$

where $\otimes$ denotes a convolution operation. Equation (3.20) can be interpreted as the spreading of a delta function at D by the inverse Fourier transform of the signal spectrum. When the signal experiences multiple delays due to a multipath environment, the cross-correlation can be represented as

$$R_{x_2x_1}(0) = R^0_s(\tau) \otimes \sum_i A_i\delta(t - D_i). \tag{3.21}$$

If the delays of the signal are not sufficiently separated, the spreading of the one delta function will overlap another, thereby making the estimation of the peak and TDOA difficult if not impossible. The frequency function $\Psi_G(f)$ can be chosen to ensure a large peak in the cross-correlation $x_1(t)$ and $x_2(t)$, resulting in a narrower spectra and better TDOA resolution. However, in doing so, the peaks are more sensitive to errors introduced by the finite observation time, especially in cases of low signal to noise ratio (SNR). Thus the choice of $\Psi_G(f)$ is a compromise between good resolution and stability [Kna76].

Several frequency functions, or processors, have been proposed to facilitate the estimate of $\hat{D}$. When the filters $H_1(f) = H_2(f) = 1$, $\forall(f)$, then $\Psi_G(f) = 1$, and the estimate $\hat{G}$ is simply the delay abscissa at which the cross-correlation peaks. This is considered cross-correlation processing. Other processors include the Roth Impulse

Table 3.1: GCC Frequency Functions

Processor Name	**Frequency Function $\Psi_G(f)$**
Cross-correlation	1
Roth Impulse Response	$1/G_{x_1x_1}(f)$ or $1/G_{x_2x_2}(f)$
Smoothed Coherence Transform	$1/\sqrt{G_{x_1x_1}(f)G_{x_2x_2}(f)}$
Eckart	$G_{s_1s_1}(f)/[G_{n_1n_1}(f)G_{n_2n_2}(f)]$
Hannon-Thomson or Maximum Likelihood	$\frac{\lvert\gamma_{x_1x_2}(f)\rvert^2}{\lvert G_{x_1x_2}(f)\rvert[1-\lvert\gamma_{x_1x_2}(f)\rvert^2]}$

Response processor [Rot71], the Smoothed Coherence Transform (SCOT) [Car73], the Eckart filter [Kna76],[Hah73], and the Hannan-Thomson (HT) processor or Maximum Likelihood (ML) estimator [Han73]. A list of GCC frequency functions is provided in Table 3.1

The Roth Impulse Response processor has the desirable effect of suppressing the frequency regions in which power spectral noise density, $G_{n_1n_1}(f)$ or $G_{n_2n_2}(f)$, is large and the estimate of the cross power spectral signal density, $\hat{G}_{x_1x_2}(f)$, is likely to be in error. However, the Roth processor does not minimize the spreading effect of the delta function whenever the power spectral noise density is not equal to some constant times the power spectral density of the signal, $G_{s_1s_1}(f)$ [Kna76]. Furthermore, one is uncertain as to whether the errors in $\hat{G}_{x_1x_2}(f)$ are due to frequency bands in which $G_{n_1n_1}(f)$ or $G_{n_2n_2}(f)$ large.

The uncertainty with the Roth processor led to the development of the proposed Smoothed Coherence Transform (SCOT). The SCOT processor suppresses frequency bands of high noise and assigns zero weight to bands where $G_{s_1s_1}(f) = 0$. The SCOT frequency function is given as

$$\Psi_S(f) = 1/\sqrt{G_{x_1x_1}(f)G_{x_2x_2}(f)}. \tag{3.22}$$

This results in the cross-correlation

$$R^S_{y_2y_1}(\tau) = \int_{-\infty}^{\infty} \hat{\gamma}_{x_1x_2}(f)e^{j\pi f\tau}df, \tag{3.23}$$

where

$$\hat{\gamma}_{x_1x_2}(f)\hat{=}\frac{\hat{G}_{x_1x_2}(f)}{\sqrt{G_{x_1x_1}(f)G_{x_2x_2}(f)}} \tag{3.24}$$

is the coherence estimate [Kna76]. The SCOT processor assigns weighting according to signal-to-noise (SNR) characteristics. In terms of the noise characteristics, [Hah73] realizes the SCOT as

$$|\Psi_S(f)|^2 = 1/N. \tag{3.25}$$

The SCOT frequency function, for which $H_1(f) = 1/\sqrt{G_{x_1x_1}(f)}$ and $H_2(f) = 1/\sqrt{G_{x_2x_2}(f)}$, can be interpreted as a prewhitening process. If $G_{x_1x_1}(f) = G_{x_2x_2}(f)$, then the SCOT filter is equivalent to the Roth filter. Consequently, the SCOT still produces the same broadening as the Roth function [Kna76].

The Eckart processor, similarly to the SCOT processor, suppresses frequency bands of high noise and assigns zero weight to bands where $G_{s_1s_1}(f) = 0$. The Eckart frequency function maximizes the ratio of the change in mean correlator output to the standard deviation of the correlator output due to the noise alone [Kna76]. For the model given by (3.2) and $n_1(t)$ and $n_2(t)$ having the same spectra, the Eckart frequency function in terms of the SNR characteristics is given by [Hah73] as

$$|\Psi_E(f)|^2 = S/N^2. \tag{3.26}$$

In practice, the Eckart filter requires knowledge of the signal and noise spectra [Kna76].

The previously described frequency functions have been shown to be suboptimal by [Hah73]. The HT processor, which is equivalent to a ML estimator, has been shown to be the optimal processor by [Hah73] and [Kna76]. The HT frequency function is given by

$$\Psi_{HT}(f) = \frac{|\gamma_{x_1x_2}(f)|^2}{|G_{x_1x_2}(f)|[1-|\gamma_{x_1x_2}(f)|^2]}, \tag{3.27}$$

where $|\gamma_{x_1x_2}(f)|^2$ is the magnitude-squared coherence [Car81]. For the model in (3.2) and $n_1(t)$ and $n_2(t)$ having the same spectra, the HT frequency function in terms of the SNR characteristics is given as

$$|\Psi_{HT}(f)|^2 = \frac{S/N^2}{1+2(S/N)}. \tag{3.28}$$

For low SNR, it has been shown in [Kna76] that the Eckart function is equivalent to the HT frequency function.

These GCC TDOA estimation methods have been shown to effective in reducing the effects of noise and interference [Gar92b]. However, if the noise and interference $n_1(t)$ and $n_2(t)$ in (3.2) are both temporally and spectrally coincident with $s(t)$, there is little that GCC methods can do to reduce the undesirable effects of this interference. In this situation, generalized cross-correlation methods encounter two problems. First, GCC methods experience a resolution problem. These GCC methods require the differences in the TDOAs for each signal to be greater than the widths of the cross-correlation functions so that the peaks can be resolved. Consequently, if the TDOAs are not sufficiently separated, the overlapping of cross correlations can introduce significant errors in the TDOA estimate. Second, if $s(t)$, $n_1(t)$ and $n_2(t)$ are resolvable, conventional GCC methods must still identify which of the multiple peaks is due to the signal of interest and interference. These problems arise because GCC methods are not signal selective and produce TDOA peaks for all signals in the received data unless they are spectrally disjoint and can be filtered out [Gar94].

3.2.3 Measures of TDOA Estimation Accuracy

The Cramér-Rao Lower Bound (CRLB) on the variance of an unbiased estimator is the standard benchmark against which conventional TDOA estimation methods are evaluated. The derivation of the CRLB is given in [Kna76]. The CRLB typically used is for evaluating stationary Gaussian signals in stationary Gaussian noise environments [Gar92b]. However, the BPSK PN signaling used in CDMA systems exhibit fundamental periodocities in the chip period, data period and PN code repetition period. The signal is therefore nonstationary (cyclostationary) and thus cannot be appropriately evaluated by the typical CRLB. Although the CRLB for nonstationary signals exist, it is very difficult to evaluate.

3.3 Hyperbolic Position Location Estimation

Accurate position location (PL) estimation of a source requires an efficient hyperbolic position location estimation algorithm. Once the TDOA information has been acquired, the hyperbolic PL algorithm will be responsible for producing an accurate and unambiguous solution to the position location problem. Many processing algorithms, with different complexity and restrictions, have been proposed for position location estimation based on TDOA estimates.

When base stations are placed in a linear fashion relative to the source, the estimation of the PL is simplified. Carter's beamforming method provides an exact solution for the source range and bearing [Car81]. However, it requires am extensive search over a set of possible source locations, which can become computationally intensive. Hahn's method estimates the source range and bearing from the weighted sum of ranges and bearings obtained from the TDOA's of every possible combination. This method is very sensitive to the choice of weights, which can be very complicated in obtaining, and is only valid for distant sources [Hah73]-[Hah75]. Abel and Smith provide an explicit solution that can achieve the Cramér-Rao Lower Bound (CRLB) in the small error region [Abe89].

When the base stations are placed arbitrarily relative to the source, which is typical scenario of a mobile unit within the infrastructure of a cellular/PCS system, the position fix becomes more complex. In this situation, the position location of a source is determined from the intersection of hyperbolic curves produced from the TDOA estimates. The set of equations that describe these hyperbolic curves are nonlinear and are not easily solved. If the set of nonlinear hyperbolic equations equals the number of unknown coordinates of the source, then the system is consistent and a unique solution can be determined from iterative techniques. For an inconsistent system, in which redundant range difference measurements are made, the problem of solving for the position location of the source becomes more difficult because no unique solution exists.

While direct nonlinear solutions to the inconsistent system can provide accurate results, they tend to be very computationally intensive. Consequently, linearization of

these equations is commonly used to simplify the computation of the position location solution. One method of linearizing the equations is by Taylor-series expansion and retaining the first two terms. Other methods have also been used. For most situations, linearization of the nonlinear equations of ranging PL system does not introduce undue errors in the position location estimate. However, linearization can introduce significant errors when determining a PL solution in bad geometric dilution of precision (GDOP) situations. It has been shown by Bancroft [Ban85] that eliminating the second order terms can lead to significant errors in this situation. The effect of linearization of hyperbolic equations on the position location solution is also explored by Nicholson in [Nic73] and [Nic76].

For an inconsistent system of equations, some error criteria must be determined for selecting an optimum solution. Classical techniques for solving these equations include the Least Squares (LS) and Weighted Least Squares (WLS) methods. These techniques can achieve the Maximum Likelihood (ML) estimate which maximizes the probability that a particular position estimate is the true position location. If the range difference errors are uncorrelated and Gaussian distributed with zero mean and equal variances then the LS solution provides the ML estimate [Sta94]. If the variances are unequal then the WLS solution is the ML estimate. The WLS utilizes weighting coefficients inversely proportional to the variances of the range difference estimates. However, a problem exists because the variances are either not known a priori or difficult to estimate.

For arbitrarily placed base stations and a consistent system of equations, Fang provides an exact solution to the nonlinear equations [Fan90]. For arbitrarily distributed base stations and redundant TDOA estimates, the spherical-intersection (SX) [Sch87], spherical-interpolation (SI) [Fri87], [Smi87a], [Smi87b], [Abe87], Divide and Conquer (DAC) [Abe90], Chan's method [Cha94] and the Taylor Series [Foy76], [Tor84] methods can be used. The Taylor Series estimation method provides a more accurate solution, even at reasonable TDOA noise levels, than the other methods but is also more computationally intensive. Consequently, a tradeoff between position location accuracy and computational requirements exists.

3.3.1 General Model for Hyperbolic PL Estimation

A general model for the two dimensional (2-D) PL estimation of a source using M base stations is developed. Referring all TDOA's to the first base station, which is assumed to be the base station controlling the call and first to receive the transmitted signal, let the index $i = 2, \ldots, M$, unless otherwise specified, (x, y) be the source location and (X_i, Y_i) be the known location of the ith receiver. The squared range distance between the source and the ith receiver is given as

$$\begin{aligned} R_i &= \sqrt{(X_i - x)^2 + (Y_i - y)^2} \\ &= \sqrt{X_i^2 + Y_i^2 - 2X_i x - 2Y_i y + x^2 + y^2}. \end{aligned} \tag{3.29}$$

The range difference between base stations with respect to the first arriving base station is

$$\begin{aligned} R_{i,1} &= c\, d_{i,1} = R_i - R_1 \\ &= \sqrt{(X_i - x)^2 + (Y_i - y)^2} - \sqrt{(X_1 - x)^2 + (Y_1 - y)^2}, \end{aligned} \tag{3.30}$$

where c is the signal propagation speed, $R_{i,1}$ is the range difference distance between the first base station and the ith base station, R_1 is the distance between the first base station and the source, and $d_{i,1}$ is the estimated TDOA between the first base station and ith base station. This defines the set of nonlinear hyperbolic equations whose solution gives the 2-D coordinates of the source.

Solving the nonlinear equations of (3.30) is difficult. Consequently, linearizing this set of equations is commonly performed. One way of linearizing these equations is through the use of Taylor-series expansion and retaining the first two terms [Foy76] [Tor84]. An commonly used alternative method to the Taylor-series expansion method, presented in [Fri87], [Sch87], [Smi87a] and [Abe87], is to first transform the set of nonlinear equations in (3.30) into another set of equations. Rearranging the form of (3.30) into

$$R_i^2 = (R_{i,1} + R_1)^2, \tag{3.31}$$

equation (3.29) now can be rewritten as

$$R_{i,1}^2 + 2R_{i,1}R_1 + R_1^2 = X_i^2 + Y_i^2 - 2X_i x - 2Y_i y + x^2 + y^2. \tag{3.32}$$

Subtracting (3.29) at i = 1 from (3.32) results in

$$R_{i,1}^2 + 2R_{i,1}R_1 = X_i^2 + Y_i^2 - 2X_{i,1}x - 2Y_{i,1}y + x^2 + y^2, \tag{3.33}$$

where $X_{i,1}$ and $Y_{i,1}$ are equal to $X_i - X_1$ and $Y_i - Y_1$ respectively. The set of equations in (3.33) are now linear with the source location (x, y) and the range of the first receiver to the source R_1 as the unknowns, and are more easily handled.

3.3.2 Hyperbolic Position Location Algorithms

For arbitrarily placed base stations and a consistent system of equations in which the number of equations equals the number of unknown source coordinates to be solved, Fang [Fan90] provides an exact solution to the equations of (3.33). For a 2-D hyperbolic PL system using three base stations to estimate the source location (x, y), Fang establishes a coordinate system so that the first base station (BS) is located at $(0, 0)$, the second BS at $(x_2, 0)$ and the third BS at (x_3, y_3). Realizing that for the first BS, where $i = 1$, $X_1 = Y_1 = 0$, and for the second BS, where $i = 2$, $Y_2 = 0$, the following relationships are simplified

$$\begin{aligned} R_1 &= \sqrt{(X_1 - x)^2 + (Y_1 - y)^2} = \sqrt{x^2 + y^2} \\ X_{i,1} &= X_i - X_1 = X_i \\ Y_{i,1} &= Y_i - Y_1 = Y_i. \end{aligned}$$

Using these relationships, the equation of (3.33) can be rewritten as

$$\begin{aligned} 2R_{2,1}R_1 &= R_{2,1}^2 - X_i^2 + 2X_{i,1}x \\ 2R_{3,1}R_1 &= R_{3,1}^2 - (X_3^2 + Y_3^2) + 2X_{3,1}x + 2Y_{3,1}y. \end{aligned} \tag{3.34}$$

Equating the two equations (3.34) and simplifying results in

$$y = g * x + h, \tag{3.35}$$

where

$$\begin{aligned} g &= \{R_{3,1} - (X_2/R_{2,1}) - X_3\}/Y_3 \\ h &= \{X_3^2 + Y_3^2 - R_{3,1}^2 + R_{3,1} * R_{2,1}(1 - (X_2/R_{2,1})^2)\}/2Y_3. \end{aligned}$$

Substituting equation (3.35) into the first equation in (3.34) results in

$$d * x^2 + e * x + f = 0, \tag{3.36}$$

where

$$\begin{aligned} d &= -\{(1 - (X_2/R_{2,1})^2) + g\} \\ e &= X_2 * \{(1 - (X_2/R_{2,1})^2)\} - 2g * h \\ f &= -(R_{2,1}^2/4) * \{(1 - (X_2/R_{2,1})^2)\}^2 - h^2. \end{aligned}$$

Fang's method provides an exact solution, however, his solution does not make use of redundant measurements made at additional receivers to improve position location accuracy. Furthermore, his method experiences an ambiguity problem due to the inherent squaring operation. These ambiguities can be resolved using a priori information or through use of symmetry properties.

To obtain a precise position estimate at reasonable noise levels, the Taylor-series method [Foy76], [Tor84] can be employed. The Taylor-series method linearizes the set of equations in (3.30) by Taylor-series expansion then uses an iterative method to solve the system of linear equations. The iterative method begins with an initial guess and improves the estimate at each iteration by determining the local linear least-square (LS) solution. With a set of TDOA estimates, the method starts with an initial guess (x_0, y_0) and computes the deviations of the position location estimation

$$\begin{bmatrix} \Delta x \\ \Delta y \end{bmatrix} = (\mathbf{G}_t^T \mathbf{Q}^{-1} \mathbf{G}_t)^{-1} \mathbf{G}_t^T \mathbf{Q}^{-1} \mathbf{h}_t, \tag{3.37}$$

where

$$\mathbf{h}_t = \begin{bmatrix} R_{2,1} - (R_2 - R_1) \\ R_{3,1} - (R_3 - R_1) \\ \vdots \\ R_{M,1} - (R_M - R_1) \end{bmatrix}$$

$$\mathbf{G}_t = \begin{bmatrix} [(X_1 - x)/R_1] - [(X_2 - x)/R_2] & [(Y_1 - y)/R_1] - [(Y_2 - y)/R_2] \\ [(X_1 - x)/R_1] - [(X_3 - x)/R_3] & [(Y_1 - y)/R_1] - [(Y_3 - y)/R_3] \\ \vdots & \vdots \\ [(X_1 - x)/R_1] - [(X_M - x)/R_M] & [(Y_1 - y)/R_1] - [(Y_M - y)/R_M] \end{bmatrix},$$

and $\mathbf{Q}$ is the covariance matrix of the estimated TDOA's. The values R_i for $i = 1, 2, \ldots, M$ are computed from (3.29) with $x = x_0$ and $y = y_0$. In the next iteration, x_0 and y_0 are set to $x_0 + \Delta x$ and $y_0 + \Delta y$. The whole process is repeated until Δx and Δy are sufficiently small, resulting in the estimated PL of the source (x, y). This Taylor-series method can provide accurate results, however, it requires a close initial guess (x_0, y_0) to guarantee convergence and can be very computationally intensive.

Friedlander's method [Fri87] utilizes a Least Squares (LS) and Weighted LS (WLS) error criterion to solve for the position location [Fri87]. He first transforms the linear set of equations of (3.33) into

$$X_{i,1}x + Y_{i,1}y = \frac{1}{2}(X_i^2 + Y_i^2 - X_1^2 - Y_1^2 - R_{i,1}^2) - R_{i,1}R_1, \tag{3.38}$$

then realizes this equation in matrix form as

$$\mathbf{Sx} = \mathbf{u} - \mathbf{R}_1\mathbf{p}, \tag{3.39}$$

where

$$\mathbf{S} = \begin{bmatrix} X_{i,1} & Y_{i,1} \\ \vdots & \vdots \\ X_{M,1} & Y_{M,1} \end{bmatrix}$$

$$\mathbf{x} = [x \quad y]^T$$

$$\mathbf{u} = \frac{1}{2}\begin{bmatrix} X_i^2 + Y_i^2 - X_1^2 - Y_1^2 - R_{i,1}^2 & \\ \vdots & \vdots \\ X_M^2 + Y_M^2 - X_1^2 - Y_1^2 - R_{M,1}^2 & \end{bmatrix}$$

$$\mathbf{p} = [\mathbf{R}_{i,1} \ldots \mathbf{R}_{M,1}]^T.$$

In order to eliminate the second term of 3.39, which requires knowledge of the unknown term R_1, the equation in (3.39) is premultiplied by a matrix $\mathbf{N}$ which has $\mathbf{p}$ in its null-space. Matrix $\mathbf{N}$ is defined as

$$\mathbf{N} = (\mathbf{I} - \mathbf{Z})\mathbf{D}, \tag{3.40}$$

where

$$\mathbf{D} = (diag\{\mathbf{p}\})^{-1} = \begin{bmatrix} R_{i,1} & & & 0 \\ & \ddots & & \\ & & \ddots & \\ 0 & & & R_{M,1} \end{bmatrix}^{-1}$$

$$\mathbf{Z} = \begin{bmatrix} 0 & 1 & & \\ & \ddots & \ddots & \\ & & \ddots & 1 \\ 1 & & & 0 \end{bmatrix},$$

and $\mathbf{I}$ is an identity matrix. By using singular value decomposition (SVD) on $(\mathbf{I} - \mathbf{Z})$, Friedlander eliminates the unknown R_1 parameter. The SVD of $(\mathbf{I} - \mathbf{Z})$ is given as

$$(\mathbf{I} - \mathbf{Z}) = [\mathbf{U}_k, \mathbf{u}_k] \begin{bmatrix} \eta_1^k & & & 0 \\ & \ddots & & \\ & & \eta_{M-2}^k & \\ 0 & & & 0 \end{bmatrix} [\mathbf{V}_k, \mathbf{v}_k^T], \tag{3.41}$$

where $\{\eta_1^k, \ldots, \eta_{M-2}^k\}$ are the non-zero singular values. The matrix to eliminate the second term of (3.39) is then given by

$$\mathbf{N} = \mathbf{V}_k^T \mathbf{D}, \tag{3.42}$$

and a closed form solution for the coordinates of the source is found by solving

$$\mathbf{NSx} = \mathbf{Nu}, \tag{3.43}$$

which results in $(M-2)$ linear equations in x and y. The source position can then be computed using the LS solution. A closed form solution which can be used is given by Friedlander as

$$\mathbf{x} = (\mathbf{S}^T \mathbf{N}\mathbf{N}^T \mathbf{S})^{-1} \mathbf{S}^T \mathbf{N}\mathbf{N}^T \mathbf{u}. \tag{3.44}$$

Friedlander also uses the Weighted Least Squares (WLS) solution, which provides the ML estimate in the case of zero-mean Gaussian range difference noises with unequal variance. The optimal weighting matrix is given as

$$\mathbf{W} = \{\mathbf{N}(diag\{\mathbf{p}\} + R_1\mathbf{I})\mathbf{Q}(diag\{\mathbf{p}\} + R_1\mathbf{I})\mathbf{N}^T\}^{-1}, \tag{3.45}$$

where $\mathbf{Q}$ is the covariance matrix of the range difference equations. The weighting matrix $\mathbf{W}$ is a function of the unknown parameter R_1 , which can be estimated from

$$R_1 = \frac{\mathbf{p}^T \mathbf{P} \mathbf{u}}{\mathbf{p}^T \mathbf{P} \mathbf{p}}, \tag{3.46}$$

where

$$\mathbf{P} = \mathbf{I} - \mathbf{S}(\mathbf{S}^T \mathbf{S})^{-1} \mathbf{S}.$$

The resulting WLS solution is in the form

$$\mathbf{W}^{1/2}\mathbf{N}\mathbf{x} = \mathbf{W}^{1/2}\mathbf{N}\mathbf{u}, \tag{3.47}$$

which results in a position location estimation by

$$\mathbf{x} = (\mathbf{S}^T\mathbf{N}\mathbf{W}\mathbf{N}^T\mathbf{S})^{-1}\mathbf{S}^T\mathbf{N}\mathbf{W}\mathbf{N}^T\mathbf{u}. \tag{3.48}$$

Friedlander's simulation results indicated that, when using four base stations, the LS and WLS solutions were identical. However, for more than four base stations, the WLS PL solution outperformed the LS PL solution.

The spherical-intersection (SX) method [Sch87], [Smi87b] is another commonly used approach. It assumes that R_1 is known and solves x and y in terms of R_1 from (3.33). The least squares solution of (3.29) is then used to find the R_1 and hence x and y. Since R_1 is assumed to be constant in the first step, the degree of freedom to minimize the second norm of the error vector, ψ , used in the solution is reduced [Cha94]. The solution obtained is therefore suboptimal as demonstrated in [Smi87a] and [Abe87].

Another approach called the spherical-interpolation (SI) method [Abe87], [Smi87a], [Smi87b], first solves x and y in terms of R_1, then inserts the intermediate result back into (3.33) to generate equations in the unknown R_1 only. Substituting the computed R_1 values that minimizes the LS equation error to the intermediate result produces the final result. One drawback to the SI method is it inability to produce a solution if the number of unknowns is equal to the number of equations based on the TDOA estimates, which may occur in certain situations. The SI method was shown in [Smi87a] to provide an order of magnitude greater noise immunity than the SX method. Although the SI performs better than the SX method, it assumes that the three variables x, y and R_1 in (3.33) to be independent and eliminates R_1 from those equations. Consequently, the solution is suboptimal because this relationship is ignored. The method proposed by Friedlander and the SI method have be shown in [Fri87] to be mathematically equivalent.

A divide and conquer (DAC) method, proposed by Abel [Abe90], consists of dividing the TDOA measurements into groups, each having a size equal to the number of unknowns. Solution of the unknowns is calculated for each group, then appropriately combined to provide a final solution. Although this method can achieve optimum

performance, the solution uses stochastic approximation and requires that the Fisher information be sufficiently large. The Fisher information matrix (FIM) is the inverse of the Cramér-Rao Matrix Bound (CRMB)(i.e.(FIM)=$(CRMB)^{-1}$) [Hah75]. The estimator provides optimum performance when the errors are small, thus implying a low-noise threshold in which the method deviates from the CRLB. This method requires an equal number of range difference measurements in each group, and as a result, the TDOA estimates from the remaining sensors cannot be used to improve accuracy.

An non-iterative solution to the hyperbolic position estimation problem which is capable of achieving optimum performance for arbitrarily placed sensors was proposed by Chan [Cha94]. The solution is in closed-form and valid for both distant and close sources. When TDOA estimation errors are small, this method is an approximation to the maximum likelihood (ML) estimator. Chan's method performs significantly better than the SI method and has a higher noise threshold that the DAC method before the performance deviates from the Cramér-Rao lower bound. Furthermore, it provides an explicit solution form that is not available in the Taylor-series method.

Following Chan's method [Cha94], for a three base station system (M=3), producing two TDOA's, x and y can be solved in terms of R_1 from (3.33). The solution is in the form of

$$\begin{bmatrix}\Delta x\\ \Delta y\end{bmatrix} = -\begin{bmatrix} X_{2,1} & Y_{2,1}\\ X_{3,1} & Y_{3,1}\end{bmatrix}^{-1} \times \left\{ \begin{bmatrix}R_{2,1}\\ R_{3,1}\end{bmatrix} R_1 + \frac{1}{2}\begin{bmatrix} R_{2,1}^2 - K_2 + K_1\\ R_{3,1}^2 - K_3 + K_1\end{bmatrix}, \right\} \tag{3.49}$$

where

$$\begin{aligned} K_1 &= X_1^2 + Y_1^2\\ K_2 &= X_2^2 + Y_2^2\\ K_3 &= X_3^2 + Y_3^2. \end{aligned}$$

When (3.49) is inserted into (3.29), with $i = 1$, a quadratic equation in terms of R_1 is produced. Substituting the positive root back into (3.49) results in the final solution. There may exist two positive roots from the quadratic equation that can produce two different solutions, resulting in an ambiguity. This problem can be resolved by using a *priori* information. The answer to this method is the same as the spherical-intersection method (SX) given in [Sch87].

For four or more base stations, the PL system is overdetermined because there are more measurements of TDOA than the number of unknowns. The original set of nonlinear TDOA equations are transformed into another set of linear equations with an extra variable. A weighted linear LS provides an initial solution and a second weighted LS gives an improved position estimate through the use of the known constrain of the source coordinates and the extra variable. Letting $\mathbf{z}_a = [\mathbf{z}_p^T, R_1]^T$ be the unknown vector, where $\mathbf{z}_p = [x, y]^T$, the error vector ψ, with TDOA noise, derived from (3.33) is

$$\psi = \mathbf{h} - \mathbf{G}_a \mathbf{z}_a^0, \tag{3.50}$$

where

$$\mathbf{h} = \frac{1}{2} \begin{bmatrix} R_{2,1}^2 - X_2^2 - Y_2^2 + X_1^2 + Y_1^2 \\ R_{3,1}^2 - X_3^2 - Y_3^2 + X_1^2 + Y_1^2 \\ \vdots \\ R_{M,1}^2 - X_M^2 - Y_M^2 + X_1^2 + Y_1^2 \end{bmatrix}$$

$$\mathbf{G}_a = - \begin{bmatrix} X_{2,1} & Y_{2,1} & R_{2,1} \\ X_{3,1} & Y_{3,1} & R_{3,1} \\ \vdots & \vdots & \vdots \\ X_{M,1} & Y_{M,1} & R_{M,1} \end{bmatrix}.$$

Denoting the noise free value of $\{*\}$ as $\{*\}^0$, when $d_{i,j} = d_{i,j}^0 + n_{i,j}$ is used to express $R_{i,1}$ as $R_{i,1}^0 + cn_{i,1}$ and noting from (3.30) that $R_i^0 = R_{i,1}^0 + R_i^0$, the error vector ψ is found to be

$$\begin{aligned} \psi &= c\mathbf{B}\mathbf{n} + 0.5c^2 \mathbf{n} \odot \mathbf{n} \\ \mathbf{B} &= diag\{R_2^0, R_3^0, \ldots, R_M^0\}, \end{aligned} \tag{3.51}$$

where $\odot$ represents the Schur product. The TDOA estimates found by the general cross-correlation methods with Gaussian data is asymptotically normally distributed when the signal to noise (SNR) is high [Car81]. Consequently, the noise vector $\mathbf{n}$ is also asymptotically normal and the covariance matrix of the error vector can be evaluated. In practice, the condition $cn_{i,1} \ll R_i^0$ is usually satisfied and the second term on the right of (3.51) can be ignored. Therefore, the error vector ψ becomes a Gaussian random vector with covariance matrix given by

$$\mathbf{\Psi} = \mathbf{E}[\psi\psi^T] = c^2 \mathbf{B}\mathbf{Q}\mathbf{B} \tag{3.52}$$

where $\mathbf{Q}$ is the TDOA covariance matrix. The elements of $\mathbf{z}_a$ are related by (3.29), which means that (3.50) is still a set of nonlinear equations in x and y variables.

The approach to solving this nonlinear problem is to first assume that there is no relationship between x, y and R_1. They can then be solved by a least squares estimation. The final solution is obtained by imposing the known relationship (3.29) to the result via another LS computation. This two step procedure is an approximation of a true ML estimator for the source location. By considering the elements of $\mathbf{z}_a$ independent, the ML estimate of $\mathbf{z}_a$ is

$$\begin{aligned} \mathbf{z}_a &= arg\,min\{(\mathbf{h}-\mathbf{G}_a\mathbf{z}_a)^T\mathbf{\Psi}^{-1}(\mathbf{h}-\mathbf{G}_a\mathbf{z}_a)\} \\ &= (\mathbf{G}_a^T\Psi^{-1}\mathbf{G}_a)^{-1}\mathbf{G}_a^T\mathbf{\Psi}^{-1}\mathbf{h}, \end{aligned} \tag{3.53}$$

which is the generalized LS solution of (3.50). The equation of (3.53) cannot be solved because $\mathbf{\Psi}$ is not known since $\mathbf{B}$ contains the true distances between the source and the sensors. Further approximation is necessary in order to make the problem solvable.

When the source is far away, each R_i^0 for i=2,3,4,...,M is close to R^0 so that $\mathbf{B} \approx R^0\mathbf{I}$, where R^0 designates the range and $\mathbf{I}$ is the identity matrix size (M-1). Since scaling of $\mathbf{\Psi}$ does not affect the answer, an approximation of (3.53) is

$$\mathbf{z}_a \approx (\mathbf{G}_a^T\mathbf{Q}^{-1}\mathbf{G}_a)^{-1}\mathbf{G}_a^T\mathbf{Q}^{-1}\mathbf{h}. \tag{3.54}$$

If the source is close, (3.54) is used first to obtain an initial solution to estimate $\mathbf{B}$. The final answer is then computed from (3.53). Although (3.53) can be iterated to provide an even better answer, simulations show that applying (3.53) once is sufficient to give an accurate answer.

The covariance of position estimate $\mathbf{z}_a$ is obtained by evaluating the expectations of $\mathbf{z}_a$ and $\mathbf{z}_a\mathbf{z}_a^T$ from (3.53), however this is difficult because $\mathbf{G}_a$ contains random quantities $r_{i,1}$. The covariance matrix is computed by using a perturbation approach. In the presence of noise

$$R_{i,1} = R_{i,1}^0 + c\,n_{i,1}. \tag{3.55}$$

The matrix $\mathbf{G}_a$ and vector $\mathbf{h}$ can be expressed as $\mathbf{G}_a = \mathbf{G}_a^0 + \Delta\mathbf{G}_a$ and $\mathbf{h} = h^0 + \Delta\mathbf{h}$. Since $\mathbf{G}_a^0\mathbf{z}_a^0 = \mathbf{h}^0$, (3.50) implies that

$$\psi = \mathbf{\Delta h} - \mathbf{\Delta G}_a\mathbf{z}_a^0. \tag{3.56}$$

Letting $\mathbf{z}_a = \mathbf{z}_a^0 + \Delta\mathbf{z}_a$. Then from (3.53)

$$(\mathbf{G}_a^{0T} + \Delta\mathbf{G}_a^T)\mathbf{\Psi}^{-1}(\mathbf{G}_a^0 + \Delta\mathbf{G}_a)(\mathbf{z}_a^0 + \Delta\mathbf{z}_a) = (\mathbf{G}_a^{0T} + \Delta\mathbf{G}_a^T)\mathbf{\Psi}^{-1}(\mathbf{h} + \Delta\mathbf{h}). \quad (3.57)$$

Retaining only the linear perturbation terms and then using (3.51) and (3.56), $\mathbf{\Delta z}_a$ and its covariance matrix is

$$\begin{aligned} \Delta\mathbf{z}_a &= c(\mathbf{G}_a^T\mathbf{\Psi}^{-1}\mathbf{G}_a)^{-1}\mathbf{G}_a^T\mathbf{\Psi}^{-1}\mathbf{Bn} \quad (3.58)\\ cov(\mathbf{z}_a) &= \mathbf{E}[\Delta\mathbf{z}_a\Delta\mathbf{z}_a^T] = (\mathbf{G}_a^{0T}\mathbf{\Psi}^{-1}\mathbf{G}_a^0)^{-1}, \end{aligned}$$

where the square error term in (3.51) has been ignored and (3.52) has been used to give $cov(\mathbf{z}_a)$.

The position estimation $\mathbf{z}_a$ assumes x, y and R_i are independent; however, they are related by (3.29). Therefore, we can incorporate this relationship to get an improved estimate. When the bias is ignored because of small errors in the TDOA estimates, the vector $\mathbf{z}_a$ is a random vector with its mean centered at the true value with covariance matrix (3.58). Hence the elements of $\mathbf{z}_a$ can be expressed as

$$z_{a,1} = x^0 + e_1, \quad z_{a,2} = y^0 + e_2, \quad z_{a,3} = R_1^0 + e_1, \quad (3.59)$$

where e_1, e_2 and e_3 are the estimation errors of $\mathbf{z}_a$. Subtracting the first two elements of $\mathbf{z}_a$ by X_1 and Y_1, and then squaring the elements gives another set of equations

$$\psi^{'} = \mathbf{h}^{'} - \mathbf{G}_a^{'}\mathbf{z}_a^{'0}, \quad (3.60)$$

where $\psi^{'}$ is a vector denoting the inaccuracies in $\mathbf{z}_a$. Substituting (3.59) into (3.60) results in

$$\begin{aligned} \Psi_1^{'} &= 2(x^0 - X_1)e_1 + e_1^2 \approx 2(x^0 - X_1)e_1\\ \Psi_2^{'} &= 2(y^0 - Y_1)e_2 + e_2^2 \approx 2(y^0 - Y_1)e_2 \quad (3.61)\\ \Psi_3^{'} &= 2R_1^0 e_3 + e_3^2 \approx 2R_1^0 e_3. \end{aligned}$$

The approximation to the ML procedure used here is valid only if the errors e_i are small. The covariance matrix of $\psi^{'}$ is given by

$$\begin{aligned} \mathbf{\Psi}^{'} &= [\psi^{'}\psi^{'T}]4\mathbf{B}^{'}cov(\mathbf{z}_a)\mathbf{B}^{'} \quad (3.62)\\ \mathbf{B}^{'} &= diag\{x^0 - X_1, y^0 - Y_1, R_1^0\}. \end{aligned}$$

Since ψ is Gaussian, then it follows that $\psi^{'}$ is also Gaussian, thus the ML estimate of $\mathbf{z}_a^{'}$ is

$$\mathbf{z}_a^{'} = (\mathbf{G}_a^{'T}\mathbf{\Psi}^{'-1}\mathbf{G}_a^{'})^{-1}\mathbf{G}_a^{'T}\mathbf{\Psi}^{'-1}\mathbf{h}^{'}. \tag{3.63}$$

The matrix $\mathbf{\Psi}^{'}$is not known since it contains the true values of the position. Nevertheless, $\mathbf{B}^{'}$ can be approximated by using the values $\mathbf{z}_a$ and $\mathbf{G}_a^0$ in (3.58) approximated by $\mathbf{G}_a$ and $\mathbf{B}$ in (3.52) approximated by the values computed from (3.54).

If the source is distant, then the covariance matrix can be approximated as

$$cov(\mathbf{z}_a) \approx c^2 R^{0^2}(\mathbf{G}_a^{0T}\mathbf{Q}^{-1}\mathbf{G}_a^0)^{-1}, \tag{3.64}$$

and (3.63) reduces to

$$\mathbf{z}_a^{'} \approx (\mathbf{G}_a^{'T}\mathbf{B}^{'-1}\mathbf{G}_a\mathbf{Q}^{-1}\mathbf{G}_a\mathbf{B}^{'-1}\mathbf{G}_a^{'})^{-1}(\mathbf{G}_a^{'T}\mathbf{B}^{'-1}\mathbf{G}_a\mathbf{Q}^{-1}\mathbf{G}_a\mathbf{B}^{'-1}\mathbf{G}_a^{'})\mathbf{h}^{'}. \tag{3.65}$$

Matrix $\mathbf{G}_a^{'}$ is constant. By taking the expectations of $\mathbf{z}_a^{'}$ and $\mathbf{z}_a^{'}\mathbf{z}_a^{'T}$, the covariance matrix of $\mathbf{z}_a^{'}$ is

$$cov(\mathbf{z}_a^{'}) = (\mathbf{G}_a^{'T}\mathbf{\Psi}^{'-1}\mathbf{G}_a^{'})^{-1}. \tag{3.66}$$

Finally, the position location estimation is obtained from as

$$\mathbf{z}_p = \sqrt{\mathbf{z}_a^{'}} + \begin{bmatrix} X_1 \\ Y_1 \end{bmatrix} \tag{3.67}$$

or

$$\mathbf{z}_p = -\sqrt{\mathbf{z}_a^{'}} + \begin{bmatrix} X_1 \\ Y_1 \end{bmatrix}.$$

The proper solution is selected to be the one which lies in the region of interest. If one of the coordinates of $\mathbf{z}_a^{'}$ is close to zero, the square root in (3.67) may become imaginary. If this occurs, the imaginary component is set to zero. The covariance matrix of the position location estimate can be determined from $\mathbf{z}_a^{'}$ in (3.60), with $x = x^0 + e_x$ and $y = y^0 + e_y$. Thus from (3.60)

$$\begin{aligned} z_{a,1}^{'} - (x^0 - X_1)^2 &= 2(x^0 - X_1)e_x + e_x^2 \\ z_{a,2}^{'} - (y^0 - Y_1)^2 &= 2(y^0 - Y_1)e_y + e_y^2. \end{aligned} \tag{3.68}$$

The errors e_x and e_y are relatively small compared to x^0 and y^0, thus we can eliminate e_x^2 and e_y^2. Then using (3.52), (3.58) , (3.62) and (3.67), the covariance matrix, $\mathbf{\Phi}$, of

position location estimate, $\mathbf{z}_p$,is found to be

$$\begin{aligned} \mathbf{\Phi} &= cov(\mathbf{z}_p) = \frac{1}{4}\mathbf{B}^{''-1} cov(\mathbf{z}_a^{'})\mathbf{B}^{''-1} \\ &= c^2(\mathbf{B}^{''}\mathbf{G}_a^{'T}\mathbf{B}^{'-1}\mathbf{G}_a^{0T}\mathbf{B}^{-1}\mathbf{Q}^{-1}\mathbf{B}^{-1}\mathbf{G}_a^{0}\mathbf{B}^{'-1}\mathbf{G}_a^{'}\mathbf{B}^{''})^{-1}, \end{aligned} \tag{3.69}$$

where

$$\mathbf{B}^{''} = \begin{bmatrix} (x^0 - X_1) & 0 \\ 0 & ((y^0 - Y_1) \end{bmatrix}.$$

To summarize Chan's method, the location of a distant source can be estimated by using equations (3.54), (3.65) and (3.67). The covariance matrix of the PL estimate is determined from (3.69). For locating near sources, (3.54) is used to give an approximation of $\mathbf{B}$, then used in (3.53), (3.63) and (3.67) to produce a PL solution. The covariance matrix of the PL estimates can then be determined from (3.69). Chan's method offers a closed form solution which can achieve the CRLB. However, it does so when the range difference errors are assumed to be small. His method also requires a *priori* knowledge of the approximate location and distance of the source to resolve ambiguities in the PL solution.

The hyperbolic PL estimation algorithms presented offer different accuracy's and complexities. The Taylor-series LS method offers accurate position location estimation at reasonable noise levels and is applicable to any number of range difference measurements, but can be computational intensive. Fang's method provides an optimal solution when the system of equations is consistent but does not make use of redundant measurements. Friedlander's approach reduces the computational requirements for the solution but does is suboptimal because it eliminates a fundamental relationship. Chan's method offers a closed form solution, thus eliminating the need for an iteration approach, but requires *a priori* information to eliminate ambiguities. The optimal PL algorithm for a given situation depends on the geometrical configuration of the base stations, the number of coordinates of the source to be solved and range difference measurements utilized, computational requirements and complexity, assumptions on the statistical nature of the channel and desired accuracy.

3.4 Measures of Position Location Accuracy

A set of benchmarks is required to evaluate the accuracy of the hyperbolic position location technique. A commonly used measure of PL accuracy is the comparison of the mean square error (MSE) of the position location solution to the theoretical MSE based on the Cramér-Rao Lower Bound (CRLB). Another commonly used measure of PL accuracy is the circle of error probability (CEP). The effect of the geometric configuration of the base stations on the accuracy of the position location estimate is measured by the geometric dilution of precision (GDOP). A simple relationship exists between the GDOP and CEP measures. Lee in [Lee75a] and [Lee75b] provides a novel procedure for assessing the accuracy of hyperbolic multilateration PL systems and limitations of the accuracy's. Hepsaydir and Yates provide a performance analysis of position locationing systems using existing CDMA networks in [Hep94].

3.4.1 MSE and the Cramér-Rao Lower Bound

A commonly used measure of accuracy of a PL estimator is the comparison of the mean squared error (MSE) of the PL solution to the theoretical MSE based on the Cramér-Rao Lower Bound on the variance of unbiased estimators. The classical method for computing the MSE of a 2-D position location estimate is

$$MSE = \varepsilon = \mathbf{E}[(x - \hat{x})^2 + (y - \hat{y})^2], \tag{3.70}$$

where (x, y) is the coordinates of the source and $(\hat{x}, \hat{y})$ is the estimated position of the source. The root-mean square (RMS) position location error, which can also be used as a measure of PL accuracy, is calculated as the square root of the MSE

$$RMS = \sqrt{\varepsilon} = \sqrt{\mathbf{E}[(x - \hat{x})^2 + (y - \hat{y})^2]}. \tag{3.71}$$

To gauge the accuracy of the PL estimator, the calculated MSE or RMS PL is compared to the theoretical MSE based on the Cramér-Rao Lower Bound (CRLB). The conventional CRLB sets a lower bound for the variance of any unbiased parameter estimator and is typically used for a stationary Gaussian signal in the presence of stationary Gaussian noise [Gar92b]. For non-Gaussian and nonstationary (cyclostationary) signals and noise, alternate methods have been used to evaluate the performance of the estimators [Gar92b]. The derivation of the CRLB for Gaussian noise is

provided in [Cha94], [Kna76], [Hah73] and [Hah75]. The CRLB on the PL covariance is given by Chan [Cha94] as

$$\mathbf{\Phi} = c^2(\mathbf{G}_t^T\mathbf{Q}^{-1}\mathbf{G}_t)^{-1}, \tag{3.72}$$

where $\mathbf{G}_t$ is defined in (3.37) with $(x, y, R_i) = (x^0, y^0, R_i^0)$, which are the actual coordinates of the source and the range of the first base station to the source, and matrix $\mathbf{Q}$ is the TDOA covariance matrix. The sum of the diagonal elements of $\mathbf{\Phi}$ defines the theoretical lower bound on the MSE of the PL estimator. Matrix $\mathbf{Q}$ may not be known in practice; however, if the noise power spectral densities are similar at the receivers, it can be replaced be a theoretical TDOA covariance matrix with diagonal elements of σ_d^2 and $0.5\sigma_d^2$ for all other elements, where σ_d^2 is the variance of the TDOA estimate [Cha94].

3.4.2 Circular Error Probability

A crude but simple measure of accuracy of position location estimates that is commonly used is the circular error probability (CEP) [Tor84] [Foy76]. The CEP is a measure of the uncertainty in the location estimator relative to its mean. For a 2-D system, the CEP is defined as the radius of a circle which contains half of the realizations of the random vector with the mean as its center. If the position location estimator is unbiased, the CEP is a measure of the uncertainty relative to the true transmitter position. If the estimator is biased and bound by bias B, then with a probability of one-half, a particular estimate is within a distance B + CEP from the true transmitter position. Figure 3.2 illustrates the 2-D geometrical relations.

The CEP is a complicated function and is usually approximated. Details of its computation can be found in [Foy76] and [Tor84]. For hyperbolic position location estimator the CEP is approximated with an accuracy within approximately 10 % as

$$CEP \approx 0.75\sqrt{\sigma_x^2 + \sigma_y^2}, \tag{3.73}$$

where σ_x^2 and σ_y^2 are the variances in the estimated position [Tor84].

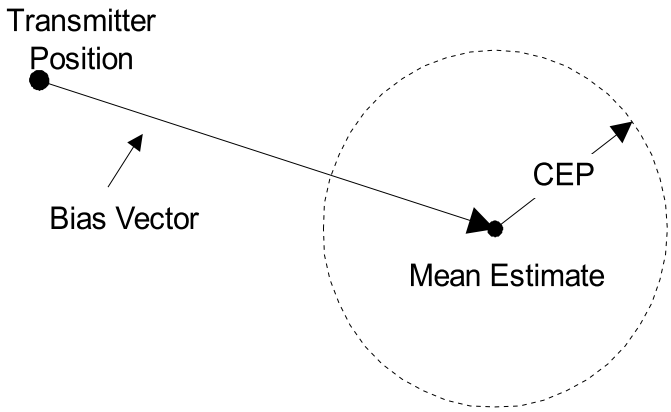

Figure 3.2: Circle of Error Probability

3.4.3 Geometric Dilution of Precision

The accuracy of Range-Based PL systems depends to a large extent on the geometric relationship between the base stations and the source to be located. One measure that quantifies the accuracy based on this geometric configuration is called the geometric dilution of precision (GDOP) [Wel86] [Tor84] [Ban85] [Lee75a]. The GDOP is defined as the ratio of the RMS position error to the RMS ranging error. The GDOP for an unbiased estimator and a ranging system is given by [Jor84] as

$$GDOP = \sqrt{tr[(\mathbf{A}^T\mathbf{A})^{-1}]}, \tag{3.74}$$

where $\mathbf{A}$ is express in equation (3.20) and tr indicates the trace of the resulting matrix. The GDOP for an unbiased estimator and a 2-D hyperbolic system is given by [Tor84] and [Lee75a] as

$$\begin{aligned} GDOP &= \left(\sqrt{(c\sigma_x)^2 + (c\sigma_y)^2}\right) \Big/ \sqrt{(c\sigma_s)^2} \\ &= \left(\sqrt{\sigma_x^2 + \sigma_y^2}\right) \Big/ \sigma_s, \end{aligned} \tag{3.75}$$

where $(c\sigma_s)^2$ is the mean squared ranging error and $(c\sigma_x)^2$ and $(c\sigma_y)^2$ are the mean square position errors in the x and y estimates. The GDOP is related to the CEP by

$$CEP \approx (0.75\sigma_s)GDOP. \tag{3.76}$$

The GDOP can be used as a criterion for selecting a set of base station from a large set whose measurements produce minimum PL estimation error or for designing base station location within new systems.

3.5 Chapter Summary

This chapter introduced the TDOA estimation techniques and hyperbolic PL algorithms used in the hyperbolic position location method. A general model for the TDOA estimation problem was developed and the generalized cross-correlation (GCC) techniques commonly used for time delay estimation were presented. The effect of the frequency functions on the TDOA estimation and the importance of the choice of frequency function was discussed. Although GCC methods do facilitate the estimation of the TDOA, they do encounter problems which are critical to the position location problem. Firstly, GCC require the differences in the TDOA for each signal to be greater than the widths of the cross-correlation functions so that the correlation peaks can be resolved. If not separated sufficiently, overlapping of cross-correlation functions corrupt the TDOA estimate. Furthermore, because GCC methods are not signal-selective, they produce correlation peaks for all signals and are faced with the problem of identifying the TDOA estimate of interest. Signal-selective TDOA estimation techniques outperform GCC methods; however, they do not offer any advantages over GCC methods when the spectrally overlapping noise and interference exhibit the same cycle frequency as the signal of interest, which is encountered in multiuser CDMA systems.

A general range difference position location model was formulated and the hyperbolic algorithms used to provide solutions to the range difference equations were presented. For the problem of geolocating mobile units within a cellular infrastructure, the algorithms applicable to arbitrarily placed base station were reviewed. Fang's PL method, Friedlanders Least Square (LS) and Weighted LS PL method, the iterative Taylor-series LS PL method and Chan's closed form PL method were described in detail. The advantages and disadvantages of the various PL algorithms were discussed. Finally, the measures of position location accuracy commonly used to evaluate hyperbolic position location algorithms were reviewed.

Chapter 4

Simulation Model

4.1 Introduction

In this chapter, the simulation models and general assumptions for the CDMA reverse channel and hyperbolic position location system are presented. A general position location procedure is given. For simplicity, it is assumed that the user requesting E-911 service is stationary. The reverse channel transmitter and receiver implementations and operation of the CDMA system model is discussed. The AWGN, multipath and shadowing mobile radio channel models used in the simulations are provided. The TDOA estimation technique and hyperbolic PL algorithm used in the hyperbolic position location system is reviewed. Finally performance measures utilized to evaluate the hyperbolic position location technique are indicated. The performance of the hyperbolic PL technique is evaluated for a macrocellular and microcellular environment. All operational parameters, such a path loss exponent, distance of mobile from base station handling call, required base station received power, were selected to maintain system integrity and reflect typical values.

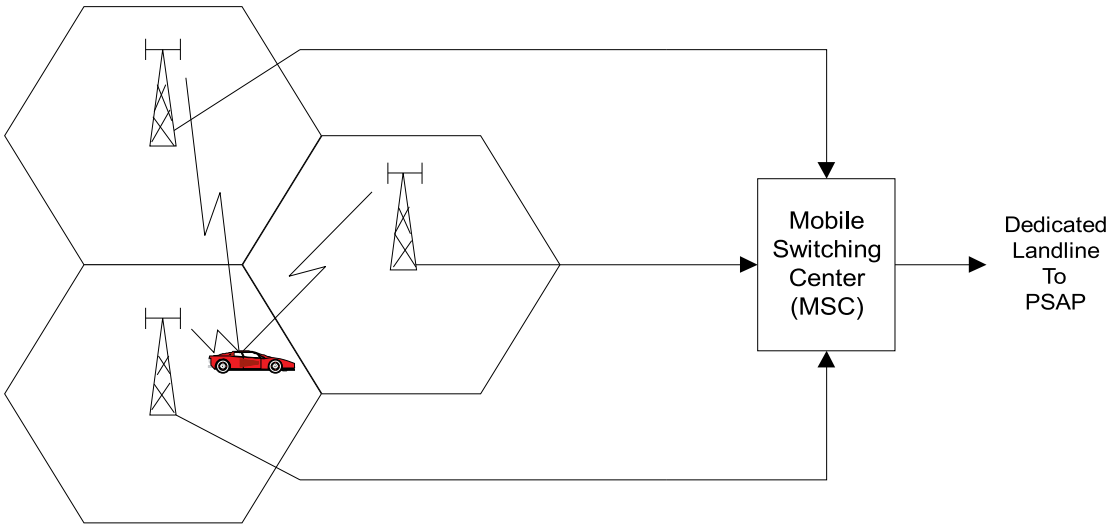

Figure 4.1: Position Location Configuration

4.2 Position Location Procedure

The general procedure for providing E-911 service to mobile wireless users is presented. When an E-911 call is initiated, it is assumed that the base station handling the call, referred to as the *controlling* base station and designated as BS#1, is able to recognize the call as an emergency call. Upon recognition of the E-911 call, the controlling BS notifies the Master Switching Center (MSC), which then monitors the mobiles signal from all available neighboring base stations. Since the MSC continually monitors the signal strength of a mobile unit from multiple base station for soft-handoff purposes, the base stations receiving the signal with the strongest strength can be easily recognized. It is assumed that the three or four base stations receiving the users signal with the highest power is selected by the MSC from the available set of base stations.

At this time, each base station selected is instructed to take a "snapshot" of the users demodulated baseband PN spread signal and relay this information to the MSC. Perfect timing synchronization between base stations as provided by CDMA timing is assumed. The MSC estimates the TDOA between all neighboring base stations and the controlling base station, then calculates the PL estimate of the mobile unit. The PL information is then transferred along a dedicated landline to the nearest PSAP. Figure 4.1 provides an illustration of a physical layer for a three BS PL configuration.

4.3 CDMA System Model

The base station configuration used for the CDMA system is based on a hexagonal cellular layout with major radius defined by R. Two base station configurations, corresponding to whether three and four base stations are being used, were established. Figure 4.2 illustrates the base station locations when three base stations are used. Figure 4.3 illustrates the base station locations when four base stations are used. Selection of the base station configuration was based on the shortest transmitter-receiver distances between the mobile unit and any neighboring base station. Unless otherwise specified, the base stations and the mobile unit are coplanar. For a macrocellular CDMA environment, a cell radius of $R = 5\ km$ is used, and for a microcellular environment, a cell radius of $R = 1\ km$ is used.

The mobile unit transmitter is modeled as the DS/SS transmitter indicated by Figure 2.4 in Chapter 2. It is assumed that the mobile unit uses a half-wave dipole antenna with unity gain and has a maximum output power of 1W. A center frequency channel and signal bandwidth of 1900MHz and 1.2288 MHz respectively, which is indicative of CDMA operation within the PCS spectrum, and perfect RF modulation and demodulation is assumed. All simulations were performed on baseband rectangular shaped BPSK signals. The BPSK modulation data is spread by a pseudo-noise (PN) spreading sequence with chip duration of $T_c = 813.8\ ns$. The spread spectrum signal is modeled as

$$s(t) = a(t)b(t), \tag{4.1}$$

where both the PN spread sequence $a(t)$ and the information bearing signal $b(t)$ are binary nonreturn-to-zero waveforms with unit amplitude. Because information content is not of importance, a random BPSK PN sequence was generated and used as the transmitted signal $s(t)$.

The long PN spreading sequence used in the IS-95 CDMA cellular standard introduces a processing gain of $N = 4$ chips/symbol after the 1/3 rate convolutional encoder and 64-ary orthogonal modulator introduce a processing gain of $N = 32$. As a result, an IS-95 system introduces a total processing gain of $N = 128$ chips/bit. Therefore, a processing gain of $N = 128$ was assumed for all simulations.

The base station receiver model used is the DS/SS receiver model indicated by Figure 2.5 in Chapter 2. It is assumed that each base station is utilizing omni directional isotropic antennas with unity gain. The received signal is demodulated to the base-band spreading sequence. A "snapshot" of the PN spread sequence required for TDOA estimation is captured immediately after demodulation. It is assumed that the PN spreading code used for any one user within access interference is negligible. Throughout, it is assumed that all base station clocks are perfectly synchronized using a common reference, such as CDMA time. Consequently, relative clock drift and bias is assumed to be zero. Perfect acquisition and synchronization of the users PN code is also assumed.

Closed-loop CDMA power control is used for all simulations. Perfect power control is assumed so that the total power level of each user on the receiving antenna is the same, thus eliminating the near-far effect. The base station adjusts the transmitting power of the mobile unit accordingly to maintain the required received power level at the receiver. Unless otherwise specified, it is assumed that the controlling base station requires sufficient power levels to maintain a SNR of 18 dB from all users within the cell.

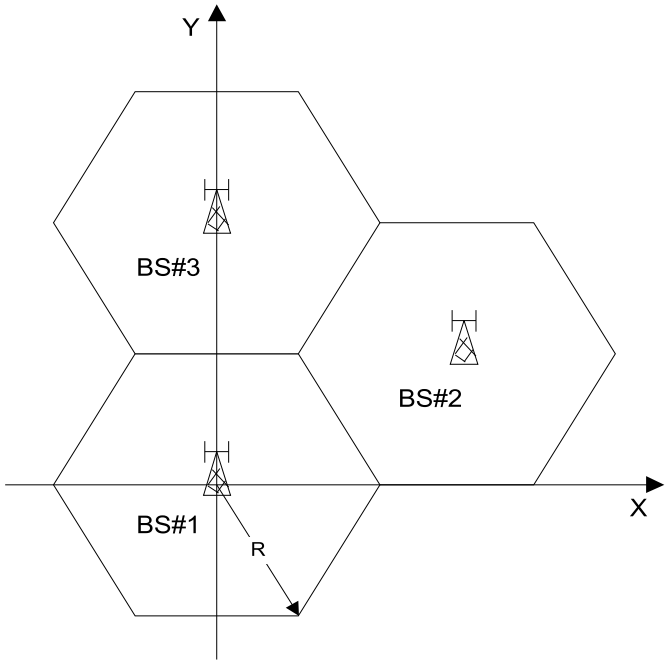

Figure 4.2: 3 Base Station Configuration

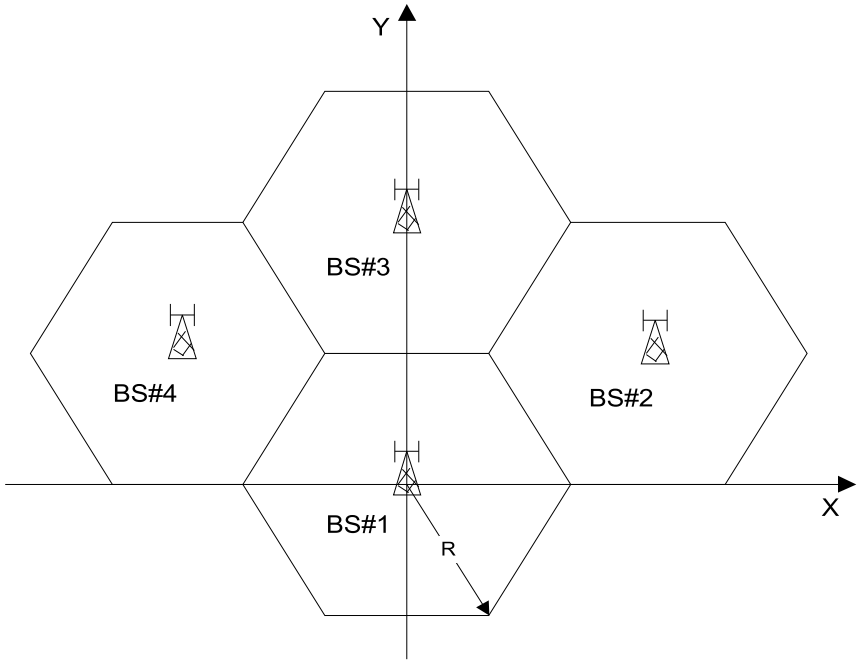

Figure 4.3: 4 Base Station Configuration

4.4 Mobile Radio Reverse Channel Models

4.4.1 Received Signal Model

This section describes how the received signal at each base station is generated. To generate the signals, a three or four base station configuration and mobile location is selected. Based on the distance of the mobile to each base station, the propagation delays, d_1, d_2 and d_3, assuming a signal propagation speed of $c = 3 \times 10^8$ m/s, of the transmitted signal to each base station is determined. Assuming a three base station configuration, the relative delays, $d_{2,1}$ and $d_{3,1}$, with respect to the controlling base station, BS#1, is then caculated from

$$d_{2,1} = d_2 - d_1 \tag{4.2}$$

$$d_{3,1} = d_3 - d_1. \tag{4.3}$$

A random BPSK signal with unity signal power is generated for each base station, then sampled and shifted according to the relative delays experienced. The signals are then passed through an additive white Gaussian noise (AWGN) channel, where the noise power is scaled according to the signal-to-noise ratio (SNR) of the received waveform. The received signals at the neighboring base stations are time shifted versions of the received signal at BS#1.

$$r_1(t) = s(t) + n(t) \tag{4.4}$$

$$r_2(t) = s(t - d_{2,1}) + n(t) \tag{4.5}$$

$$r_3(t) = s(t - d_{3,1}) + n(t). \tag{4.6}$$

Received signal power levels at each base station, and consequently SNRs, are adjusted according to the channel path loss exponent n and distance of the mobile to the base stations. Multipath components of the signal were added in the multipath simulations and the effects of shadowing on the signal propagation delay time and power level were included in the simulations of shadowed cellular environments. The received signals are then processed by the TDOA estimator and hyperbolic position location algorithm to provide an estimate of the mobiles location.

4.4.2 Path Loss Model

The log distance path loss model was used to determine received power levels as a function of transmitter-receiver separation distance. The log distance path loss model is based on theoretical analysis and measurements that indicate that the average received signal power decreases logarithmically with distance. The average large-scale path loss for an arbitrary transmitter-receiver separation is expressed as a function of distance by using the path loss exponent n.

$$PL(dB) = PL(d_o) + 10nlog\left(\frac{d}{d_o}\right). \tag{4.7}$$

In equation (4.7), $PL(d_0)$ is the path loss at the close-in reference distance d_0 and d is the distance from the mobile to the base station. The close-in reference distance must be chosen so that it lies in the far field, or *Fraunhofer region*, of the transmitting antenna so that the near-field effects do not alter the reference path loss [Rap96]. The far-field distance of a transmitting antenna is defined as the region beyond the far-field distance d_f. The far-field distance d_f is related to the largest dimension of the antenna, D_a, and the carrier frequency.

$$d_f = \frac{2D_a^2}{\lambda}. \tag{4.8}$$

For a half-wave dipole antenna used at the PCS carrier frequency of 1900 MHz, the largest linear dimension of the mobile units antenna is approximately 0.08 meters, which results in a Fraunhofer distance of 0.08 meters. Therefore, a close-in reference distance of 10 meters was selected for simulations within microcellular environments, and a close-in reference distance of 1 km was selected for simulations within macro-cellular environments.

Given a required base station received power of $Pr(d)$ dBm, the power received at the close-in reference distance d_0 using the log distance path loss model is

$$P_r(d_0)\ dBm = P_r(d)\ dBm + 10nlog\left(\frac{d}{d_o}\right)\ dB. \tag{4.9}$$

The transmitting power of the mobile in watts is then calculated from

$$P_t = P_r(d_0) \times \frac{(4\pi)^2 d_o^2 L}{G_t G_r \lambda^2}, \tag{4.10}$$

where $P_r(d_o)$ is expressed in watts, G_t and G_r are the gains of the transmitting and receiving antenna respectively, and L is the system loss factor not associated with propagation losses. For all simulations, it is assumed that the transmitting and receiving antennas have unity gain and the system loss factor L=1. The signal power received at each base station is then calculated using the log-distance path loss model described

$$P_r(d)\ dBm = P_r(d_o)\ dBm - 10nlog\left(\frac{d}{d_o}\right)\ dB. \tag{4.11}$$

4.4.3 Signal-to-Noise Ratio

Having determined the required mobile unit transmit power and the received signal power $P_r(d)$ at each of the base stations, the SNR at each base station is calculated using the relationship

$$SNR = 10log_{10}\left(\frac{P_r}{P_n}\right)\ dB, \tag{4.12}$$

where P_n is the noise power. The noise power is defined as

$$P_n = kTB, \tag{4.13}$$

where k is Boltzman's constant, T is the thermal noise temperature in Kelvins, and B is the bandwidth of the transmitted signal. For all simulation, T is assumed to be 295 kelvin. The calculated SNR, or equivalently E_b/N_o, is used to scale the noise components added to the signal described in Section 4.4.4.

4.4.4 Additive White Gaussian Noise Channel

A zero-mean additive white Gaussian noise channel is used in all simulations. The noise, $n(t)$, is added to the transmitted signal, $s(t)$, so that the received signal is represented as

$$r(t) = s(t) + n(t). \tag{4.14}$$

The SNR of the received signal is defined as the ratio of the signal power, P_s, to the noise power, P_n.

$$SNR = \frac{P_s}{P_n}. \tag{4.15}$$

In the simulation of digital communications systems, the SNR is commonly evaluated as E_b/N_o, where E_b is the transmit energy per bit and N_o is a function of the noise power spectral density. The energy per bit in terms of the transmit signal power is given as

$$E_b = P_s T_{bit}, \tag{4.16}$$

where T_{bit} is the duration of a bit. Because of the coding gain, N, provided by the PN spreading sequence and the sampling of the signal by N_s, the energy is spread over many more symbols, and T_{bit} is equal to the number of symbols and samples used to represent each bit.

$$T_{bit} = N\ N_s. \tag{4.17}$$

The noise power, assuming a AWGN channel with two-sided power spectral density of $N_o/2$, is given by

$$\sigma_n^2 = \frac{N_o}{2}. \tag{4.18}$$

Unity signal power, $P_s = 1$, is used for all simulation. Therefore, the noise power, σ_n^2, is scaled to simulate a particular SNR. The noise power for a given SNR is calculated using

$$\sigma_n^2 = \frac{N\ N_s}{2\ (E_b/N_o)}. \tag{4.19}$$

Therefore, zero-mean Gaussian noise components with variance given by Equation 4.19 is added to the signal in Equation 4.14.

4.4.5 Multipath Channel Model

This section describes the multipath model used in this research. For wideband signals, as used in CDMA, the channel bandwidth is considerably smaller than the signal bandwidth. This leads to frequency selective fading which introduces intersymbol interference (ISI) in the time domain. As a result, the received signal will consist of multiple copies of the original signal, which are attenuated and time delayed. To minimize computation, it is assumed that the channel exhibits slow fading. In slow fading channels, the channel impulse response changes at a rate much slower then the transmitted baseband signal. Therefore the impulse response of the channel is assumed to remain constant over a data collection interval. A simple tapped delay

line model is used to simulated the multipath channel, resulting in a received signal given by

$$r(t) = s(t) + n(t) + \sum_{i=1}^{M} \alpha_i s(t - \tau_i) + n_i(t - \tau_i), \tag{4.20}$$

where τ_i and α_i are the relative delay and signal power of the ith multipath component, and M is the number of multipath components present. Only coherent multipath was considered; the multipath components constructively combine with the LOS signal. The effect of multipath on the PL accuracy is observed as a function of a chip interval delay and relative power multipath with respect to the LOS signal and the number of multipath components present.

4.4.6 Shadowing Channel Model

In simulations evaluating the effect of obstruction due to man-made or natural structure, the knife-edge diffraction model of [Rap96] was used. Figure 4.4 illustrates the geometry used. It is assumed that the obstruction has height h and is infinitely wide. It is apparent from the figure that the wave travels a longer distance than the LOS path. Assuming that $h << d_1, d_2$ and $h >> \lambda$, the difference between the direct LOS and diffracted path, called the *excess path length*, can be approximated as

$$\Delta \approx \frac{h^2(d_1 + d_2)}{2(d_1 d_2)}. \tag{4.21}$$

The excess propagation delay due to the longer diffracted distance can be determined from

$$\Delta t = \Delta / c, \tag{4.22}$$

where c is the speed of signal propagation. When shadowing is caused by an object, such as a mountain or building, the attenuation caused by diffraction can be estimated by calculating the *Frensel-Kirchoff* diffraction parameter v and using the Fresnel integral in [Rap96]. An approximate solution to the Fresnel integral, which was used in the simulations, is provided by [Lee85]. The diffraction parameter v is a dimensionless parameter and is given as

$$v = h\sqrt{\frac{2(d_1 + d_2)}{\lambda d_1 d_2}}. \tag{4.23}$$

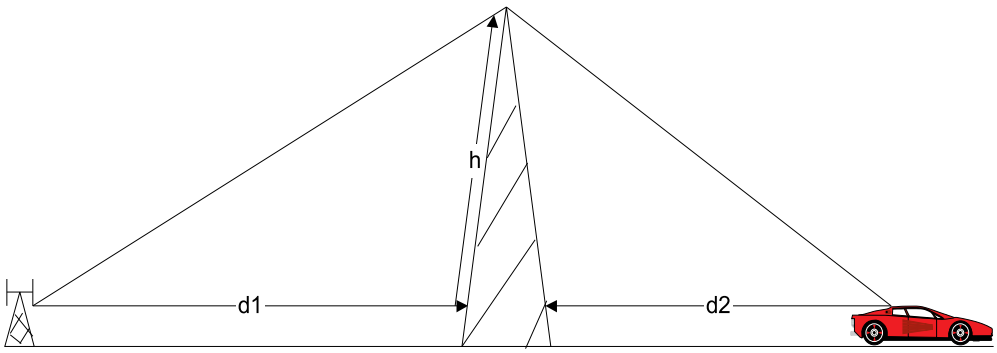

Figure 4.4: Knife-Edge Diffraction Model

The approximations to the Fresnel integral provided by Lee is given as

$$G_d(dB) = 0 \qquad v \leq -1 \qquad (4.24)$$

$$G_d(dB) = 20log(0.5 - 0.62v) \qquad -1 \leq v \leq 0 \qquad (4.25)$$

$$G_d(dB) = 20log(0.5exp(-0.95v)) \qquad 0 \leq v \leq 1 \qquad (4.26)$$

$$G_d(dB) = 20log\left(0.4 - \sqrt{0.1184 - (0.38 - 0.1v)^2}\right) \qquad 1 \leq v \leq 2.4 \qquad (4.27)$$

$$G_d(dB) = 20log\left(\frac{0.225}{v}\right) \qquad v > 4. \qquad (4.28)$$

The effect of shadowing on the PL accuracy is observed as a function of the excess path length (or excess propagation delay) and power attenuation due to the obstruction.

4.5 Hyperbolic Position Location Technique

The hyperbolic PL technique utilized in the simulations consisted of a cross-correlation TDOA estimator and the Taylor-series Least Squares (LS) PL algorithm. The cross-correlation TDOA estimation technique was selected because of its simplicity. It provides unbiased TDOA estimation and allows for observation of the relative effect due to different channel and system parameters. The MATLAB cross correlation function, *xcorr*, was used to perform the cross correlation of signal snapshots acquired at the base stations. Because generalized cross correlation techniques are not signal selective, they are unable to distinguish between correlation peaks generated from line-of-sight (LOS) and multipath components. Therefore, for all simulations, it is assumed that the maximum correlation peak is due to the LOS signal.

The TDOA estimation errors in the absence of interference and signal noise are assumed to be due to the uncertainity in the peak correlation estimation by the cross-correlation estimator. The TDOA estimator errors are modeled as a zero-mean Gaussian random variable with variance σ_d^2. The TDOA estimates were simulated by adding zero-mean Gaussian noise with variance σ_d^2 to the TDOA's calculated by the cross-correlation delay estimator. Throughout this thesis, the accuracy of the TDOA estimator is defined as the standard deviation of the peak correlation estimator.

The Taylor-series LS PL algorithm was used because of its ability to provide accurate results at reasonable TDOA noise levels. It is a simple method that is can be applied to an arbitrary number of range difference measurements, thus eliminating the need for multiple PL algorithms. The PL solution to the set of range difference Equations of 3.30 generated from the TDOA estimates is determined from Equations 3.37 and 3.29. The TDOA covariance matrix $\mathbf{Q}$ used in Equation 3.37 is generated from 1000 TDOA estimation iterations. The deviates Δx and Δy are caculated and used to update the estimated x and y until both deviates are ≤ 0.01. To facilitate convergence of the Taylor-series PL method, the actual mobile position was used as the initial guess. When large TDOA errors are encountered, the Taylor-series method may not always converge. In this situation, the iterative Taylor-series method is halted and a non-solution is declared. Non-solution were not used in the performance evaluation of hyperbolic PL technique.

4.6 Performance Measures

The performance measures used to evaluate the accuracy of the hyperbolic position location technique include the root-mean square (RMS) PL error, geometric dilution of precision (GDOP) and circle of error probability (CEP). The classical RMS measure of Equation 3.71 was used to evaluate the position location accuracy of the hyperbolic PL estimation technique. The GDOP factor, as defined by Equation 3.75, was used to evaluate PL errors due to base station configuration. The CEP of Equation 3.73 was utilized as a simple measure of accuracy. Comparison of the simulation results to the Cramér Rao Lower Bound (CRLB) was performed whenever applicable. The CRLB was calculated using Equation 3.72, where $\mathbf{G}_t$ is defined in Equation (3.37) with $(x, y, R_i) = (x^0, y^0, R_i^0)$, which are the actual source and the range of the first base station to the source, and matrix $\mathbf{Q}$ is the TDOA covariance matrix. It was assumed that the signal and noises are white and the SNR at each of the receivers is identical. Consequently, the theoretical TDOA covariance matrix $\mathbf{Q}$ is found to be σ_d^2 all diagonal elements and $0.5\ \sigma_d^2$ for all other elements, where σ_d^2 is the TDOA variance.

4.7 Chapter Summary

This chapter presented the simulation models and assumptions used in the software. The general position location procedure was described. The CDMA system parameters and operation were indicated. The AWGN, multipath and shadowing channel models were described. The TDOA estimation technique and hyperbolic PL algorithm used in the simulations and measures of accuracy used to evaluate PL accuracy were indicated.

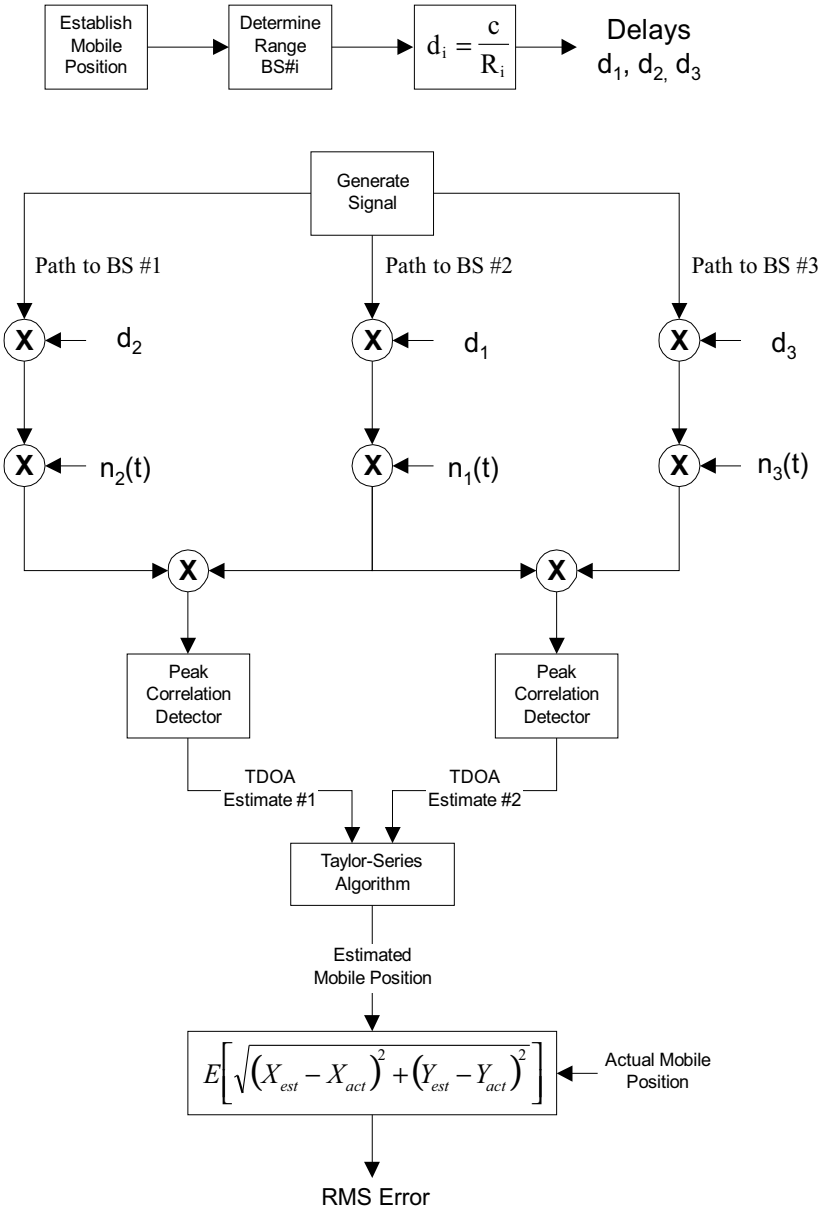

Figure 4.5: Block Diagram for Simulation

Chapter 5

Experimental Results

5.1 Introduction

In this chapter, we present the results of the simulations. The hyperbolic position location (PL) technique described in Chapter 3 and the CDMA system described in Chapter 2 are simulated using the concepts and models described in Chapter 4. The simulation results are intended to evaluate the performance of the hyperbolic PL technique when used in the reverse channel of a CDMA system.

The effect of mobile radio channel conditions, CDMA system operation and configuration on the performance of the hyperbolic PL technique is reported. Simulation results demonstrate the effect of the number of base stations utilized, the location of the mobile unit within the cell, and the cell environment on PL performance. The effect of the CDMA closed-loop power control on the accuracy and ability of the PL method is presented. The effect of path loss and the length of the observation window over which the signal is used for TDOA estimation on performance is evaluated. Performance evaluation of the hyperbolic PL system in multipath and shadowing mobile radio environments is also performed.

Monte Carlo simulations for a single user CDMA system were performed in all simulations. The effect of multiple access interference is not included in the evaluation of the hyperbolic PL system. In all simulations, the mobile unit is located within the coverage area of BS#1 and all location values are reported in meters.

Table 5.1: Number of Base Stations vs MSE of CRLB, Chan's Model, and the Hyperbolic PL Simulation Model

# of BS	CRLB	Chan	Simulation Model
4.0	328.82	346.86	353.00
5.0	143.94	147.57	148.37
6.0	44.06	44.38	44.70
7.0	38.54	38.64	39.09
8.0	38.53	38.63	39.03
9.0	36.47	36.55	36.90
10.0	33.73	33.80	34.07

5.2 Validation of Hyperbolic PL Model

Validation of the PL system models used in the simulations is critical in establishing the reliability of the experimental results. Therefore, validation of the hyperbolic PL estimation model, which is comprised of a cross-correlation TDOA estimator and a Taylor-series Least Squares PL algorithm, was performed.

To validate the PL system model, a simple simulation was performed and compared to the simulation results of [Cha94]. In the simulation, ten coplanar receiver's were placed at the following locations: $(x_1 = 0, y_1 = 0)$, $(x_2 = -5, y_2 = 8)$, $(x_3 = 4, y_3 = 6)$, $(x_4 = -2, y_4 = 4)$, $(x_5 = 7, y_5 = 3)$, $(x_6 = -7, y_6 = 5)$, $(x_7 = 2, y_7 = 5)$, $(x_8 = -4, y_8 = 2)$, $(x_9 = 3, y_9 = 3)$ and $(x_{10} = 1, y_{10} = 8)$. The source was located at $(x_m = -50, y_m = 250)$. It was assumed that both signal and noises are white random processes and the SNR at each receiver is identical. Therefore, the TDOA covariance matrix $\mathbf{Q}$ is found to be σ_d^2 for diagonal elements and $0.5\sigma_d^2$ for all other elements. The TDOA noise power was set to $\sigma_d^2 = 0.00001/c^2$ and the MSE PL error for a different number of receivers, obtained from 10,000 iterations, was compared to the theoretical MSE based on the Cramér Rao Lower Bound (CRLB).

Table 5.1, which provides the simulation results, indicates that the hyperbolic PL model does approach the Cramér Rao Lower Bound. Furthermore, the results are in very close agreement with those reported by Chan in [Cha94]. As such, the operation of the software implementation of the hyperbolic position location system model was verified and reliable results can be reported.

5.3 Base Stations and TDOA Accuracy

The results presented in this section evaluates the performance of the hyperbolic PL technique as a function of the number of base stations utilized and the accuracy of the TDOA estimator. The performance of the hyperbolic PL technique in a macrocellular and microcellular CDMA system and AWGN channel is performed. The simulation results can be used as a baseline performance of the hyperbolic position location method.

5.3.1 Macrocellular Environment

The results presented here evaluate the performance of a hyperbolic PL system utilizing three and four base stations in a macrocellular CDMA environment. In the simulations, the base station configurations indicated by Figures 4.2 and 4.3 and a cell size of $R = 5$ km were used. For the three base station configuration, the base stations were located at BS#1=$(0, 0)$, BS#2=$(7500, 4330)$ and BS#3=$(0, 8660)$. For the four base station configuration, an additional base station was located at BS#4=$(-7500, 4330)$. The mobile unit was located near the cell boundary at $(x_m = 1480.7, y_m = 4068.2)$. The same mobile position was used in each simulation. Figure 5.1 illustrates the location of the mobile within a three base station configuration

The first simulation was performed for a path loss factor of $n = 2.5$ and an observation window of 1000 chips. Figure 5.2 indicates the results of the simulation. As stated previously, the Taylor-series PL algorithm can provide precise position location estimates that approach the CRLB even at reasonable TDOA noise levels. This is evident from the simulation results of both configurations. The RMS PL accuracy from both base station configurations closely follows the CRLB when the TDOA estimation errors are small. However, as the TDOA noise levels increase, the deviation from the CRLB increases. At very high TDOA noise levels, the RMS PL error begins to sharply increase and evaluation of the hyperbolic PL method becomes difficult because convergence of the iterative Taylor-series method is not guaranteed.

As explained in Chapter 2, redundant TDOA measurements can improve position location accuracy. The plot clearly shows the performance gains from redundant

measurements. The four base station configuration offers approximately 1 dB better TDOA noise tolerance and approximately 17% better RMS PL accuracy over a three base station configuration. At a TDOA accuracy of -60 dB, or 1 μs, the four base station configuration provides approximately 50 meter better RMS PL accuracy than a three base station configuration. While these results indicate the performance benefit of using redundant measurements, it should be noted that the mobile unit is ideally located. In the simulation, the mobile unit is close to the cell boundary so that the received power levels are sufficiently high enough at neighboring base stations to facilitate the TDOA estimation between them. At the given mobile location and the path loss factor, the SNR's at the base stations are 18.0, 14.4, 16.8 and 10.1 dB respectively. In following simulations, the degradation in PL performance as a mobile deviates from this ideal location is demonstrated.

A second simulation was performed for a path loss factor of $n = 3.6$, which is typical of urban cellular environments. Figure 5.3 illustrates the results of the simulation. The figure indicates that the three base station configuration provides reasonable PL performance. However, in contrast to the previous simulation, the results indicate that redundant TDOA measurements do not offer improved performance. For a channel path loss of $n = 3.6$, the SNR's at the base stations were found to be 18.0, 12.8 16.3 and 6.5 dB respectively. The results suggest that, while the SNR's at BS#1-BS#3 are sufficiently high enough to facilitate accurate TDOA estimation, the SNR level at the fourth, and most distant base station, is not. Consequently, the performance gains from the redundant TDOA measurement are offset by the inaccuracies in the measurement because of low signal quality. In following simulations, the effect of path loss and the SNR's at the neighboring base stations is demonstrated.

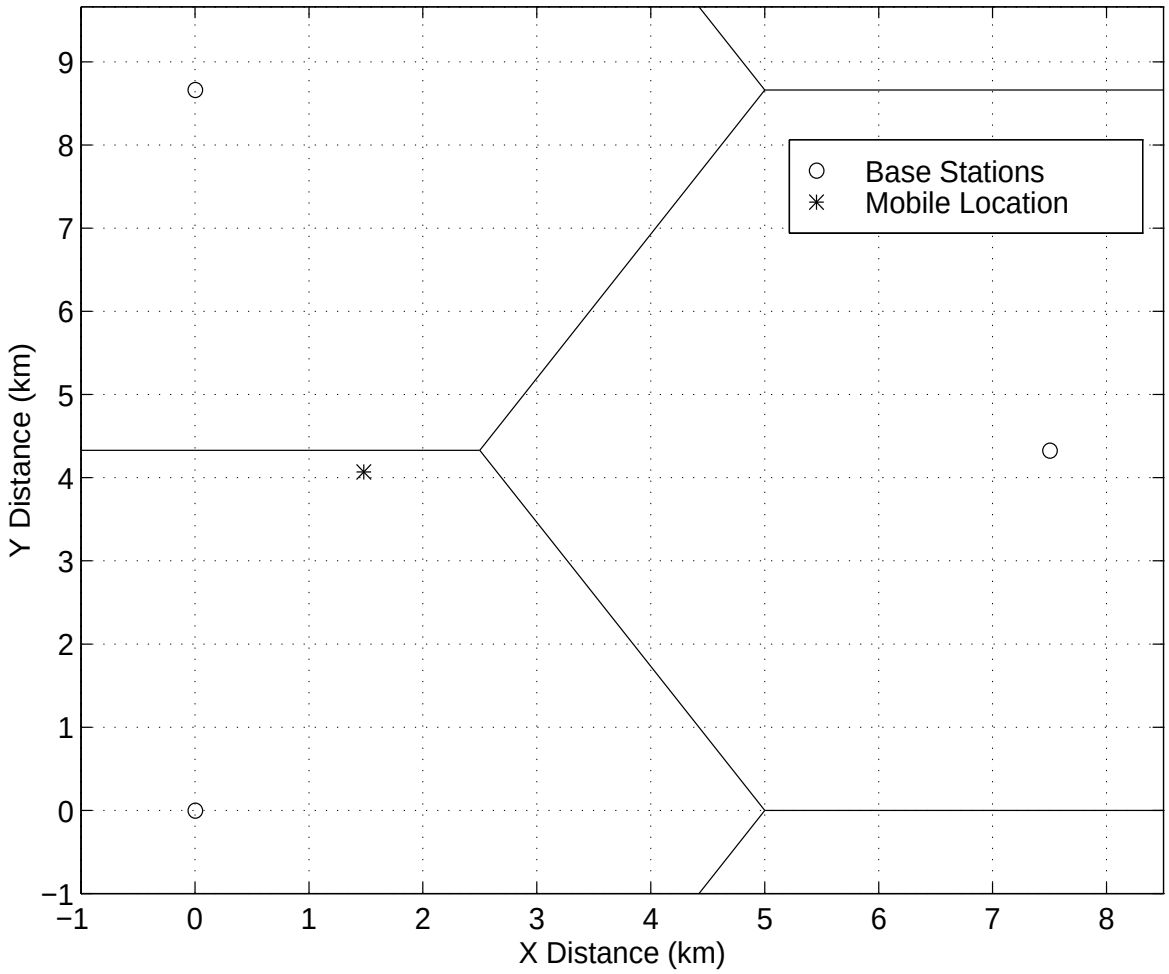

Figure 5.1: Mobile Position within a 3 Base Station Macrocellular Configuration

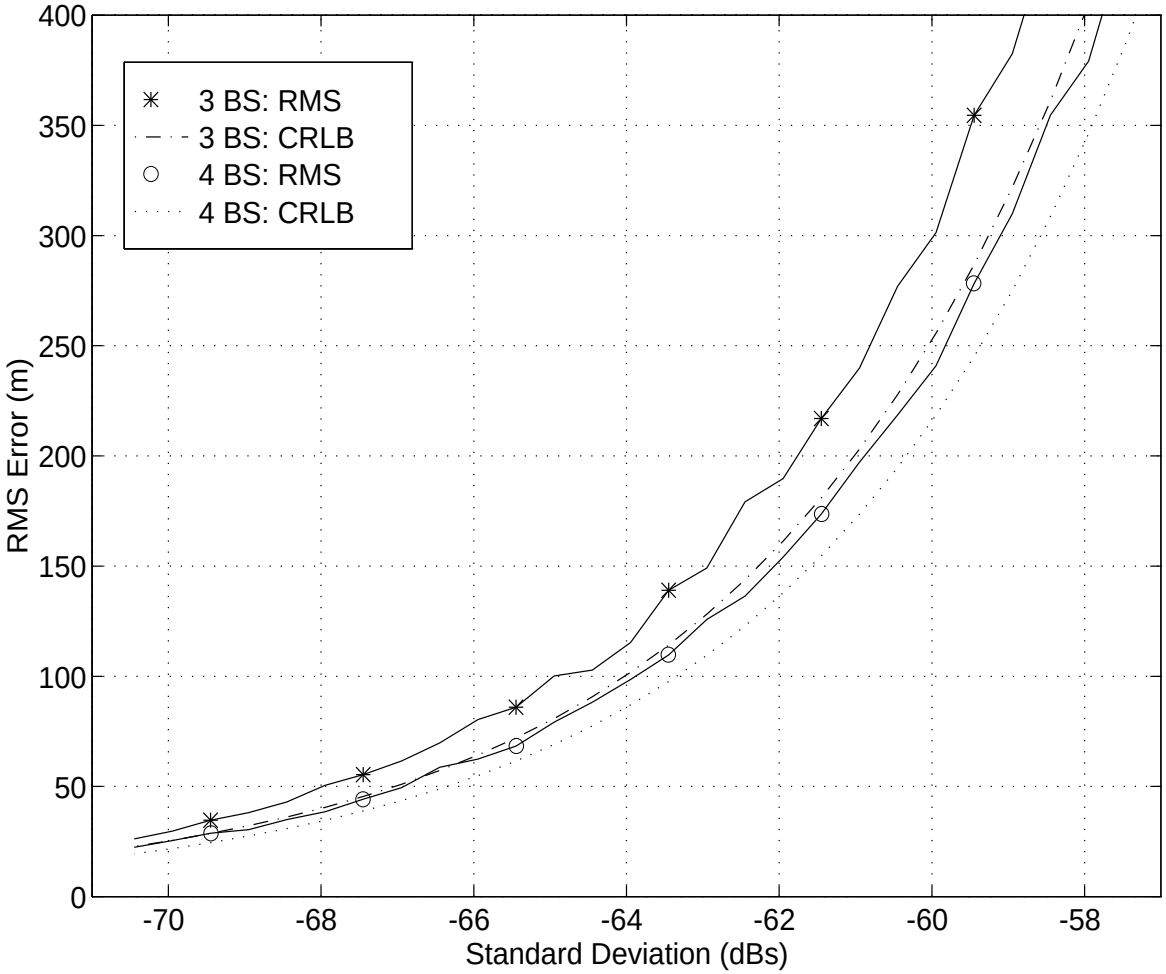

Figure 5.2: RMS PL Error vs TDOA Estimation Accuracy for 3 and 4 Base Station Configuration in an AWGN Reverse Channel of a CDMA Macrocellular System (R=5 km, n=2.5)(Standard Deviation = Accuracy)

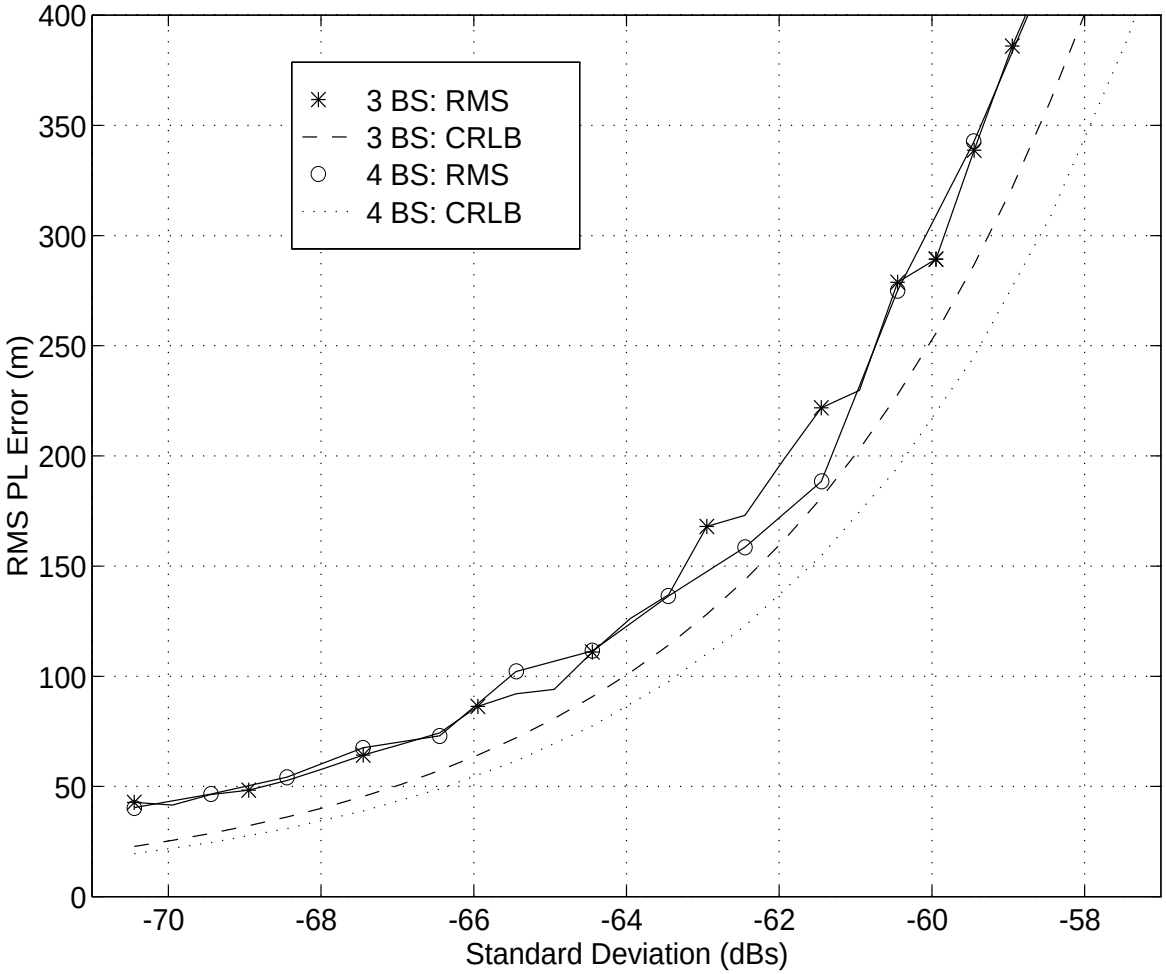

Figure 5.3: RMS PL Error vs TDOA Estimation Accuracy for 3 and 4 Base Station Configuration in an AWGN Reverse Channel of a CDMA Macrocellular System (R=5 km, n=3.6)(Standard Deviation = Accuracy)

5.3.2 Microcellular Environment

In a similar simulation, the performance of the hyperbolic PL technique within a microcellular CDMA environment was evaluated. The same base station configurations as indicated by Figures 4.2 and 4.3 were used. For the three base station configuration, the base stations were located at BS#=$(0, 0)$, BS#2=$(1500, 866)$ and BS#3=$(0, 1732)$. For the four base station configuration, an additional base station was located at BS#4=$(-1500, 866)$.

The mobile position was located near the cell boundary at $(x_m = 281, y_m = 772)$ and the SNRs at the neighboring base stations are sufficiently high enough to facilitate the TDOA estimation between base stations. The simulation was performed for a cell size of $R = 1$ km, path loss of $n = 3.5$ and a 1000 chip observation window. Figure 5.4 indicates the location of the mobile within a three base station microcellular system and Figure 5.5 presents the results of the simulation.

From the figure, it can be seen that the PL performance from both base station configurations follows closely with the CRLB at lower TDOA errors. As with the macrocellular system, the PL estimation accuracy begins to deviate from the CRLB at higher TDOA error levels. At higher TDOA noise levels, the RMS PL error performance of both hyperbolic PL system configurations sharply increase. As before, the simulation results clearly indicates the performance gains due to redundant range difference measurements. The four base station configuration in the microcellular environment offers approximately 1 dB better noise tolerance and approximately 17% better RMS accuracy than the three base station configuration and is able to provide precise position location estimates for a much wider range of TDOA noise levels.

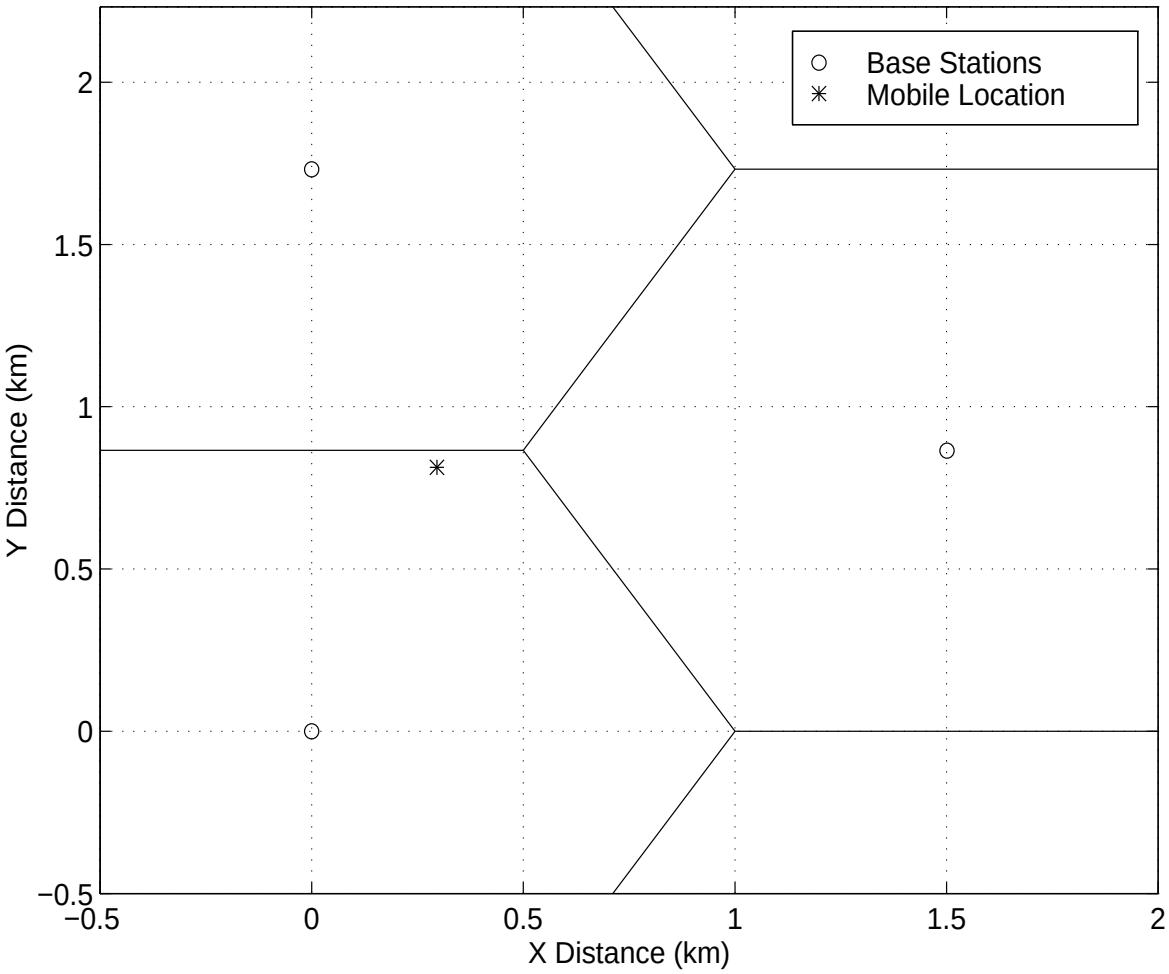

Figure 5.4: Mobile Position within a 3 Base Station Microcellular Configuration

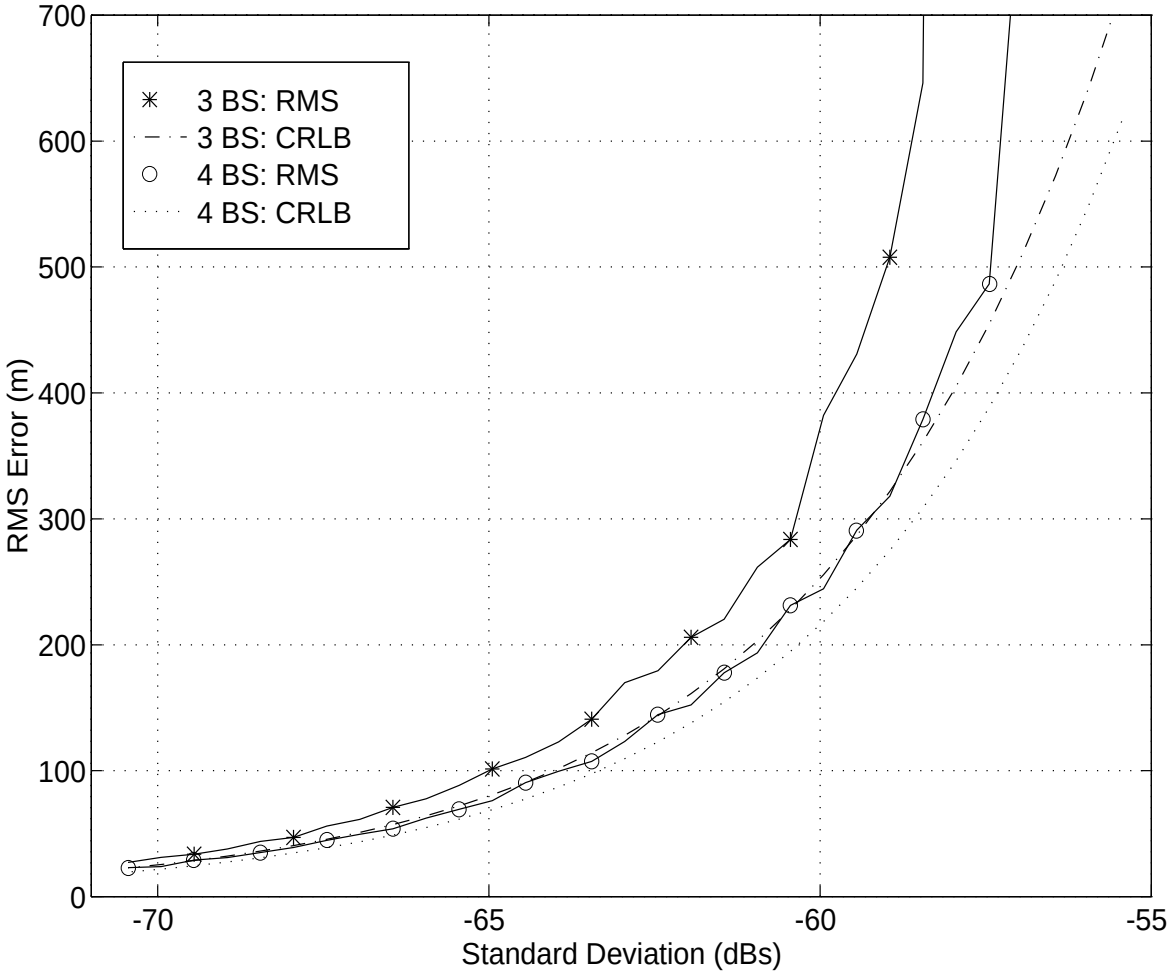

Figure 5.5: RMS PL Error vs TDOA Estimation Accuracy for 3 and 4 Base Station Configuration in an AWGN Reverse Channel of a CDMA Microcellular System (R=1km, n=3.5)

5.3.3 Microcell versus Macrocell

In the previous simulations, the mobile unit was located at the relatively same position within the cellular system. Thus it is interesting to compare the results of the previous simulations. A comparison of the performance of the hyperbolic PL system in 3 base station microcellular and macrocellular CDMA systems is provided in Figure 5.6.

Figure 5.6 indicates the RMS PL performance of both system configurations is identical for small TDOA errors and closely follow the CRLB. However, the performance of the microcellular system deviates from the CRLB more quickly than for the macrocellular systems. At higher TDOA estimation errors, the microcellular system appears to reach a threshold and the RMS PL error begins to sharply increase, while the RMS PL performance of the macrocellular system continues to follow the CRLB. The results suggest that microcellular systems may be more sensitive to TDOA estimator accuracy than macrocellular systems and that performance of the PL system improves as the spatial diversity between base station increases.

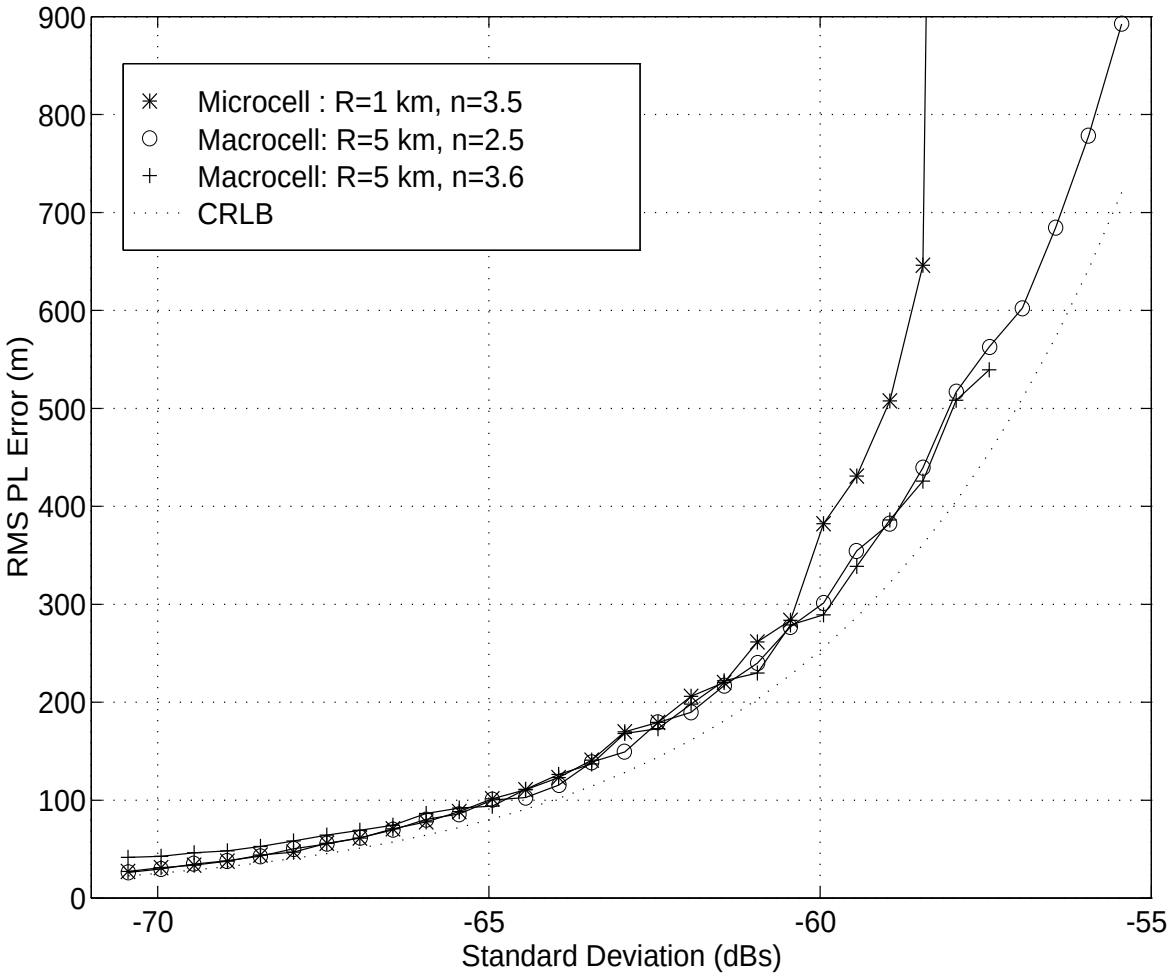

Figure 5.6: RMS PL Error vs TDOA Accuracy for a 3 base station microcellular and macrocellular CDMA system

5.4 Location of Mobile

In this section, the performance of the hyperbolic PL system as a function of the location of the mobile user within a CDMA system is evaluated. The RMS PL error for various mobile positions is determined and compared to the CRLB. The effect of base station geometry, as indicated by the geometric dilution of precision (GDOP) and the circle of error probability (CEP) factors, on the accuracy of the PL estimate for each location is also evaluated.

The three base station configuration of Figure 4.2 was used, and mobile locations within the cell are indicated in Figure 5.7. The coordinates of each mobile position are provided in Table 5.2. In the simulation, a cell radius of $R = 5$ km, path loss of $n = 3.6$ and TDOA noise level of $\sigma_d = 407$ ns were used. In order to evaluate the relative effect of the location of the mobile unit on the PL accuracy, the SNRs at all base station were made sufficiently high enough in order to not influence the results.

Table 5.3 provides the MSE, RMS and theoretical MSE and RMS results for each mobile position. The simulation results indicate that PL accuracy improves as the mobile moves farther away from the controlling base station, BS#1, and to a point symmetrical to all base stations. An improvement of approximately 38% in RMS PL accuracy is realized when the mobile moves from position #1 to position #9. Furthermore, improvement in performance is realized as the difference between the RMS PL results and the CRLB decreases from 40% to 15%.

As indicated in Chapter 2, the accuracy of PL estimate is best when the hyperbolas defined by the range difference equations intersect at 90 degrees. A degradation in performance is experienced when the intersection deviates from this ideal condition. Table 5.4, which provides the GDOP and CEP factors for each position, illustrates the effect of the base station geometry on the performance of the hyperbolic PL system. The smaller the GDOP factor the better the configuration of the base stations. Higher GDOP factors indicate that the base station configuration deviates from the optimal configuration, which is reflected in the RMS PL results of Table 5.3. As the mobile becomes more symmetrically located with respect to the base stations, the base station geometry improves, which leads to better PL performance.

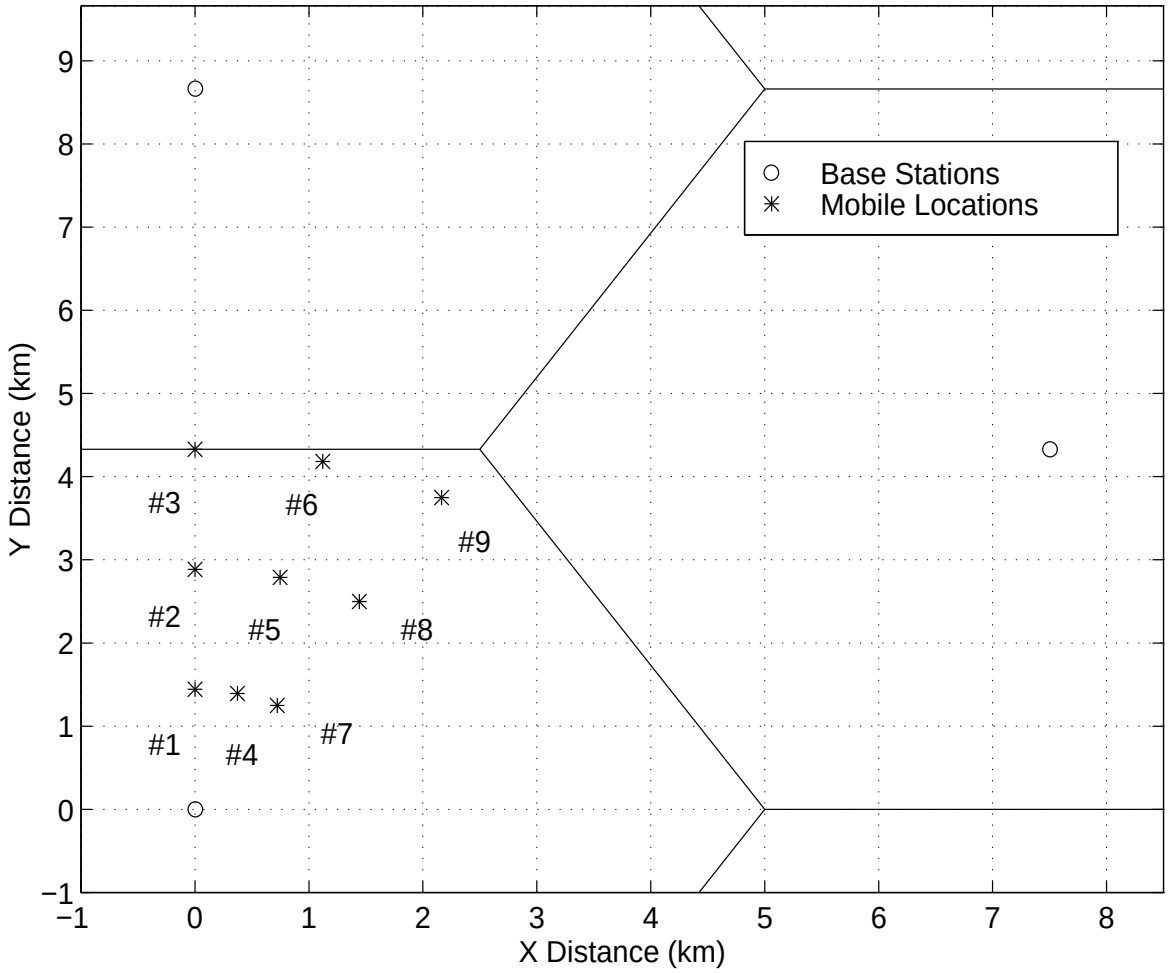

Figure 5.7: Mobile Locations within a 3 Base Station Configuration

Table 5.2: Coordinates of Mobile Positions in Figure

Position	**X**	**Y**
#1	0.00	1443.09
#2	0.00	2886.17
#3	0.00	4329.26
#4	373.50	1393.92
#5	747.00	2787.83
#6	1120.50	4181.75
#7	721.54	1249.75
#8	1443.09	2499.50
#9	2164.63	3749.25

Table 5.3: MSE and RMS Position Location Error and Cramér Rao Lower Bound for Each Mobile Locations

Position	**CRLB : MSE**	**MSE**	**CRLB : RMS**	**RMS**
#1	17109.18	33510.20	130.80	183.06
#2	15453.50	26206.10	124.31	161.88
#3	14901.16	23063.71	122.07	151.87
#4	15049.38	24036.60	122.68	155.04
#5	12554.10	19269.02	112.05	138.81
#6	11127.22	17265.02	105.49	131.40
#7	14412.38	22139.76	120.05	148.79
#8	11692.43	19169.56	108.13	138.45
#9	10139.00	13118.55	100.69	114.54

Table 5.4: Geometric Dilution of Precision and Circle of Error Probability Results

Position	**GDOP**	**CEP**
#1	1.377	137.65
#2	1.282	121.77
#3	1.259	113.36
#4	1.267	114.41
#5	1.044	104.53
#6	0.969	98.35
#7	1.268	111.87
#8	1.101	103.92
#9	0.920	85.68

5.5 Path Loss

This section evaluates the effect of the path loss factor on the performance of the hyperbolic PL system. To evaluate the effect of path loss on PL performance, the RMS PL error was determined at three mobile positions for a range of path loss factors. In the simulation, a three base station configuration with cell radius of $R = 5$ km, an observation window of 2000 chips and TDOA estimator accuracy of $\sigma_d = 10$ ns were used. The locations of the mobile unit within the cell are indicated in Figure 5.8. The path loss factor was varied from $n = 2.5$ to 4. For simplicity, it was assumed that each channel experiences the same path loss.

As the simulation results in Figure 5.9 indicate, at lower path loss factors, the PL performance for all three mobile locations is unaffected as only a slight increase in PL error is experienced. However, at higher path loss factors, while the PL system continues to provide precise PL estimates for the two farther mobile locations, the PL error of the closer mobile location begins to sharply increase. The more distant mobile locations require higher transmit power levels to maintain a specific SNR. This improves the signal power levels at the neighboring base stations. Furthermore, because the mobile is closer to the cell boundary, it is also closer to the neighboring base stations. These smaller transmitter-receiver distances reduce the attenuation experienced by the signal. Even though the channel path loss increases, the higher transmit power and closer proximity compensates for the signal attenuation, which results in precise PL estimation. In contrast to the two farther mobile locations, the closer mobile location needs to transmit at lower power levels to maintain adequate SNR at the controlling BS. This reduces the available power at the neighboring base stations. Furthermore, the distance to the neighboring base stations increases and the signal experiences much greater attenuation. As a consequence, PL performance suffers because of poor signal quality.

The results from this simulation indicate that, depending on the location of the mobile, path loss may or may not have a significant influence on PL performance and that only slight changes in the location of the mobile can significantly effect the sensitivity of the hyperbolic PL systems performance to the path loss of the propagation channel.

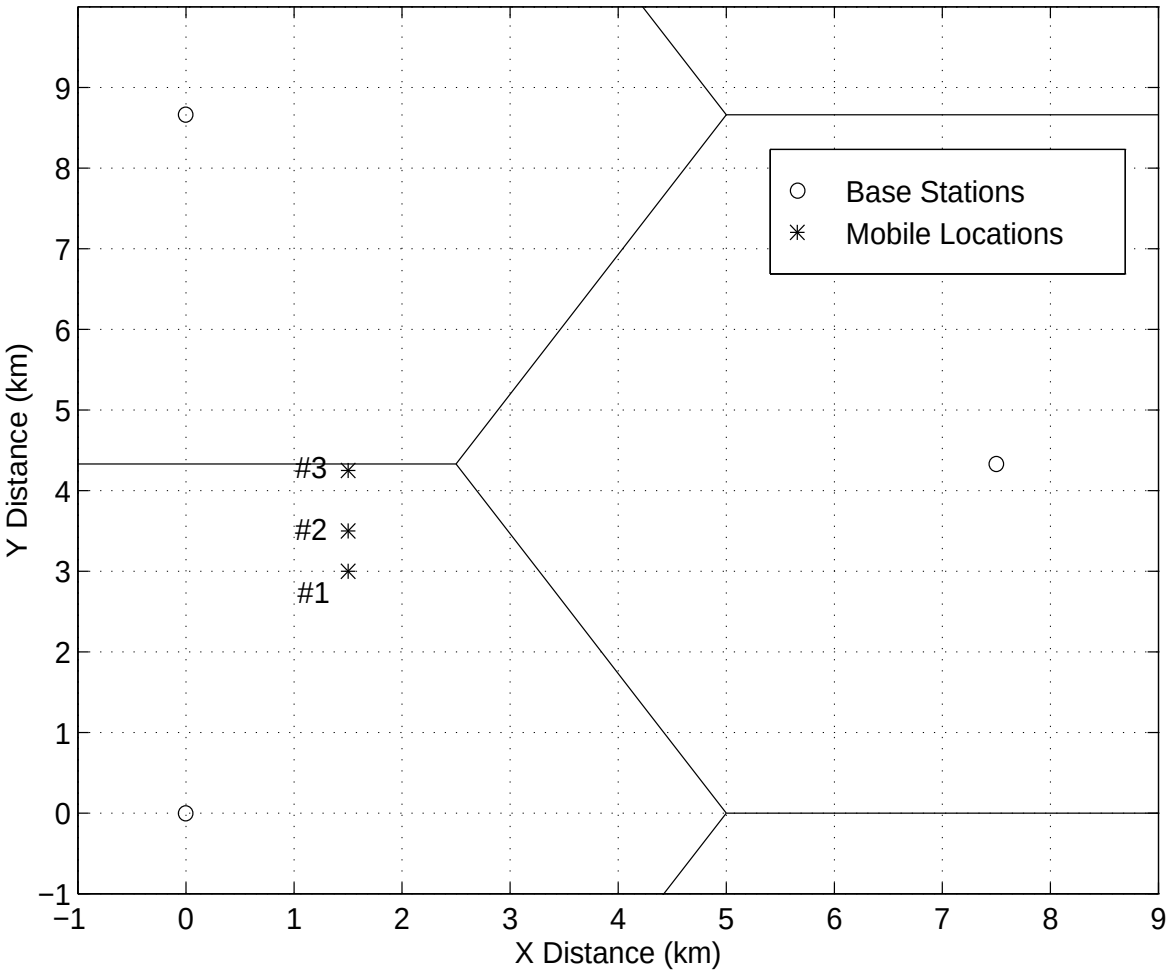

Figure 5.8: Mobile Location within a 3 Base Station Configuration

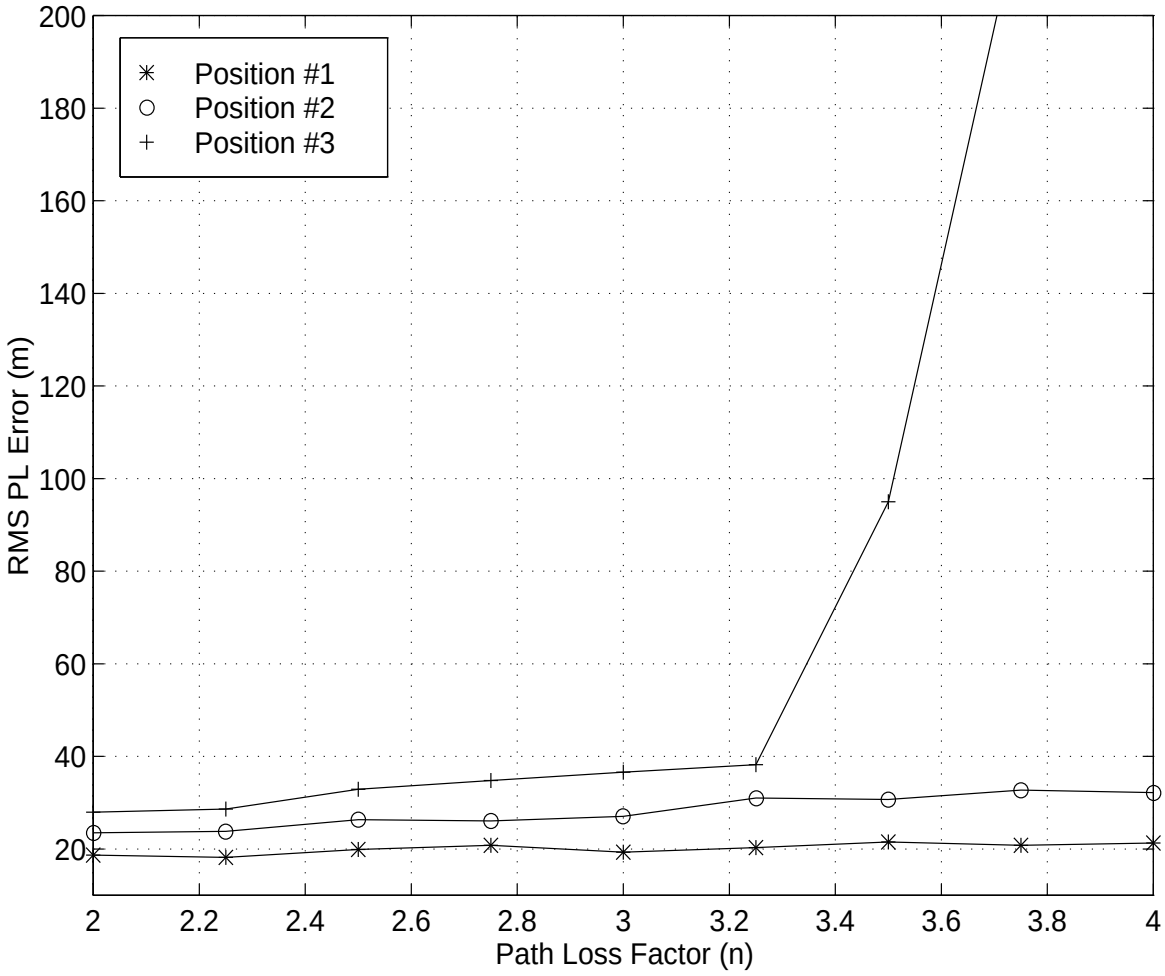

Figure 5.9: RMS PL Error vs Path Loss Factor for 3 Mobile Positions (R=5km, T=2000 chips)

5.6 Performance under CDMA Power Control

The results presented here demonstrate the effect of CDMA closed-loop power control on the performance of the hyperbolic PL system. To evaluate the effect of the power control scheme, the RMS PL accuracy at several mobile locations, extending from the cell boundary towards the controlling base station, was determined. Under CDMA power control, it is assumed that the mobile unit is required to maintain an SNR of 18 dB at the controlling base station.

To evaluate the effect of power control, several different simulation cases were performed. In the first case, a path loss factor of $n = 2.5$, a 2000 chip observation window and TDOA estimator accuracy of $\sigma_d = 285$ ns were used. In the second case, a path loss factor of $n = 3.6$, a 5000 chip observation window and TDOA estimator accuracy of $\sigma_d = 10$ ns were used. The three and four base station configurations of Figure 4.2 and Figure 4.3, with cell radius of $R = 5$ km, and an AWGN channel were used in the simulations. The locations of the mobile unit within the cell is indicated in Figure 5.10. The simulation results for the first case is provided in Figure 5.11 and Figure 5.12 illustrates the RMS PL error results for the second case.

The results from both cases indicate that both BS configurations provide acceptable PL results when the mobile is close to the cell boundary. In the region around the cell boundary, the SNRs at all BS's is sufficiently high enough to permit accurate TDOA estimation between BS's. However, as the mobile reduces its transmit power as it moves closer to the controlling base station, lower SNRs are experienced at the neighboring BS's. This results in a gradual increase in PL error. When the SNR at the neighboring BS's reaches much lower levels, RMS PL error begins to sharply increase, providing unacceptable PL accuracy. The simulation results indicate that a SNR threshold level, in which the PL error begins to sharply increase, exists. In the first simulation, the SNR threshold level at the neighboring base stations was found to be approximately 10 dB, while in the second simulation, which utilizes a longer observation window, a threshold level of approximately 7 dB was experienced.

The simulation results also indicate that redundant range difference measurements made from additional base stations do not always improve PL performance. When signals are received at low SNR, the TDOA estimate and resulting PL estimate will be

inaccurate. Although the nearest neighboring base stations recieve the users signal with adequate SNR, it appears that the corrupted range difference measurement from the fourth, and most distant base station, introduces significant errors in the PL estimate.

Most importantly, the results from the first case suggest that under closed-loop CDMA power control, hyperbolic PL systems will only meet FCC 2-D requirements on accuracy for approximately 40% of the coverage area. While the second case offers better performance, it still does not provide complete coverage of the cell. Issues concerning cell coverage and the effect of the observation window on the operational range of the hyperbolc system are dealt with in the following section.

In a third simulation, the three base station configuration of the first simulation was repeated for a path loss factor of $n = 3.6$ and compared to the simulation results of the first case. As seen by Figure 5.13, the different path loss factors do not appear to have a significantly influence on PL performance. The higher path loss factor are compensated for by the higher transmit power required of the mobile to maintain adequate SNR at the controlling base station.

Now we consider the situation in which the mobile is instructed to transmit at maximum power when the call is recognized as an E-911 emergency request. Figure 5.14 compares the PL performance between a mobile under the CDMA power control and when the mobile is able to transmit at maximum power. While the increased power level provides only slight improvement in the PL accuracy, dramatic improvements in the coverage area over which effective PL estimation can be performed is experienced. However, this improvement in PL coverage area comes at the expense of system capacity. Because the mobile does not reduce transmit power as it moves closer to the controlling base station, the interference level due to the mobile increases, causing the near-far effect. This reduces the signal quality of all other users and results in an increase in dropped calls.

The simulation results presented here clearly demonstrate that position location coverage is severely limited under CDMA closed-loop power control. Methods which mitigate this power control problem must be developed if universal coverage of PL systems is to become a reality. Although cell coverage of PL systems can be extended if transmit powers are increased, system capacity is severely effected.

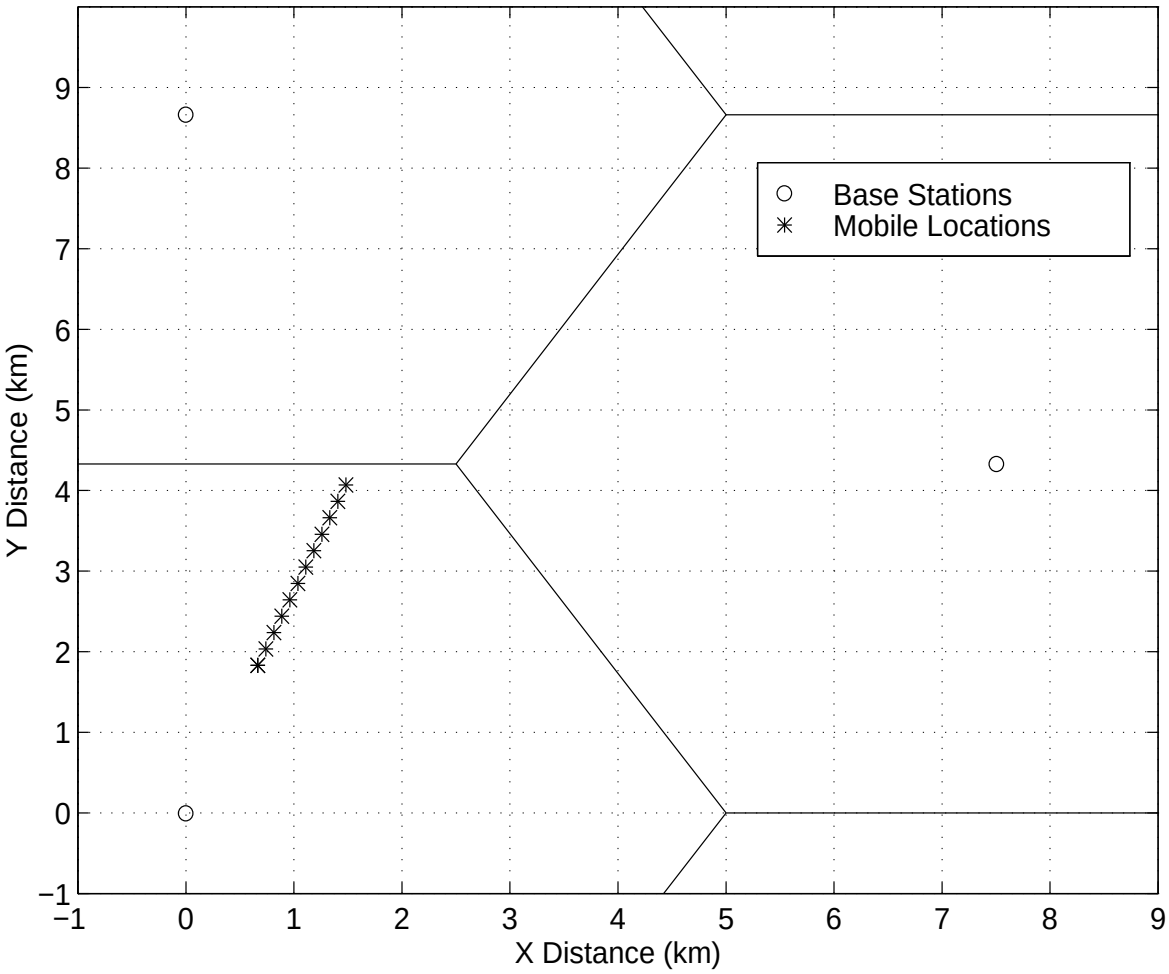

Figure 5.10: Mobile Positions in a 3 Base Station Macrocellular Configuration

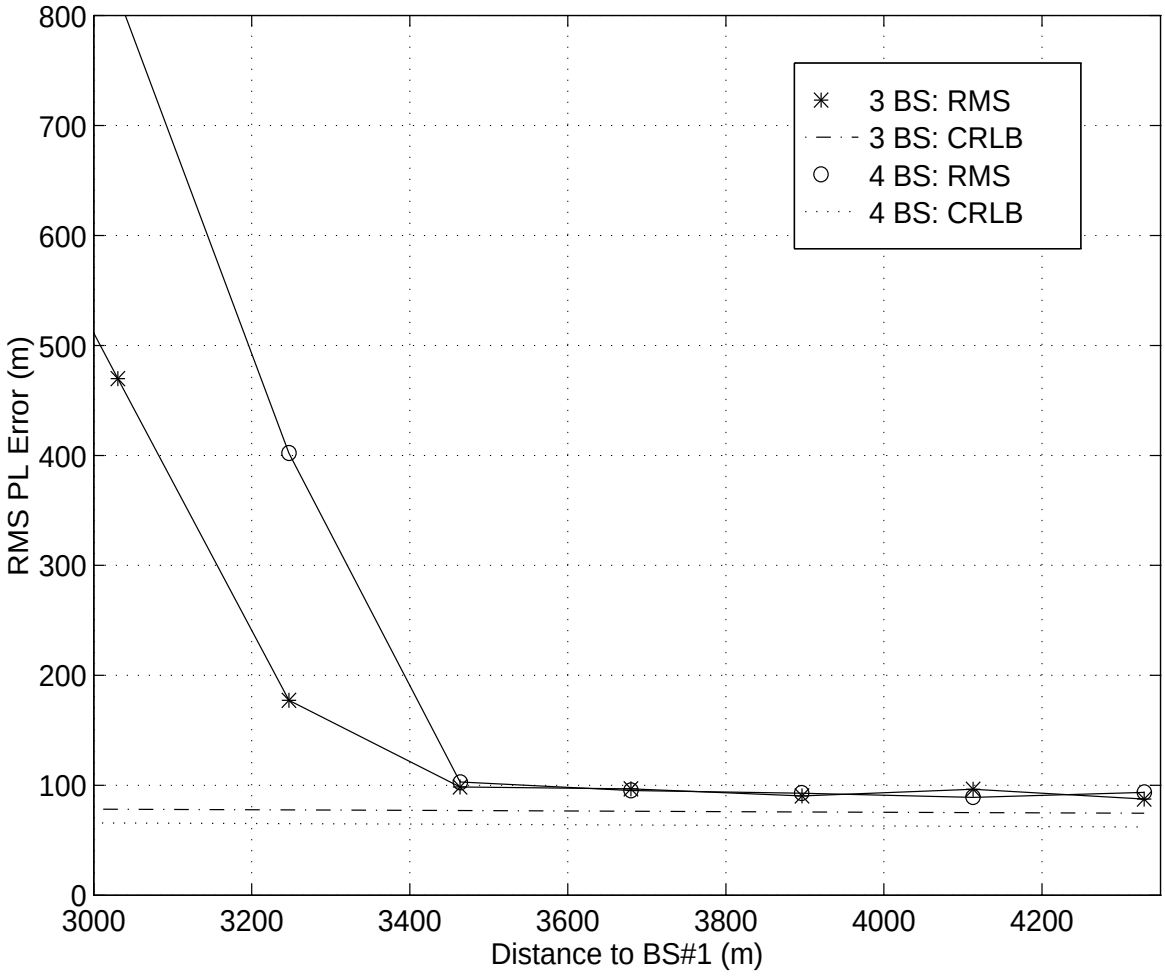

Figure 5.11: RMS PL Error vs Distance of Mobile to BS# 1 in a 3 and 4 Base Station Configuration: Closed-Loop Power Control (n=2.5, T= 2000 chips, $\sigma_d = 285$ ns)

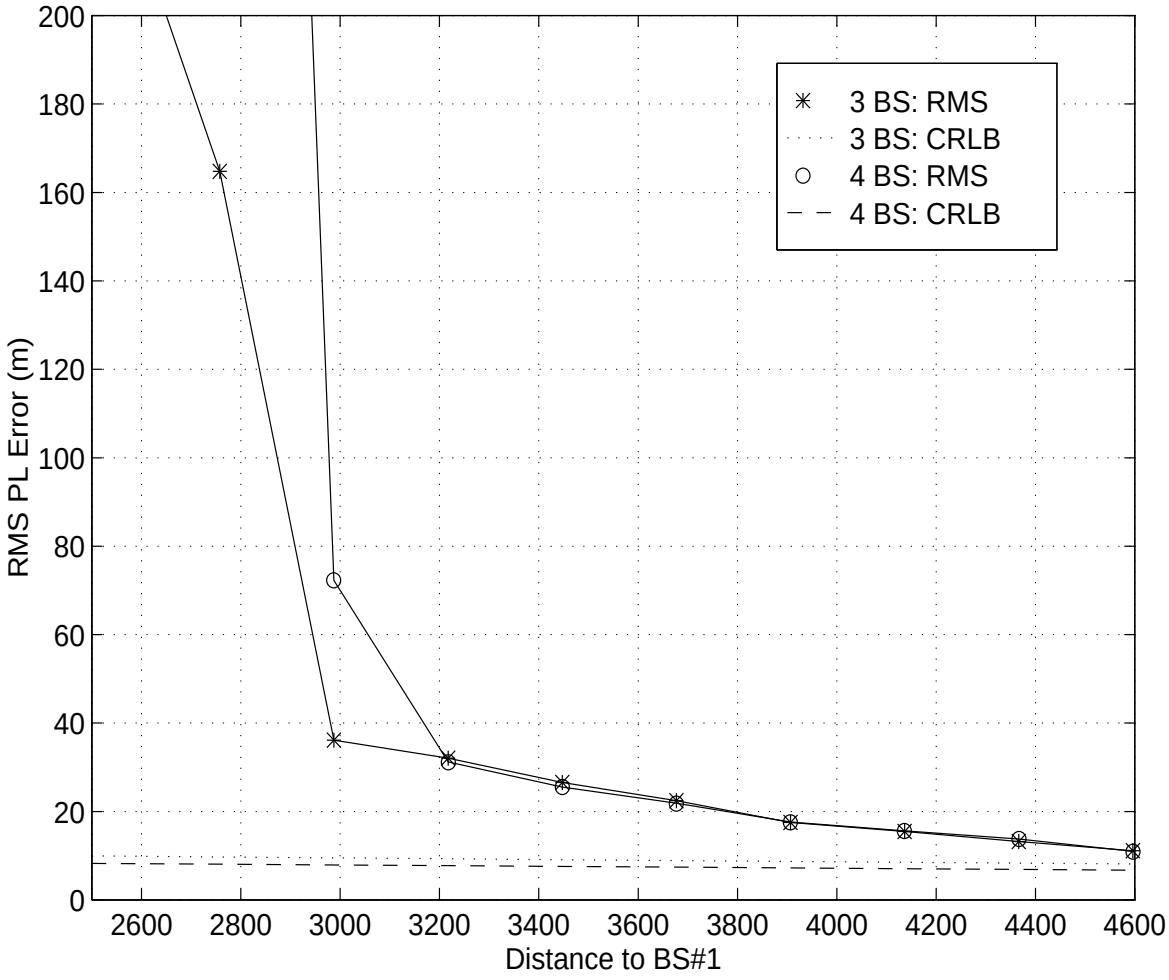

Figure 5.12: RMS PL Error vs Distance of Mobile to BS# 1 in a 3 and 4 Base Station Configuration: Closed-Loop Power Control (n=3.6, T= 5000 chips, $\sigma_d = 10$ ns)

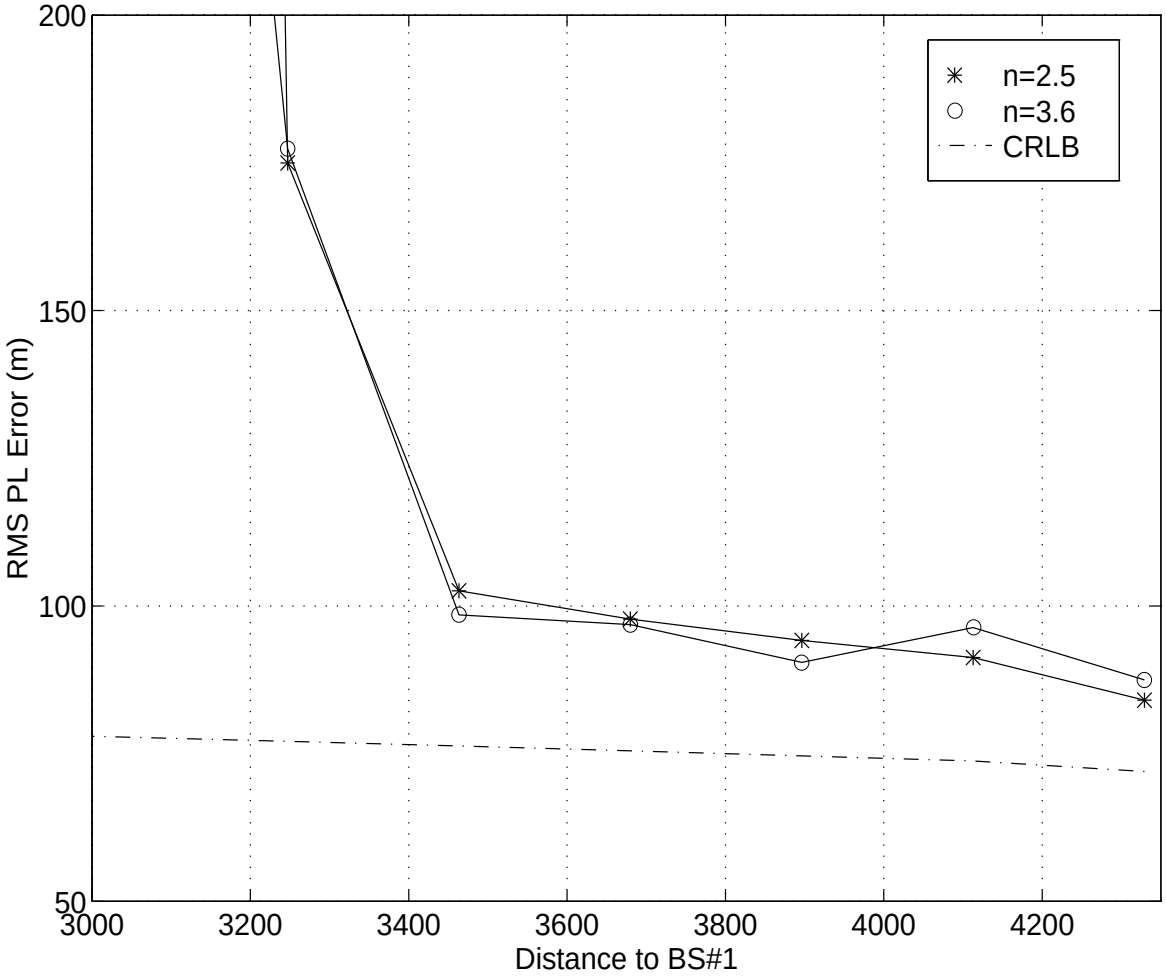

Figure 5.13: RMS PL Error vs Distance of Mobile to BS# 1 for Path Loss n = 2.5 and 3.6 in a 3 Base Station Configuration: Closed-Loop Power Control (T=2000 chips, $\sigma_d = 285$ ns)

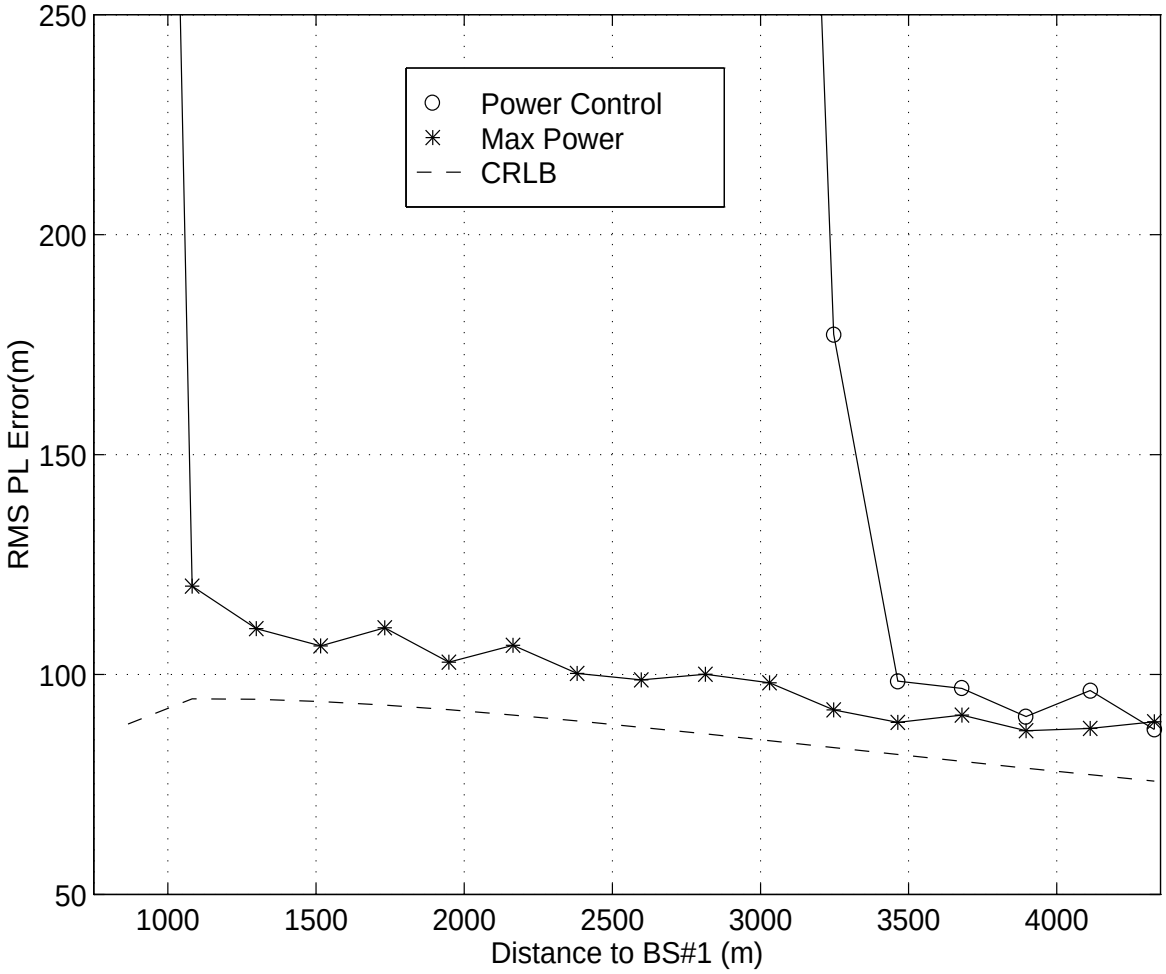

Figure 5.14: RMS PL Error vs Distance of Mobile to BS# 1 in a 3 Base Station Configuration: Mobile under Closed-Loop Power Control and Transmitting a Maximum Power (n=2.5, T= 2000 chips, $\sigma_d = 285$ ns)

5.7 Observation Window Length

While it has been shown that the signal power levels at the neighboring base stations can influence PL performance, PL accuracy and cell coverage are also influenced by the length of the observation interval over which the signal is captured at each base station and correlated to provide a TDOA estimate. In this section we investigate the effect of the length of the observation window on PL performance.

To evaluate the effect of the observation length, the RMS PL error of several mobile positions, extending from the cell boundary towards the controlling base station, for different observation window lengths were determined. In the simulation, a three base station configuration with a cell size of $R = 5$ km, path loss factor of $n = 3.6$ and TDOA estimator accuracy of $\sigma_d = 10$ ns were used. Observation lengths of 1000, 2000, 5000, and 10,000 chips, which corresponds to a signal interval of approximately 0.8 ms, 1.6 ms, 4 ms and 8 ms respectively, were used. The locations of the mobile within the cell are the same as those indicated in Figure 5.10.

Figure 5.15, which illustrates the results from the simulation, clearly indicates the improvement in PL estimation accuracy as the observation window increases. Near the cell boundary, an observation window of 1000 chips is sufficient to provide reasonable PL estimation. However, a doubling of the observation window provided approximately 20% better PL accuracy, while a observation window with an order of magnitude greater length provided approximately 66% better performance. As the observation window increases, a relatively constant improvement in PL performance is experienced.

As the mobile moves from the cell boundary towards the controlling base station, lower transmit power levels are required of the mobile unit and the distance between the mobile unit and neighboring base stations increases. This results in lower signal powers at the neighboring base stations. As the SNRs decrease, the correlation strength of the PN sequences over the smaller observation windows are unable to overcome the effects of low signal powers and the PL error rises sharply. However, longer observation windows improve the correlation properties of the observed PN sequences between base stations and is able to maintain accurate TDOA estimation and PL accuracy over a much greater range.

More importantly, the simulation results indicate how longer observation windows can extend the coverage region of the hyperbolic PL system. An improvement in coverage of approximately 10% is experienced when the observation window is doubled from 1000 to 2000 chips, and a 40% improvement when the observation window increases by an order of magnitude. The results also demonstrate the ability of longer observation windows to overcome the effects of low received SNR levels at the base stations. In these simulations, a slow fading channel was assumed. If the channel exhibits fast fading, in which the impulse response of the channel does not remain constant over the observation window, it is expected that longer obervation times can be used to improve the correlation properties between corrupted received signals, resulting in improvements in PL performance. It should be noted that the improvements in PL performance due to the increased length of the observation window comes at the expense of increased computational time and resources. However, the improvements in PL accuracy and coverage offset these added requirements.

As observed in the previous simulation, a threshold level for each of the observation windows exist. The SNR threshold levels for the 1000, 2000, 5000 and 10,000 chip observation windows were found to be approximately 13, 10, 7, and 2 dB respectively. Thus an improvement in the dynamic range of the PL system is achieved for a longer observation windows. In order to evaluate the cell coverage based on these SNR threshold levels, a contour plot indicating the coverage pattern was developed. Figure 5.16 illustrates cell coverage pattern based on various SNR levels at the neighboring base stations. As one can see, depending on the location of the mobile, the operational range of the hyperbolic system varies. The greatest range of coverage occurs for mobile locations symmetrically between base stations, with a decrease in range as the position deviates from this ideal location.

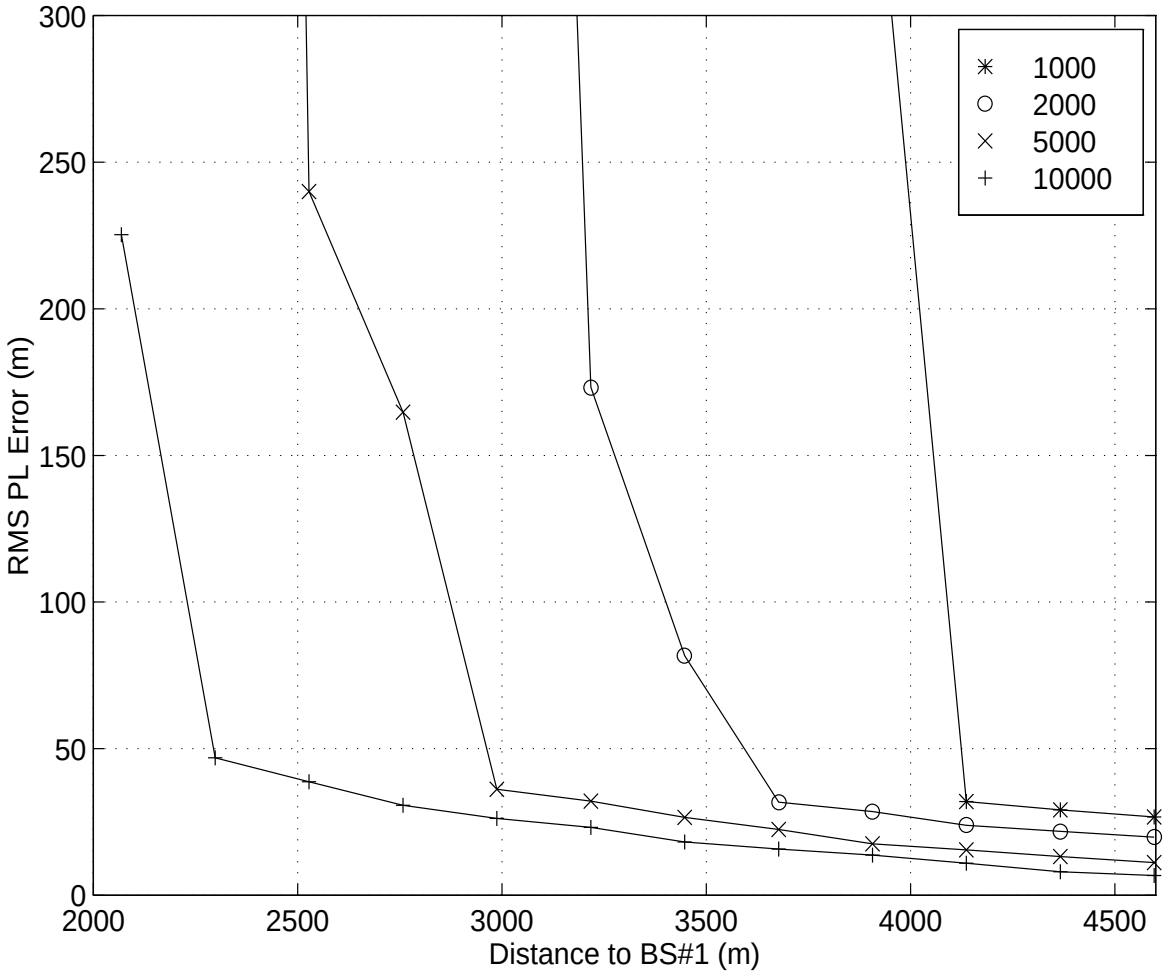

Figure 5.15: RMS PL Error vs Distance to BS#1 for Observation Windows of 1000, 2000, 5000, and 10,000 chips (R=5km, n=3.6)

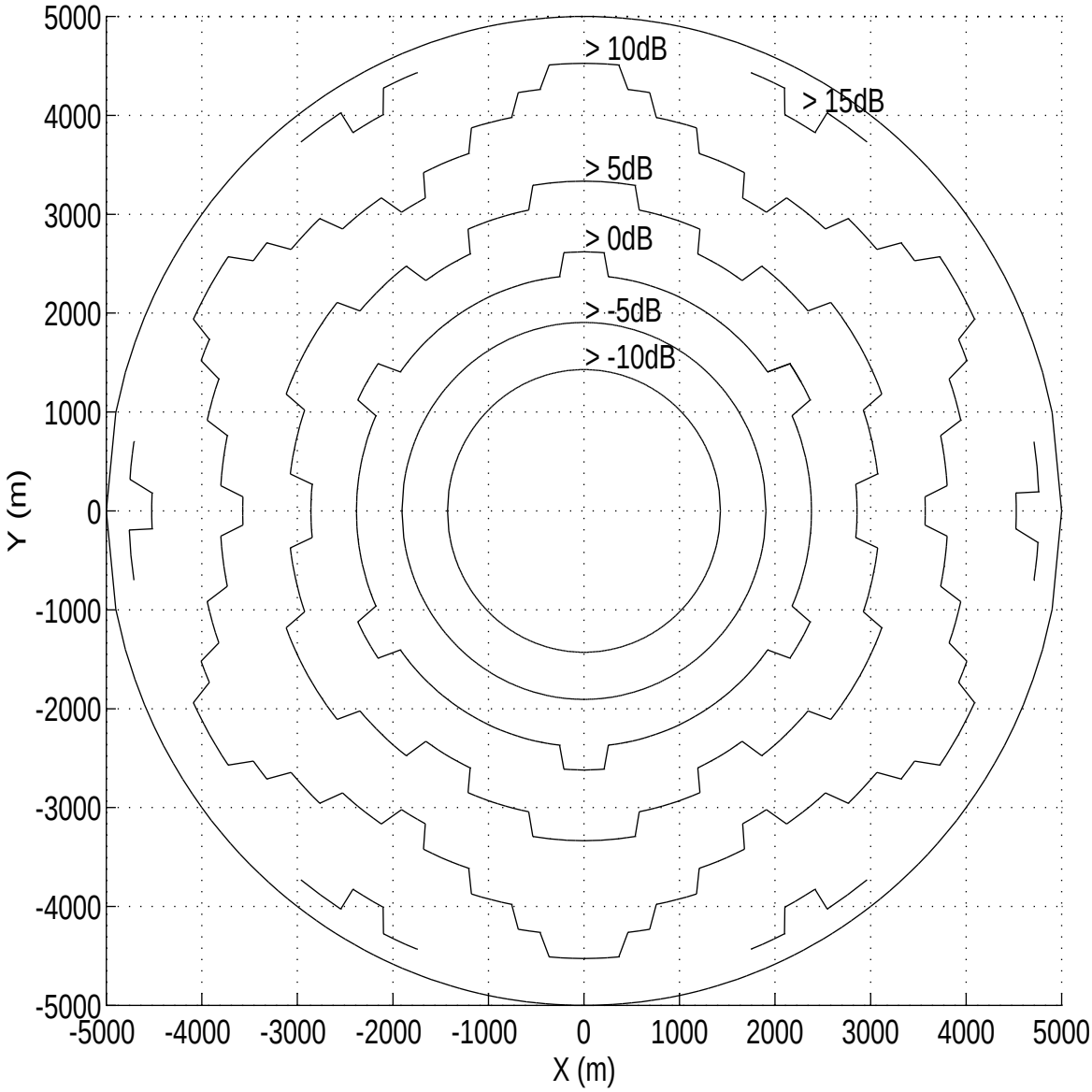

Figure 5.16: Cell PL Coverage based on SNR's at Neighboring Base Stations

5.8 Performance in Multipath

In this section, the performance of the hyperbolic PL system in the presence of multipath is examined. To evaluate the effects of multipath, a single multipath component is introduced in the channel to BS#1. The delay and signal strength of the multipath component relative to the LOS signal is varied and the effect on the PL performance is determined. The mobile position and base station locations are the same as indicated in Figure 5.1. A cell radius of $R = 5$ km and path loss of $n = 2.5$ were used. With the mobile at this location, the SNR at each base station is sufficiently high enough to facilitate the TDOA estimation between them. To evaluate the relative effect of the multipath, the TDOA noise level was set to $\sigma_d = 28.5$ ns.

The results for multipath signal strengths of $\alpha = 0.1, 0.5, 0.7, 0.8$, and 0.9 are provided in Figure 5.17. From the plot, it can be seen that as the relative signal strength of the multipath component increases so does the RMS PL error introduced by the multipath. At relative signal strengths of one-half or less, the hyperbolic PL estimator is able to follow the CRLB with only slight deviation. However, significant errors are introduced by multipath of higher relative strengths. For a multipath component with signal strength of $\alpha = 0.8$ arriving 1/6 of a PN chip later than the LOS, the multipath introduces approximately 2.5 times greater RMS PL error and for a multipath signal strength of $\alpha = 0.9$, approximately 5 fold increase in RMS PL error is experienced.

The results for multipath components with relative power of $\alpha = 0.7, 0.8, 0.9$, and 1 are shown in Figure 5.18. The plot indicates that when an equal power multipath components are present, the TDOA estimate and resulting RMS PL error is dominated by the multipath signal component. Although the LOS and multipath have identical power, the additional correlation between the delayed multipath and the delayed signals at neighboring BS's results in a higher correlation peak then the correlation due to the LOS signal.

This clearly illustrates a major drawback of using generalized cross-correlation (GCC) TDOA estimation methods. As discussed previously, GCC methods are not signal selective, and thus are unable to discern between correlation peaks caused by the LOS and multipath signal components. As a result, the assumption that the peak correlation is due to the LOS can result in significantly worse PL performance.

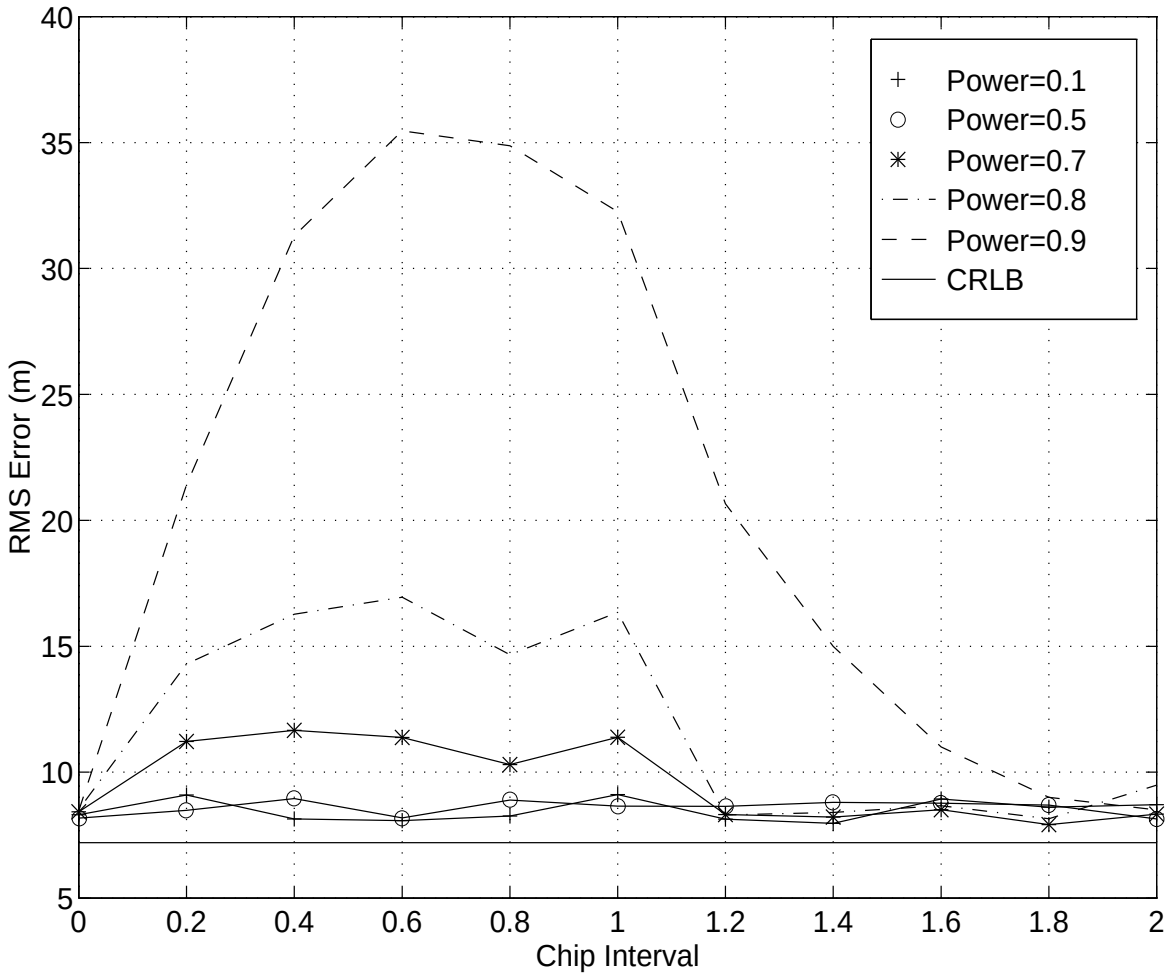

Figure 5.17: RMS PL error vs Relative Power of Multipath and Fractional Chip Delay of Multipath Component

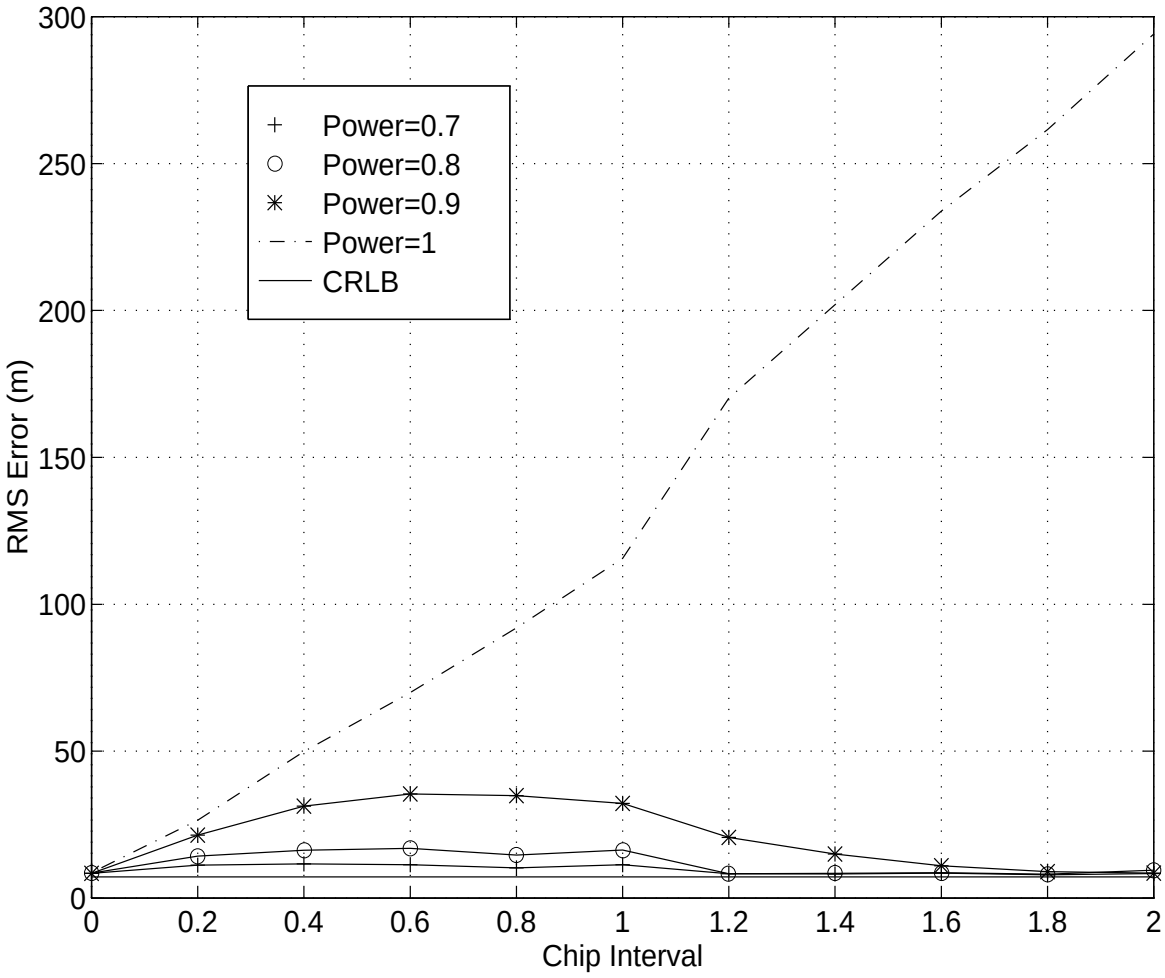

Figure 5.18: RMS error vs Relative Power of Multipath and Fractional Chip Delay of Multipath Component

5.9 Performance in Shadowed Channels

This section examines the effect of shadowed mobile environments on the performance of the hyperbolic PL system. To evaluate the effects of shadowing, the knife-edge diffraction model presented in Chapter 4 was implemented. A base station height of 50 meters was used and the mobile was assumed to be ground level. The simulations were performed for the three base station configuration of Figure 5.1 with cell radius of $R = 5$ km, path loss of $n = 2.5$ and TDOA estimator accuracy of $\sigma_d = 250$ ns. In the simulations, the mobile is required to maintain a SNR of 18 dB.

In the first simulation, an obstruction is introduced in the channel to BS#1. The height of the obstruction is varied and the effect of the excess path length and signal attenuation on the PL performance is observed. The obstruction was located 250 meters from BS#1 and the mobile was located at $(x_m = 500, y_m = 750)$. Figure 5.19 provides the results from the simulation. When the mobile is subjected to shadowed radio environments, the obstruction causes signal attenuation. As a result, the mobile must transmit at higher levels to maintain adequate SNR at the controlling base station. The higher transmit power required of the mobile improves the SNRs experienced at the neighboring base stations. This improves TDOA estimation and results in better PL performance as indicated by the plot. The excess propagation time experienced by the signal due to the increased path length did not appear to impact performance.

In the second simulation, an obstruction is introduced in the channel of a BS#3. The obstruction is located 250 meters from BS#3 and the mobile is located within the coverage area of BS#1 at $(x_m = 1500, y_m = 4250)$. The results of the simulation are provided in Figure 5.20. The figure clearly illustrates the degradation in performance due to shadowing of the mobiles propagating signal. As the obstruction height increases, attenuation of the signal propagating to BS#3 increases, resulting in lower SNR. As the SNR at BS#3 continues to decrease, the TDOA estimates results in worse PL estimation. While the obstruction improved the PL performance in the previous simulation, it clearly degrades performance in this simulation.

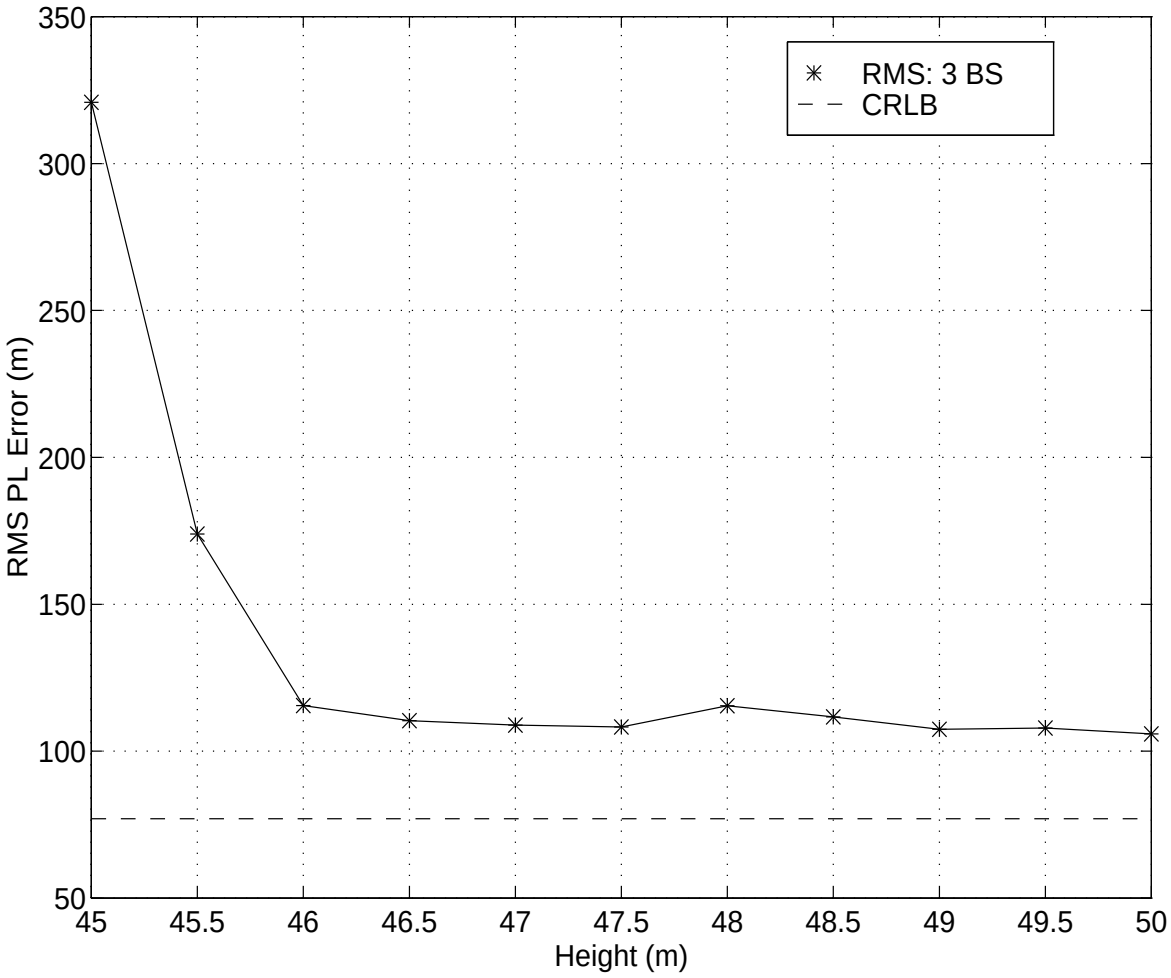

Figure 5.19: RMS PL error vs Height of Obstruction in the Channel to BS#1 for a 3 Base Station Configuration

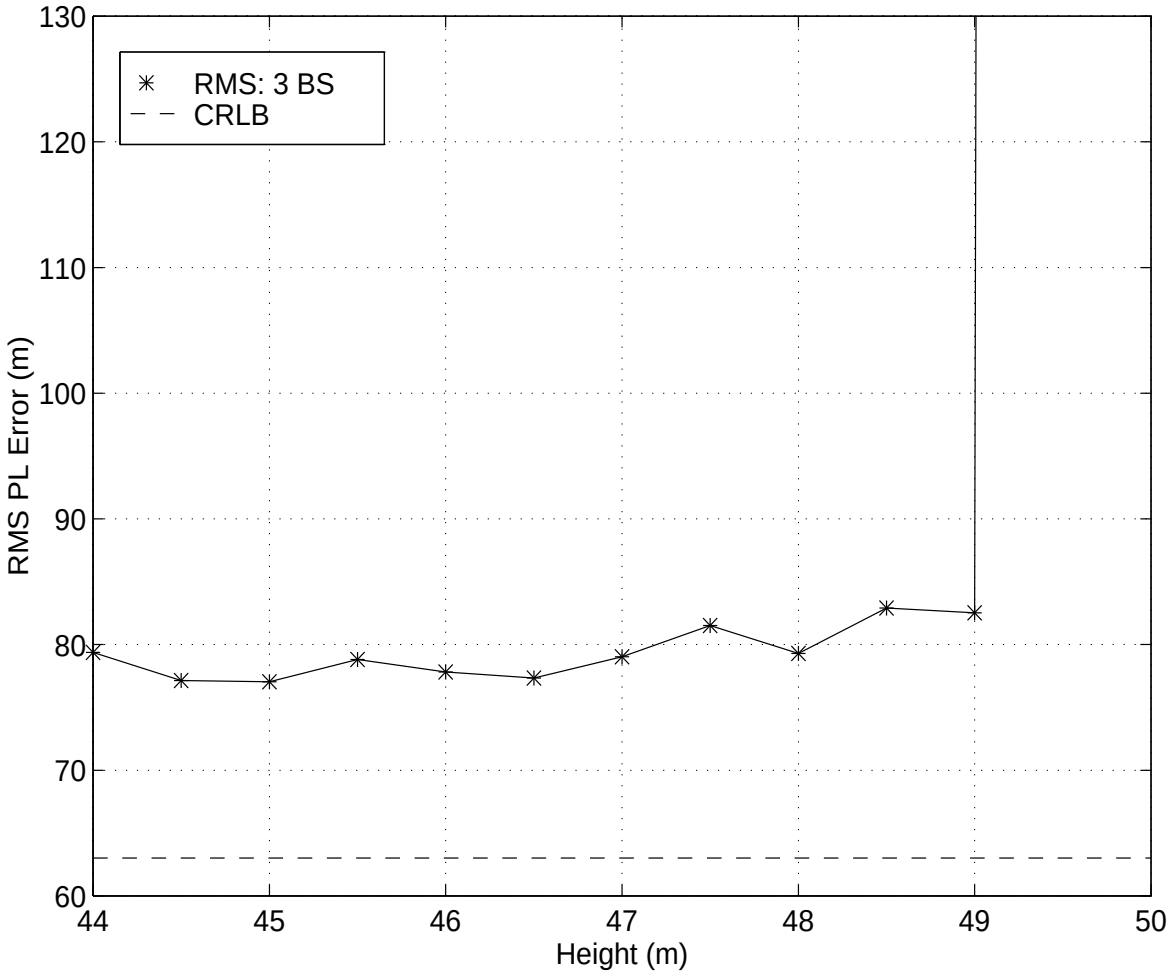

Figure 5.20: RMS PL error vs Height of Obstruction in the Channel to BS#3 for a 3 Base Station Configuration

5.10 Chapter Summary

This chapter provided a summary of the performance of the hyperbolic position location technique in a CDMA systems. The effect of various CDMA system parameters and channel conditions were investigated. The RMS PL performance of the hyperbolic PL system in a macrocellular and microcellular systems were presented. The effect of the TDOA estimation accuracy and the performance gains due to redundant TDOA measurements was illustrated. The degradation in PL performance due to the closed-loop power control scheme used in CDMA systems was presented. The performance of the PL system in multipath and shadowed mobile radio environments was demonstrated. Discussion of these results is provided in the following chapter.

Chapter 6

Conclusions and Future Work

This thesis provides an overview of hyperbolic position location techniques and evaluates the performance of hyperbolic PL systems within CDMA systems. The application of PL techniques for the geolocation of mobile users within CDMA cellular/PCS systems presents a major challenge. While the hyperbolic PL technique can provide effective PL estimation, the mobile radio channel environment and CDMA operation present practical limitations on PL performance.

The high rate pseudo-noise sequences used in CDMA systems facilitate high resolution TDOA estimation, which leads to accurate PL estimation. However, simulation results indicate that the accuracy of the TDOA estimate has a major impact on the accuracy of the PL estimate. The hyperbolic PL system can provide accurate PL estimates at low TDOA noise levels; however, RMS PL error sharply increases at higher noise levels. While both microcellular and macrocellular environments appear to be equally effected by TDOA accuracy, the size of the cells used in the CDMA system contribute to the sensitivity to the TDOA estimation accuracy.

The effect of the number of base stations used in the PL estimate was demonstrated. It was shown that redundant TDOA measurements can lead to improved PL accuracy. Simulation results indicate that an improvement of approximately 17% in PL performance and 1 dB better noise tolerance can be achieved when using four base stations versus three base stations. However, adequate signal power levels are required at all base stations if improvements in PL performance are to be expected.

Simulation results demonstrated the effect of the base station configuration on the accuracy of the PL estimate. The geometric dilution of precision factor, which indicates the influence of the base station geometry on the PL accuracy, was evaluated for numerous mobile positions within a cell. The GDOP results indicated that ideal base station geometry is such that the mobile is equidistant and symmetrically located relative to the base stations. This GDOP factor can be used in the selection of base stations for the PL estimation procedure.

The effect of the closed-loop power control scheme used in CDMA systems on the accuracy of hyperbolic PL systems was evaluated. As a mobile moves closer to the controlling base station, lower SNRs are experienced at neighboring base stations. This results in inaccurate TDOA estimates and poor PL performance. At very low SNR values, the hyperbolic position location system is unable to provide reasonable PL estimates. More importantly, simulation results indicate that up to 60% of the cell coverage area cannot be served by the PL system. CAs a result, the service provider will not be able to provide E-911 service over this area. This presents a major problem to wireless service providers using CDMA technology in meeting FCC E-911 regulations. Under CDMA power control, it was also shown that redundant measurements do not always lead to improved PL accuracy. Simulation results indicate that very low SNRs experienced at the more distant base station will introduce greater uncertainty in the redundant TDOA estimate, resulting in greater uncertainty in the PL estimate. This problem can be overcome, at the expense of system capacity, by instructing the mobile to transmit at maximum power.

The performance of the hyperbolic PL system within the presence of multipath was demonstrated. Code division multiple access system have an inherent capability for multipath interference rejection. However, multipath presents a unique problem to hyperbolic PL systems. If multipath signal components arrive within the chip interval of the LOS signal, the resulting cross-correlation and TDOA estimate will be based on both LOS and multipath signal components. In this situation, the resulting TDOA estimate will be biased and degradation in performance is experienced. If the LOS signal has greater signal power than the multipath component, then PL performance improves as the multipath component arrives farther outside of the chip interval. However, if multipath arriving within the observation window has equal or higher

signal power than then LOS signal or if the LOS propagation path is non-existent, then the TDOA estimate will be based primarily on the multipath component and a linear increase in PL error is experience as the arrival time of the multipath component increases. Because the GCC TDOA estimation methods are unable to discriminate between the correlation peak due to LOS and multipath signal components, an assumption as to which correlation peak was due to the LOS signal must be made, which can lead to inaccuracies in the PL estimate.

The effect of shadowing mobile radio environments, in which the LOS propagation path of the users signal is obstructed, on the PL performance was also demonstrated. Simulation results indicate that shadowing and CDMA power control can have both beneficial and adverse effects on PL accuracy. If the mobile radio channel to the controlling base station is obstructed, the mobile increases transmit power in order to maintain adequate SNR at the base station. This increase in transmit power effectively improves the SNRs experienced at neighboring base stations, resulting in better TDOA estimation and improved PL performance. However, if the radio channel to any of the neighboring base stations is shadowed by an obstructed of sufficient height, lower signal levels are experienced at the base station and a degradation in PL performance results.

6.1 Future Research

The performance evaluation of the hyperbolic position location technique presented in this thesis provides a general overview of the capabilities of the system. Additional research is needed to further evaluate the performance of the hyperbolic PL system within CDMA systems. Areas of future research can concentrate on two specific areas: improvements to the TDOA estimation and improved hyperbolic PL algorithms.

If improved PL performance is to be realized using the hyperbolic PL method, improved TDOA estimation techniques will be required. The cross-correlation TDOA estimation technique used in the simulations is a generalized cross-correlation (GCC) delay estimation method in its simplest form. Consequently, a performance comparison of the frequency filter functions described and improvements to PL accuracy can

be evaluated. As discussed previously, GCC methods are unable to resolve spectrally and temporally coincident signals or identify the correlation peaks due to the signal of interest and interfering signals. Time difference of arrival estimation techniques which overcome the inability's of GCC TDOA estimation methods can further improve PL performance. The simulation used in this thesis evaluated a single-user CDMA system. Future research efforts may concentrate on the performance of the hyperbolic PL system in multiuser CDMA systems and the effect of multiple access interference on PL accuracy. Methods to mitigate the correlation peaks due to other sources of interference may be investigated. Because accurate receiver tracking and high clock synchronization between base stations is desirable, receiver sensitivities, such as timing and sampling errors, clock drift and biases and base station timing biases on the PL performance can also be evaluated.

Because of the large scale nature of the cellular infrastructure, adequate signal quality at neighboring base stations becomes a significant problem. Time difference of arrival estimation methods which perform well at low SNRs would also be of importance. Other methods to mitigate the low SNR problem and improve PL accuracy, such as the use of "sniffer" receivers within the cell, can also be investigated. Another area of interest would be evaluating the effect of the observation interval, or "snapshot", taken for the TDOA estimation and signal sampling on the PL performance. Improved channel models or the use of site-specific channel information that better represent real-world mobile radio channels would also be valuable in accessing the performance of the hyperbolic PL technique.

While the accuracy of the TDOA estimate appears to be a major limiting factor in the performance of the hyperbolic PL system, the performance of the hyperbolic PL algorithm is equally important. Position location algorithms which are robust against TDOA noise and are able to provide unambiguous PL solution to the set of nonlinear range difference equations are desirable. The hyperbolic PL algorithms discussed in this thesis provide solutions to a linearized set of range difference equations. Consequently, the effect of the linearization of the range difference equations on the performance of the system, especially in bad GDOP situations, can be investigated. The Taylor-series Least Squares PL algorithm used in these simulation was selected

because of its simplicity and ability to offer accurate PL estimation even at reasonable TDOA noise levels. However, because the Taylor-series method is an iterative process, it can become computationally intensive and convergence is not guaranteed. The trade-off between computational complexity and accuracy exist for all PL algorithms. The iterative Taylor-series method provides accurate results, however, if real-time results are required, the computational complexity of the algorithm may be of more importance. Therefore, a trade-off analysis through performance comparison of the closed-form and iterative PL algorithms can be performed.

Bibliography

[Abe87] J. S. Abel and J. O. Smith, " The spherical interpolation method for closed-form passive localization using range difference measurements," *Proc. ICASSP-87* (Dallas, TX) , pp. 471-474, 1987.

[Abe89] J. S. Abel and J. O. Smith, "Source Range and Depth Estimation from Multipath Range Difference Measurements," *IEEE Transactions on Acoustics, Speech, and Signal Processing*, Vol. 37, No. 8, pp. 1157- 1165, August 1989.

[Abe90] J. S. Abel, " A divide and conquer approach to least-squares estimation," *IEEE Transactions on Aerospace and Electronic Systems*, Vol. 26, March 1990, pp. 423 - 427.

[Ban85] S. Bancroft, "An Algebraic Solution of the GPS Equations," *IEEE Transactions on Aerospace and Electronic Systems*, Vol. AES-21, No. 7, January 1985.

[Car73] G.C. Carter, A. H. Nuttall and P.C. Cable, "The smoothed coherence transform," *Proc. IEEE*, Vol. 61, pp. 1497-1498, October 1973.

[Car81] G. C. Carter, " Time Delay Estimation for Passive Sonar Signal Processing," *IEEE Transactions on Acoustics, Speech, and Signal Processing*, Vol. ASSP-29, No. 3, pp. 463-470, June 1981.

[Car87] G. C. Carter, "Coherence and Time Delay estimation," *Proc. IEEE*, Vol. 75, pp. 236-255, February 1991.

[Cha94] Y. T. Chan and K.C. Ho, "A Simple and Efficient Estimator for Hyperbolic Location," *IEEE Transactions on Signal Processing*, Vol. 42, No. 8, pp. 1905-1915, August 1994.

[Fan90] B. T. Fang, " Simple Solutions for Hyperbolic and Related Position Fixes," *IEEE Transactions on Aerospace and Electronic Systems*, Vol. 26, No. 5, pp 748- 753, September 1990.

[FCC94] FCC Regulation Proposal: Notice of Proposed Rule Making, FCC Docket 94-237, Adopted Date : Sept.19,1994 Released Date : Oct. 19,1994

[FCC96] FCC Report and Order and Further Notice of Proposed Rule Making, FCC Docket 96-264, June 12, 1996

[Foy76] W. H. Foy, " Position-Location solutions by Taylor-series estimation," *IEEE Transactions on Aerospace and Electronic Systems*, Vol. AES-12, pp. 187 - 194, March 1976.

[Fri87] B. Friedlander, " A Passive Localization Algorithm and Its Accuracy Analysis," *IEEE Journal of Oceanic Engineering*, Vol. OE-12, No. 1, pp. 234 - 244, January 1987.

[Gar92a] W. A. Gardner and C. K. Chen, "Signal-Selective Time-Difference-of-Arrival Estimation for Passive Location of Man-Made Signal Sources in Highly Corruptive Environments, Part I: Theory and Method," *IEEE Transactions on Signal Processing*, Vol. 40, No. 5, pp. 1168 - 1184, May 1992.

[Gar92b] W. A. Gardner and C. K. Chen, "Signal-Selective Time-Difference-of-Arrival Estimation for Passive Location of Man-Made Signal Sources in Highly Corruptive Environments, Part II: Algorithms and Performance," *IEEE Transactions on Signal Processing*, Vol. 40, No. 5, pp. 1185 - 1197, May 1992.

[Gar94] W. A. Gardner, Cyclostationarity in Communications and Signal Processing, IEEE Press, 1994.

[Gil96] K. S. Gilhousen, Technical Presentation at the Virginia Tech Symposium on Wireless Personal Communications, June 5-7, 1996.

[Hah73] W. R. Hahn and S. A. Tretter, "Optimum Processing for Delay-Vector Estimation in Passive Signal Arrays," *IEEE Transactions on Information Theory*, Vol. IT-19, No. 5, pp. 608-614, September 1973.

[Hah75] W. R. Hahn, "Optimum signal processing for passive sonar range and bearing estimation," *Journal of the Acoustical Society of America*, Vol. 58, No. 1, pp. 201 - 207, July 1975.

[Han73] E. J. Hannan and P. J. Thomson, "Estimating Group Delay," *Biometrika*, Vol. 60, pp. 241-253, 1973.

[Hep94] E. Hepsaydir and W. Yates, " Performance Analysis of Mobile Positioning using Existing CDMA Network," *IEEE Position Location and Navigation Systems*, pp. 190 - 192, 1994.

[Jor84] P. S. Jorgenson, "Navstar/Global Positioning System 18-satellite constellations," *Global Positioning System: Papers Published in NAVIGATION*, Washington: The Institute of Navigation, Vol. II, 1984.

[Kna76] C.H. Knapp, G.C. Carter, "The Generalized Correlation Method for Estimation of Time Delay," *IEEE Transactions on Acoustic, Speech, and Signal Processing*, Vol. ASSP-24, No. 4, pp. 320-327, August 1976.

[Law76] Lawhead, "Position Location Systems Technology," *IEEE PLANS 76*, pp. 1 - 12, 1976.

[Lee75a] H. B. Lee, "A Novel Procedure for Accessing the Accuracy of Hyperbolic Multilateration Systems," *IEEE Transactions on Aerospace and Electronic Systems*, Vol. AES-11, No. 1, pp. 2-15, January 1975.

[Lee75b] H. B. Lee, "Accuracy Limitations of Hyperbolic Multilateration Systems," *IEEE Transactions on Aerospace and Electronic Systems*, Vol. AES-11, No. 1, pp. 16-29, January 1975.

[Lee85] W. C. Y. Lee, *Mobile Communications Engineering*, McGraw Hill Publications, New York, 1985.

[Lib95] J. C. Liberti, Jr., "Analysis of CDMA Cellular Radio Systems Employing Adaptive Antennas," Dissertation, VPI&SU, MPRG-TR-95-17, September 1995.

[Nat93] "Network Reliability: A Report to the Nation," *National Engineering Consortium*, Section F, page 1, June 1993.

[Nic73] D. L. Nicholson, "Multipath sensitivity of a linearized algorithm used in time-difference-of-arrival location systems," *Digest of International Electrical and Electronics Conference and Exposition*, Paper No. 73252, October 1973.

[Nic76] D. L. Nicholson, "Multipath and ducting tolerant location techniques for automatic vehicle location systems," *Record of Papers Presented at IEEE Vehicular Technology Conference*, Washington D.C. , pp. 151-154, March 24-26, 1976.

[Par96] B. W. Parkinson, J. Spiker Jr., P. Axelrad, P. Enge, *Global Positioning System: Theory and Applications Vol. I and II*, American Institute of Aeronautics and Astronautics, Inc., Washington, D. C. , Vol. 136, 1996.

[Rap96] T. S. Rappaport, *Wireless Communications : Principles and Practice*, Prnetice-Hall Inc., Upper Saddle River, NJ, 1996.

[Rot71] P. R. Roth, "Effective measurements using digital signal analysis," *IEEE Spectrum*, Vol. 8, pp. 62 - 70, April 1971.

[Roy89] R. Roy and T. Kailath, "ESPRIT - Estimation of Signal Parameters via Rotational Invariance Techniques," *IEEE Transactions on Acoustics, Speech, and Signal Processing*, Vol. 8, pp. 62 - 70, April 1971.

[Sch87] H. C. Schau and A. Z. Robinson, "Passive Source Localization Employing Intersecting Spherical Surfaces from Time-of-Arrival Differences," *IEEE Transactions on Acoustic, Speech, and Signal Processing*, Vol. 29, No. 4, pp. 984-995, July 1989.

[Smi87a] J. O. Smith and J. S. Abel, " The Spherical Interpolation Method for Source Localization," *IEEE Journal of Oceanic Engineering*, Vol. OE-12, No. 1, pp. 246 - 252, January 1987.

[Smi87b] J. O. Smith and J. S. Abel, "Closed-Form Least-Squares Source Location Estimation from Range-Difference Measurements," *IEEE Transactions on Acoustics, Speech, and Signal Processing*, Vol. ASSP-35, No. 12, pp. 1661 - 1669, December 1987.

[Sta72] H. Staras and S. N. Honickman, "The Accuracy of Vehicle Location by Trilateration in a Dense Urban Environment," *IEEE Transactions on Vehicular Technology*, Vol. VT-21, No. 1, pp. 38 - 44, February 1972.

[Sta94] H. Stark and J. W. Woods, Probability, *Random Processes, and Estimation Theory for Engineers*, Prentice-Hall, Inc., 2nd edition, 1994

[TIA93] TIA/EIA Interim Standard-95, "Mobile Station - Base Station Compatibility Standard for Dual-Mode Wideband Spread Spectrum Cellular Systems," July 1993.

[Tor84] D. J. Torrieri, "Statistical Theory of Passive Location Systems," *IEEE Transactions on Aerospace and Electronic Systems*, Vol. AES-20, No. 2, pp. 183 - 198, March 1984.

[Tur72] G. L. Turin, W. S. Jewell and T. L. Johnston, "Simulation of Urban Vehicle-Monitoring Systems," *IEEE Transactions on Vehicular Technology*, Vol. VT-21, No. 1, February 1972, pp. 9 - 16.

[Wel86] D. Wells, "Guide to GPS Positioning," Canadian GPS Associates, 1986.

[Woe94] B. D. Woerner, J. H. Reed and T.S. Rappaport, "Simulation Issues for Future Wireless Modems," *IEEE Communications Magazine*, Vol. 32, No. 7, July 1994.

[Zie85] R. E. Ziemer and R. L. Peterson, *Digital Communications and Spread Spectrum Systems*, Macmillan Publishing Company, New York, 1985.

[Zis88] I. Ziskind and M. Wax, "Maximum Likelihood Localization of Multiple Sources by Alternating Projection," *IEEE Transactions on Acoustics, Speech, and Signal Processing*, Vol. 36, No. 10, pp. 1553 - 1560, October 1988.

Vita

George Mizusawa was born in Toyko, Japan, November 5, 1963. He received a Bachelor of Science degree in Electrical Engineering from Virginia Polytechnic Institute and State University, Blacksburg, Virginia in May 1994. He joined the graduate program at Virginia Tech in September 1994, and has been a member of the Mobile and Portable Radio Research Group since May 1995. His research interests include digital communications and CDMA interference cancellation techniques. His research effort have focused on code division division multiple access (CDMA) spread spectrum communications systems, position location techqniues for cellular/PCS system architectures, and simulation of communications systems. George is a student member of the IEEE.